EPA

Introduction to Fractured Rock Hydrogeology

Presented by Joseph Alfano

July 10, 1997

Raleigh, NC

Geology

How fractures form

- Fractures are formed by tectonic stresses within the earth's crust
  - Isostatic adjustment
    - Up and down movements of the crust to come to equilibrium with gravity
    - Uplift from removal of overburden by erosion or unloading of glacial ice sheets
    - Downward movement by loading of sediments or the advancement of a glacial ice sheet
    - Isostatic adjustments create predominately tensional fractures (example — Joints with vertical orientation)

How fractures form (cont'd.)

- Stress relief fractures are also caused by removal of overburden
- The rock under pressure at depth expands as it nears the earth's surface (overburden pressure is removed)
- Results predominantly in horizontal tensional fractures
- Stress relief fractures may occur at pre-existing planes of weakness
- Bedding planes in sedimentary rock or foliation in metamorphic rock
- Stress relief fractures decrease in number and increase in spacing with depth

How fractures form (cont'd.)

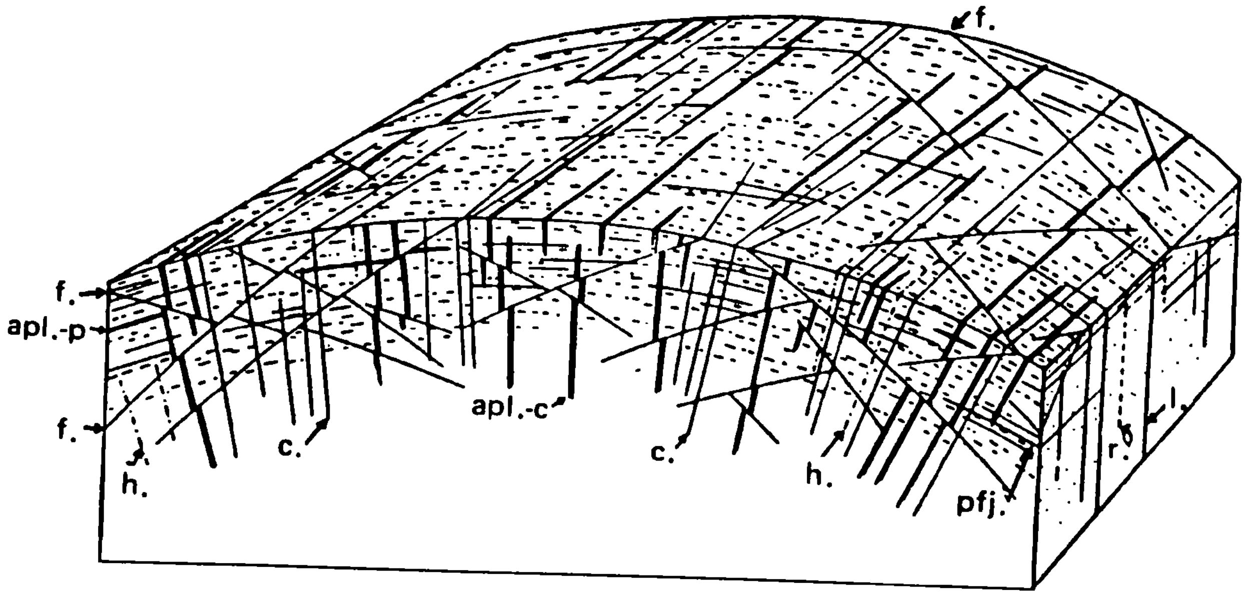

(After H. Cloos, 1992; From Balk, 1937; From Dennis, 1992)

How fractures form (cont'd.)

- Lateral tectonic forces cause faults
- Faults are fractures with a displacement and can extend for miles
- Faults occur at any angle and are compressional and tensional

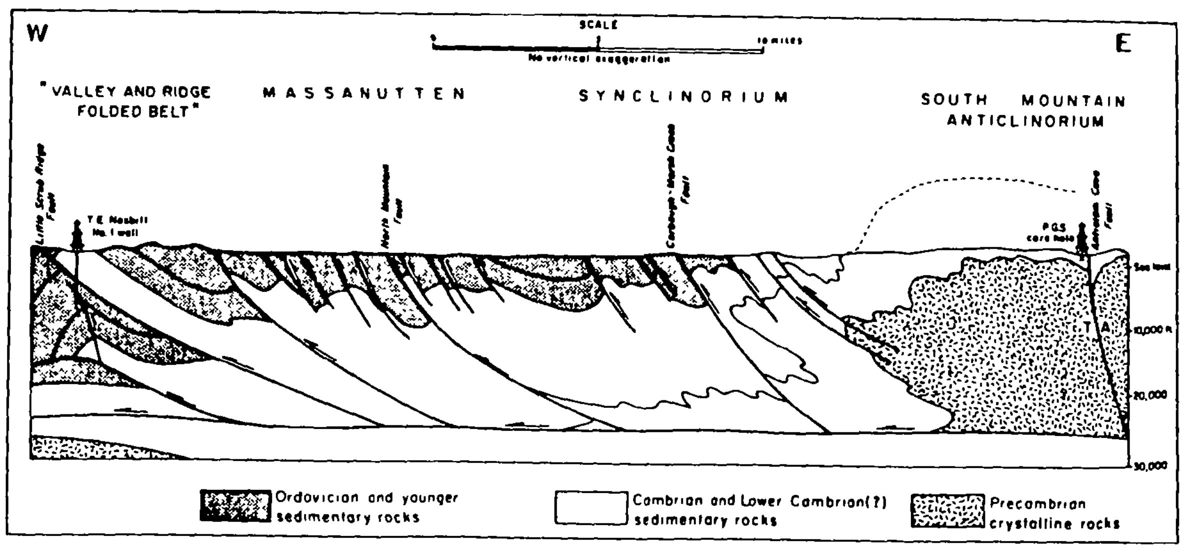

(From Root, 1970; From Spencer (1977)

How fractures form (cont'd.)

- Whether a fault or fracture is more or less permeable than the surrounding rock depends on the material that fills the fracture, if any
  - Clays → low permeability
  - Broken rock → higher permeability

- Shear zones are narrow zones in a rock body where shear stress is accommodated by plastic deformation in the mineral grains

- Shear zones can be zones of increased permeability

How fractures form (cont'd.)

- The orientation of a fracture or any planar feature is described by strike and dip
- Strike is the intersection of a horizontal plane and the plane of a fracture
- Strike is a horizontal line that is measured as an angle from geographic north or south, or as an azimuth with zero degrees at north

How fractures form (cont'd.)

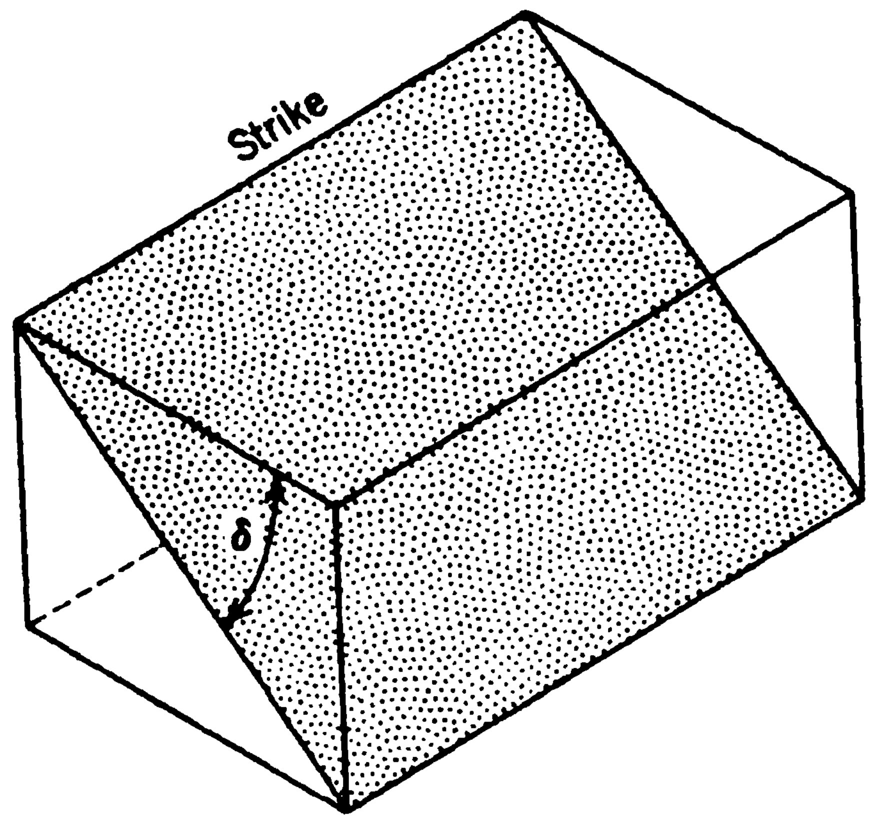

From Ragan (1973)

How fractures form (cont'd.)

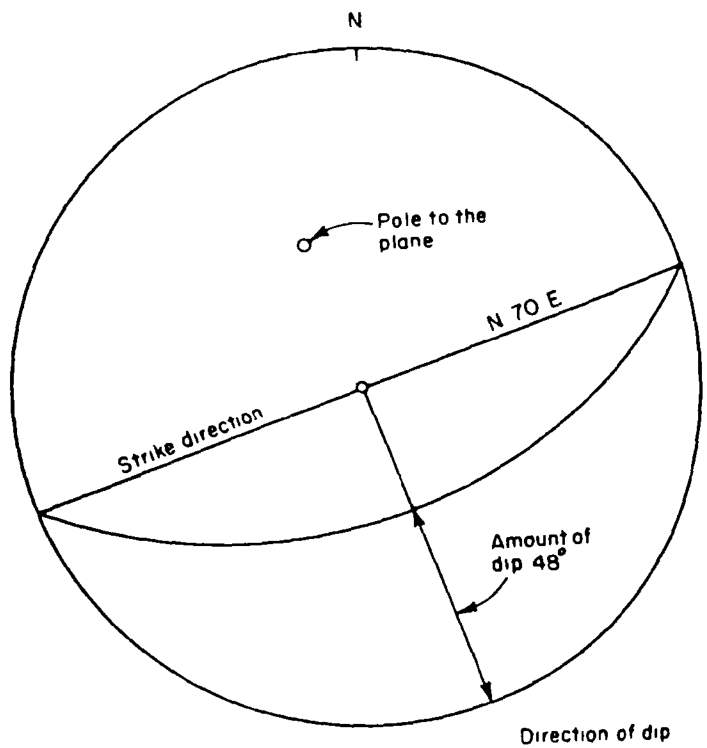

Representation of a plane by stereographic projection. From Spencer (1977)

How fractures form (cont'd.)

- Dip is the angle the fracture plane makes with the horizontal in a direction perpendicular to strike

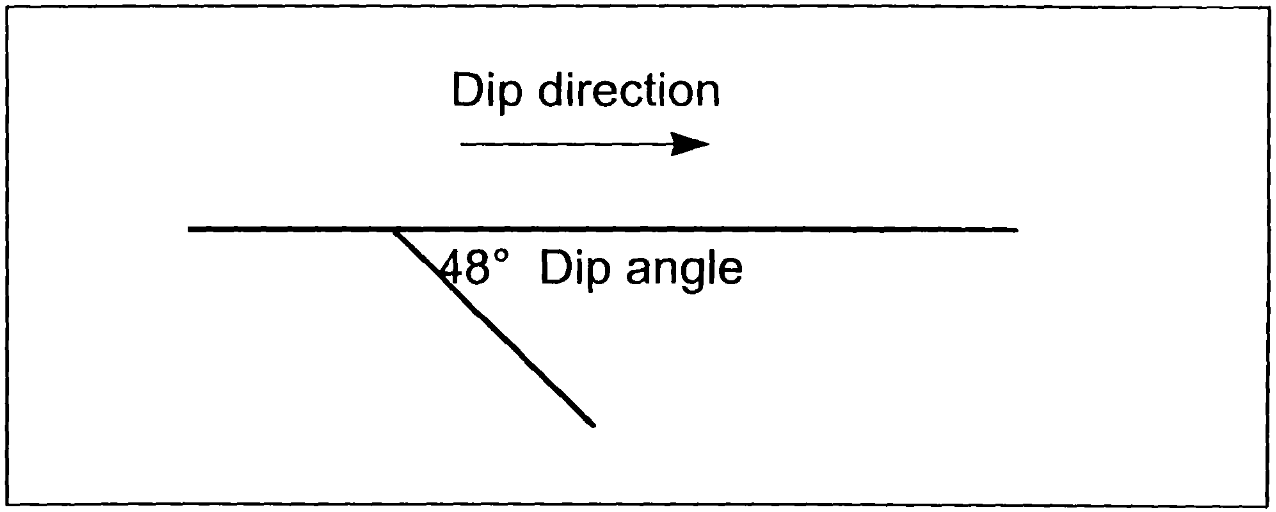

- Any planar feature is oriented by its strike and dip
  - N70°E strike, 48°E dip

Size of fractures

- Micro fractures (fissures)
  - Narrow aperature — less than 100 microns (micron = 10^{-6} meters)
  - Often limited to a single layer
  - Limited length and width
  - If interconnected can be significant
- Macro fractures
  - Wide aperature — greater than 100 microns
  - Develop across various layers
  - Can be of considerable length (miles)

Size of fractures (cont'd.)

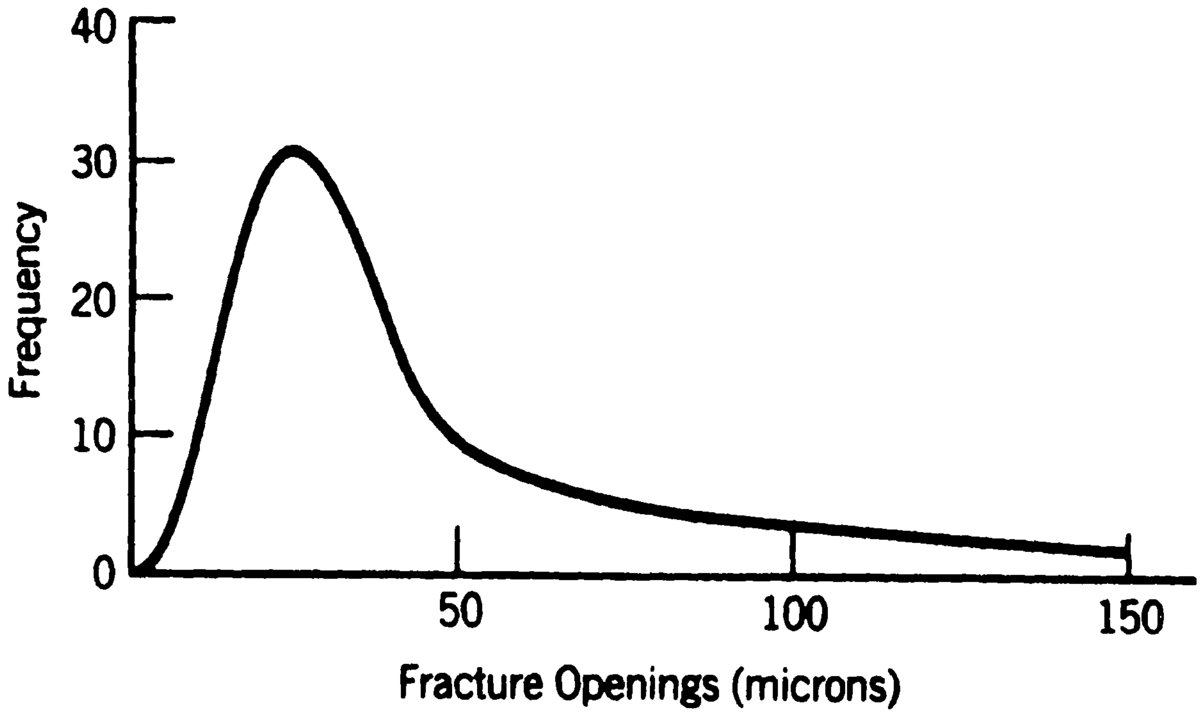

Statistical frequency curve of opening width . Reprinted with permission of Elsevier Scientific Publishing Company. From van Golf Racht (1982)

Size of fractures (cont'd.)

TABLE 1. STATISTICAL PARAMETERS OF THE DISTRIBUTION OF FRACTURE APERTURES AT EXPOSURES OF PIKES PEAK GRANITE

Parameter	(range 0·12–5·41 mm) $\log_e$ (mm)	(mm)
Arith. mean	−0·700	0·932
Geom. mean	0·000	1·000
Median	−0·100	0·905
S.D.	0·043	1·045
Skewness	−0·060	
Kurtosis	3·051	

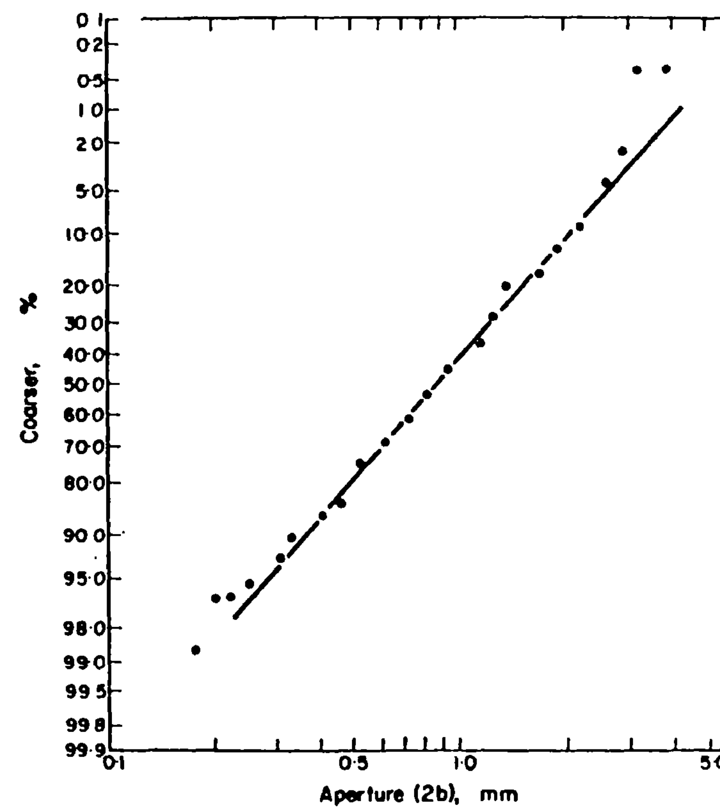

Log-probability plot of cumulative frequency of 256 apertures of exposed fractures, Pike's Peak granite (replotted from BIANCHI [24]). From Snow (1970)

Size of fractures (cont'd.)

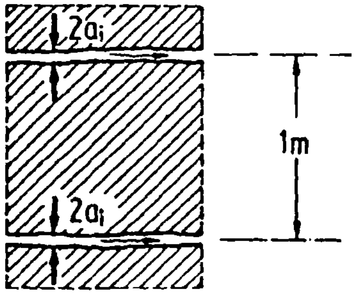

$$k_0 = \begin{cases} \dfrac{(2a_i)^3 \cdot g}{12 \cdot \nu \cdot 1\mathrm{m}} & (k/D_h \leq 0.032) \\[2ex] \dfrac{(2a_i)^3 \cdot g}{12 \cdot \nu \cdot [1 + 8.8 \cdot (k/D_h)^{1.5}] \cdot 1\mathrm{m}} & (k/D_h > 0.032) \end{cases}$$

$2a_i$	k/D_h	k_0 [m/s]	≙ k (soil)
0.1 mm	≤ 0.032	$0.6 \cdot 10^{-6}$	silt
	0.25	$0.3 \cdot 10^{-6}$	
0.2 mm	≤ 0.032	$0.5 \cdot 10^{-5}$	
	0.25	$0.2 \cdot 10^{-5}$	
0.4 mm	≤ 0.032	$0.4 \cdot 10^{-4}$	sand
	0.25	$0.2 \cdot 10^{-4}$	
0.7 mm	≤ 0.032	$0.2 \cdot 10^{-3}$	
	0.25	$0.1 \cdot 10^{-3}$	
1.0 mm	≤ 0.032	$0.6 \cdot 10^{-3}$	gravel
	0.25	$0.3 \cdot 10^{-3}$	

From Wittke (1990)

Porosity

- Primary porosity
  - Voids formed at the same time as the rock formation
  - Spaces between the sand grains

$$p = \frac{V_{voids}}{V_{total}} \times 100$$

- Secondary porosity
  - Voids formed after rock formation
    - —Faults, joints and solution cavities

$$P_{total} = P_{primary} + P_{secondary}$$

Characterization of fractures

- Orientation — strike and dip — measured with a Brunton Compass

- Size of fractures — aperature and length
  - Is the fracture filled?
    - —Minerals
    - —Clay
    - —Gravel
  - To what degree is the fracture weathered?

- Fracture density
  - Linear fracture density (average fracture frequency)
  - Number of fractures per unit length of a straight line perpendicular to fracture set (N)

Characterization of fractures (cont'd.)

$$N = \frac{\text{Total number of fractures}}{\text{Total length of sampling line}} = \frac{\text{20 fractures}}{\text{5 meters}} = \frac{\text{4 fractures}}{\text{meter}}$$

- The inverse of fracture frequency is fracture spacing (d)

$$d = \frac{\text{0.25 meters}}{\text{fracture}}$$

Roughness — is the degree fracture walls are not smooth (R_r)

- Roughness is defined as the ratio of mean irregularity (I) to the hydraulic aperature (H_r). (Sen, 1995)

$R_r < 0.032$ is smooth

$$R = \frac{I}{H}$$

$R_r > 0.032$ is rough

Lineament study

- Fracture traces and lineaments are the surface expression of the intersection of fractures and the ground surface

- Performed on aerial photographs or topographic maps

Lineament study (cont'd.)

From Lattman and Nickelsen (1958)

Lineament study (cont'd.)

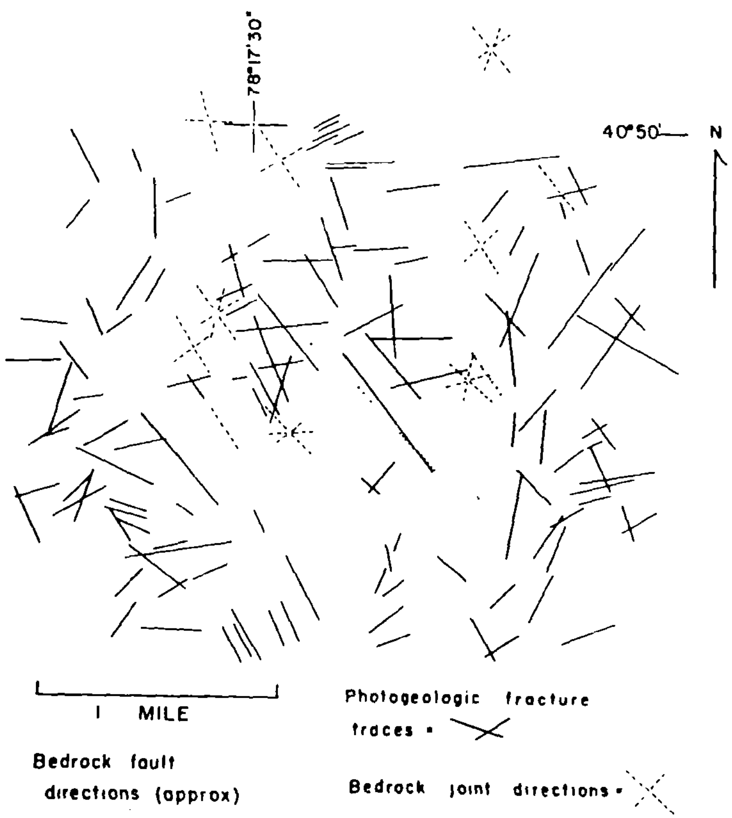

Photogeologic fracture traces and bedrock joints. From Lattman and Nickelson (1958)

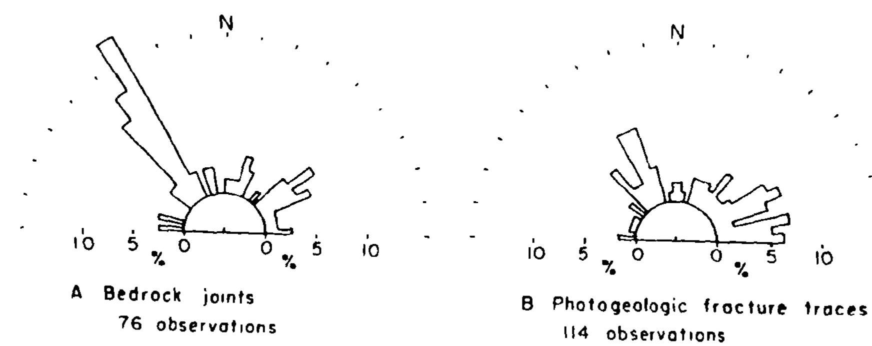

Histograms of photogeologic fracture traces and bedrock joints. From Lattman and Nickelsen (1958)

Lineament study (cont'd.)

Lineament study (cont'd.)

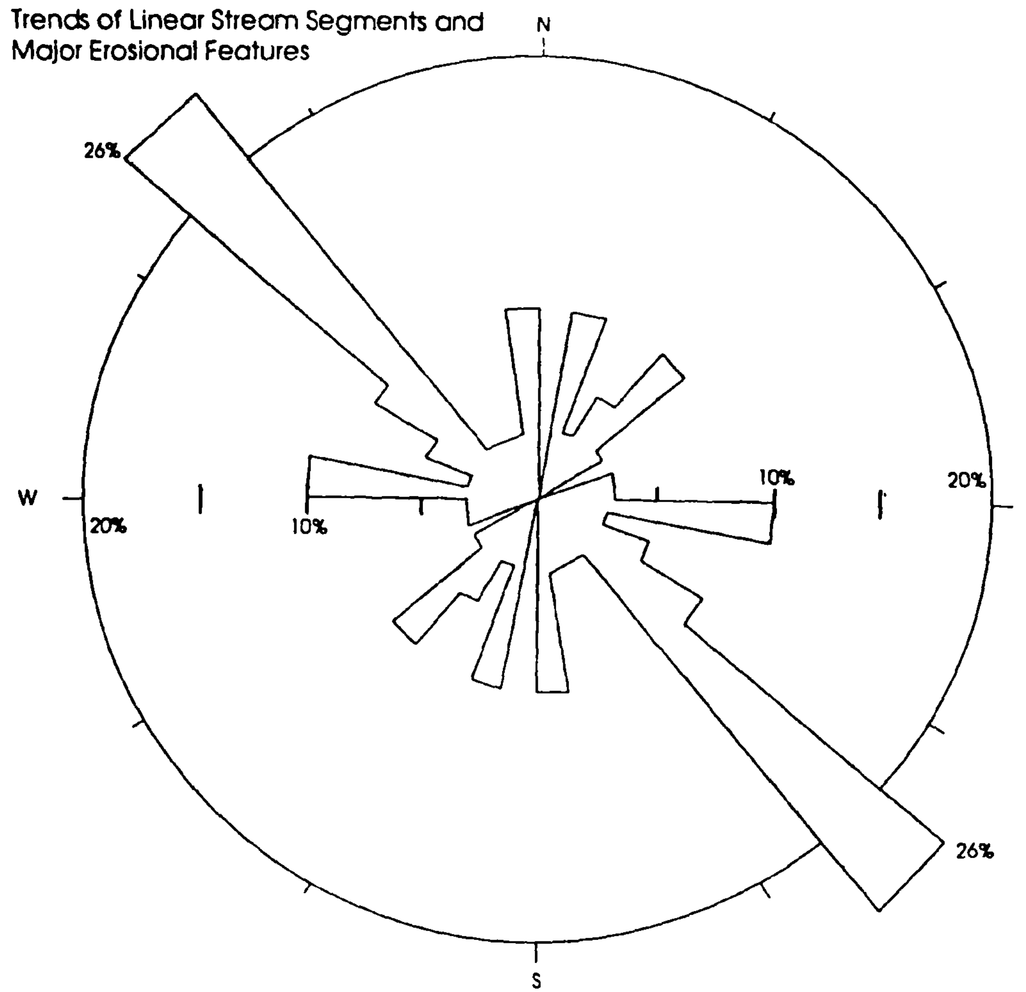

From Alfano (1993)

Follow-up lineament study with field study

- Check nature of observed lineament
  - Are they manmade or natural?

- Collect outcrop data on fracture orientation and characteristics

- Use Brunton Compass for strike and dip measurements

- Include orientation of any bedrock fabrics — Bedding planes in sediments rock and foliation in metamorphic rock

Scanline analysis

- A series of scanlines are established on the rock face. The orientation of the rock face is measured. The traverses (scanlines) are established is different direction to compensate for directional bias. Perpendicular traverses are good

- Measure the angle between the fracture trace and the scanline. Measure the distance along the scanline to the fracture trace and any cross cutting relationship between fracture traces (which fracture cut off other fractures). If the strike and dip of the fracture trace can be measured do so

- The fracture traces are plotted on a stereonet and the fracture sets established by grouping fracture traces with similar orientations

Scanline analysis (cont'd.)

- The number of fractures in a fracture set are corrected to account for the directional bias imparted by the angle the fracture trace is to the scanline. The corrected fracture frequency (N_c) is determined by

$$N_c = \frac{N_{measured}}{\sin\theta}$$

θ = Acute angle between the scanline and fracture trace

- A scanline analysis is useful when a statistical analysis of the fracture data is performed. (Priest and Hudson, 1976 and Priest, 1993)

- The 2 dimensional scanline fracture groups can be correlated with 3 dimensional orientation (strike and dip) fracture group data

Problem with surface measurements

- Problem with field survey
  - Fracture characteristic, such as aperature, weathering measured at the surface will be different then fractures at depth under the surface because fractures open up (aperature increases) as fracture near the surface (over burden pressure is decreased) and weathering is more intense near the surface

Directional bias

- The directional bias experienced in scanline analyses is also encountered when boreholes are drilled
- The vertical orientation of most boreholes will selectively locate low angle fractures and miss high angle fractures (joints)

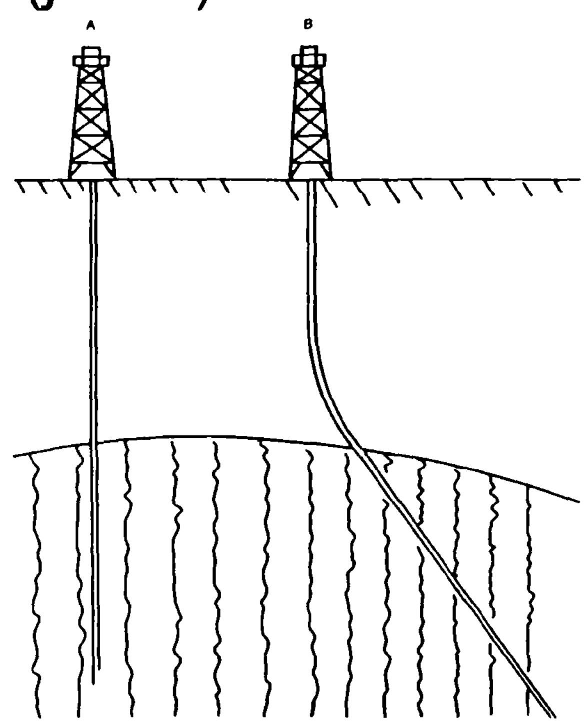

From Aquilera (1980)

Directional bias (cont'd)

- Outcrop versus core fractures

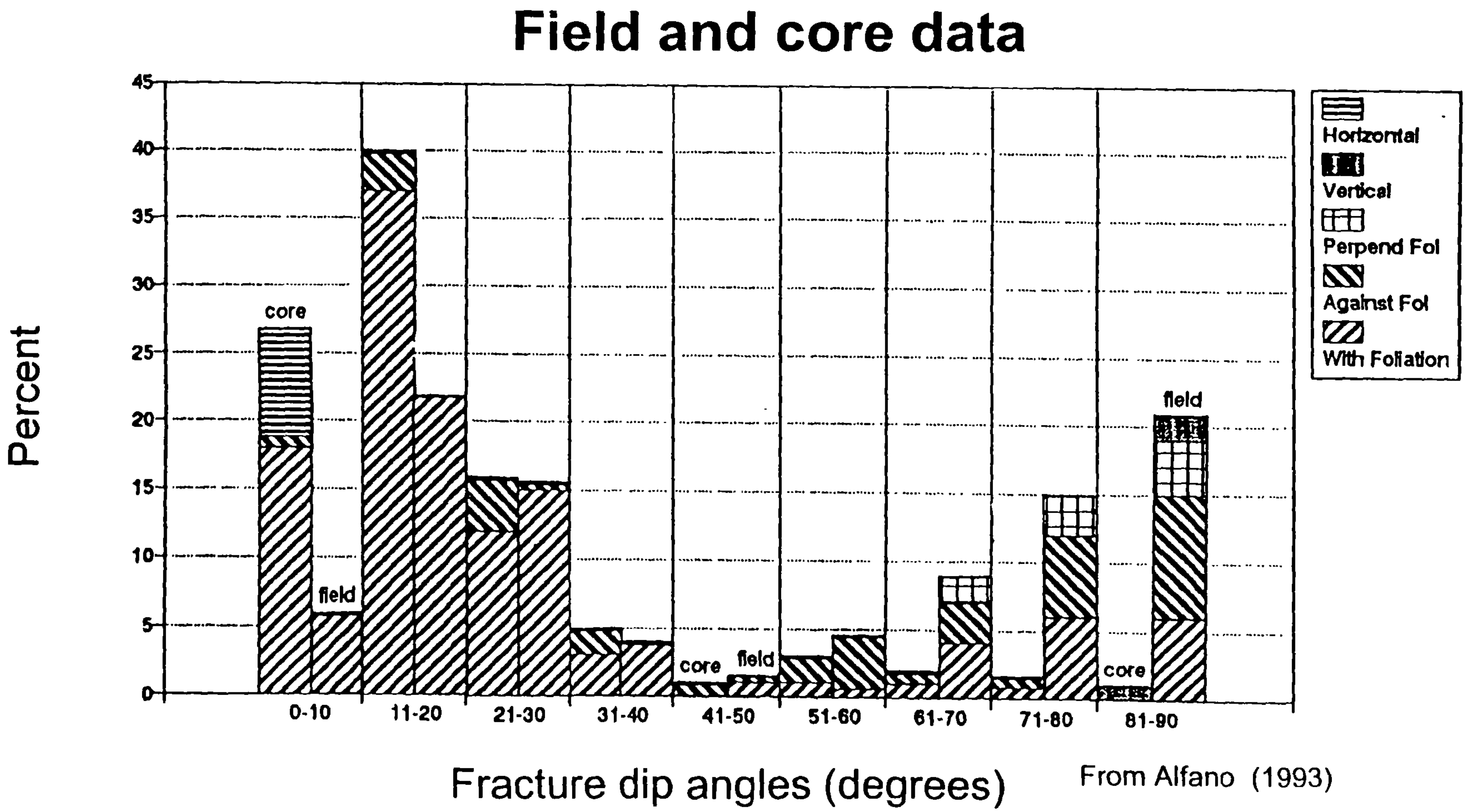

From Alfano (1993)

Core analysis

- Bedrock coring is an expensive operation and oriented coring is as much as three times more expensive than ordinary coring

- Without oriented core the orientation of the fractures are difficult to determine

- Coring can create fractures that are hard to distinguish from original fractures. Although weathering along the fracture is an indication of original fractures and which fractures are conducting water

- Intensely weathered zone obscure individual fractures

Core analysis (cont'd.)

- If original fractures are distinguishable an average fracture frequency is easy to determine (fractures per meter)
- Weathering and mineralization along fractures is directly observable
- Good lithological description

Core analysis (cont'd.)

- Problems of core analysis:
  - Coring is expensive and the analysis of the core is time consuming. Borehole geophysical methods are less expensive and less time consuming to analyze
  - Vertical cores are bias toward intersecting low angle fractures
  - High angle fractures are underrepresented

Core analysis (cont'd.)

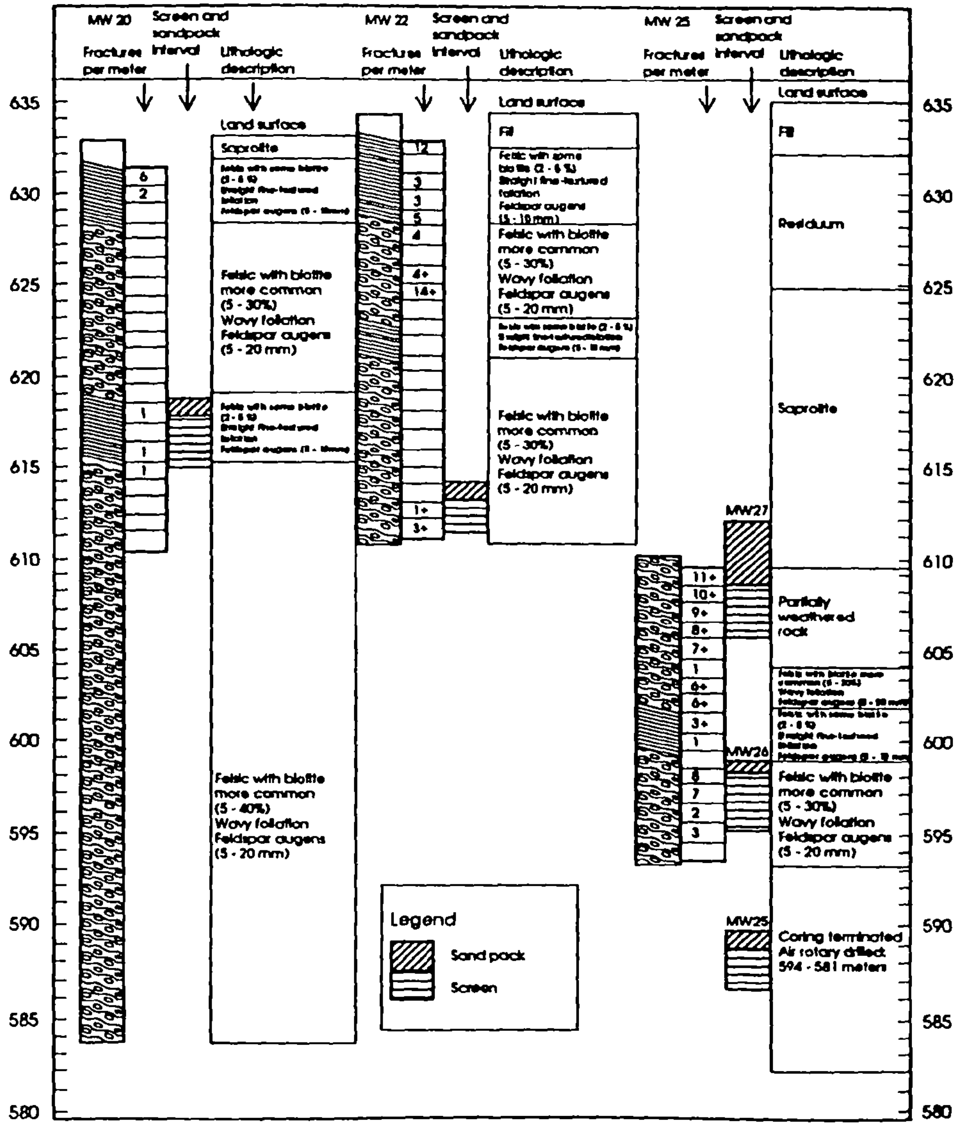

From Alfano (1993)

Core analysis (cont'd.)

- Rock quality designation — RQD used to express the degree to which the rock is competent

$$RQD = \frac{\text{Sum of the length of all pieces over 4 inches (100mm)}}{\text{Total length recovered}} \times 100$$

- Problem:
  - If a five foot core section has a fracture every foot there are four fractures but the RQD is 100%

Geophysical method

- Conventional well logs
  - Neutron logs detect porosity (fracture) by detecting the hydrogen in water
  - Density logs detects porosity by measuring scattered gamma radiation

- The above logs have a resolution of about 0.1 meters. The shallow penetration of these logs may only measure the gouging and wash out area adjacent to the borehole

Geophysical method (cont'd.)

- Caliper logs measure variation in the diameter of the borehole
- Best response for areas of washout where fracture zones (more than one fracture) or large fractures are located
- Small fractures will not show up

Geophysical method (cont'd.)

- Fluid conductivity logs
  - Detects a change in the electrical conductivity of the water
  - Need to replace the water in the well bore with low conductivity (deionized) water first so water entering the wellbore from the fractures will have higher conductance

Geophysical method (cont'd.)

- Acoustic televiewer
  - Uses reflected sonic waves to detect fracture openings or soft weathered zones
  - Can be used in clear or murky water
  - Fracture orientation is easy to determine because it is equipped with internal compass

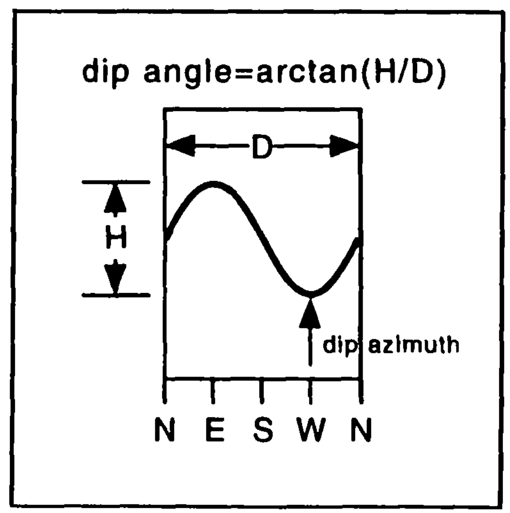

Determination of dip angle and azimuth of fracture from the ATV log. D = diameter of borehole. From Cohen (1995)

Geophysical method (cont'd.)

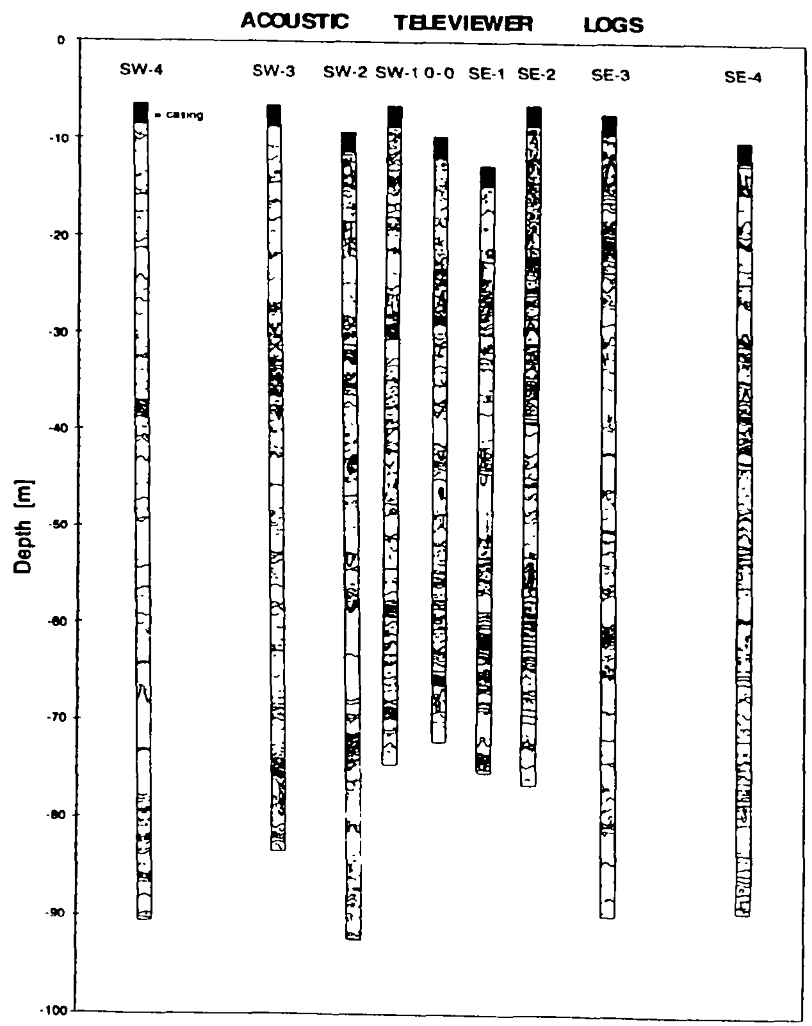

Acoustic televiewer logs of all nine wells. From Cohen (1995)

Geophysical method (cont'd.)

- Problems of televiewer
  - Gouged out closed fracture appear open
  - Individual fractures cannot be determined in intensely weathered or washed out areas
  - Fill material in fractures cannot be directly seen
  - Can only be used in water filled portion of well
  - Not all fractures conduct water
  - Must use other methods to determine conductive fractures

Geophysical method (cont'd.)

- Downhole television camera
  - Inexpensive method to get video picture of the borehole
  - Fractures and fill material directly observable
  - Borehole does not have to have water in it

- Problems of downhole television
  - Cannot see in murky water
  - Many downhole cameras do not have orientation devises (wire line)
  - Fractures hard to see in dark rocks

Geophysical method (cont'd.)

- All borehole detection methods are limited by ability to only measure conditions near the borehole where drilling damage is present
- Measurements near the borehole may not be representative of condition in the rest of the rock
- Geophysical methods for detection between boreholes or a borehole and the surface do exist
- Seismic, radar, electromagnetic tomography

Surface methods

- Electromagnetic methods
  - Uses electric and magnetic fields to detect anomalies in conductance
  - In the sounding mode (different depth but same location) horizontal fractures are detectable
  - In the profiling mode (same depth but different location) vertical and dipping fractures are detected
  - Can penetrate to 100 meters if bedrock is exposed
  - Clay-rich overburden greatly reduces depth of penetration

Surface methods (cont'd.)

- Ground-penetrating radar
  - Also uses electromagnetic energy to detect changes in electrical conductance
  - Can penetrate to 100 meters if bedrock is exposed
  - Clay-rich overburden greatly reduces depth of penetration
- If overburden obscures detail in the bedrock electromagnetic method can still define the bedrock surface
- Depression in the bedrock surface may indicate high angle fracture zones

Surface methods (cont'd.)

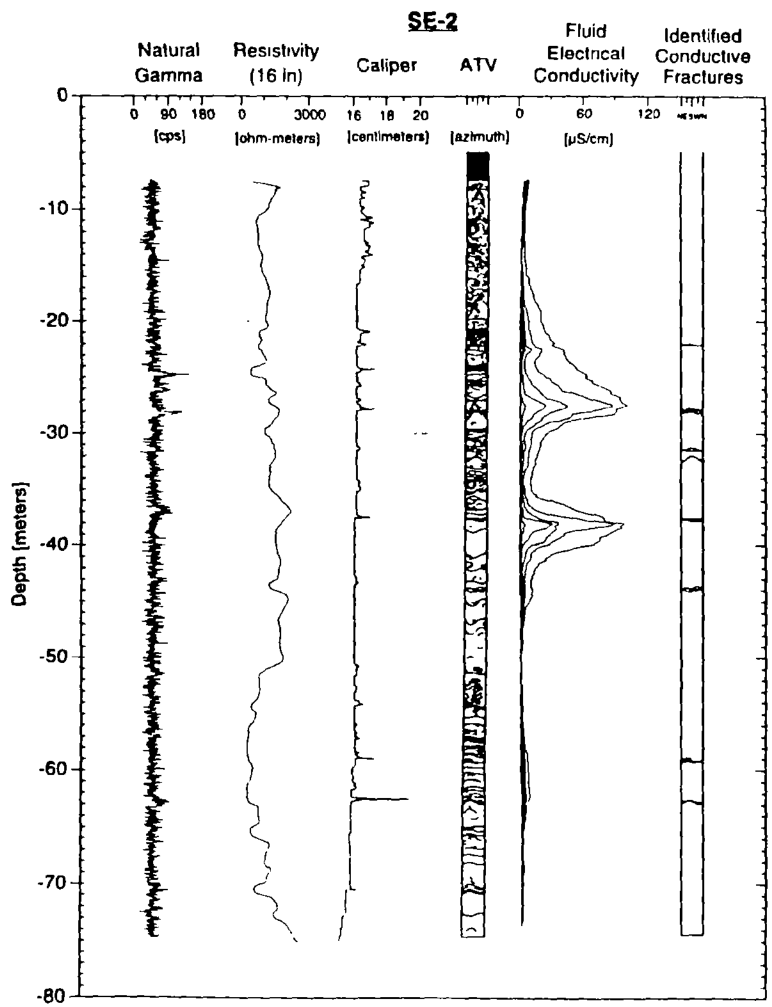

Reference from Cohen (1995)

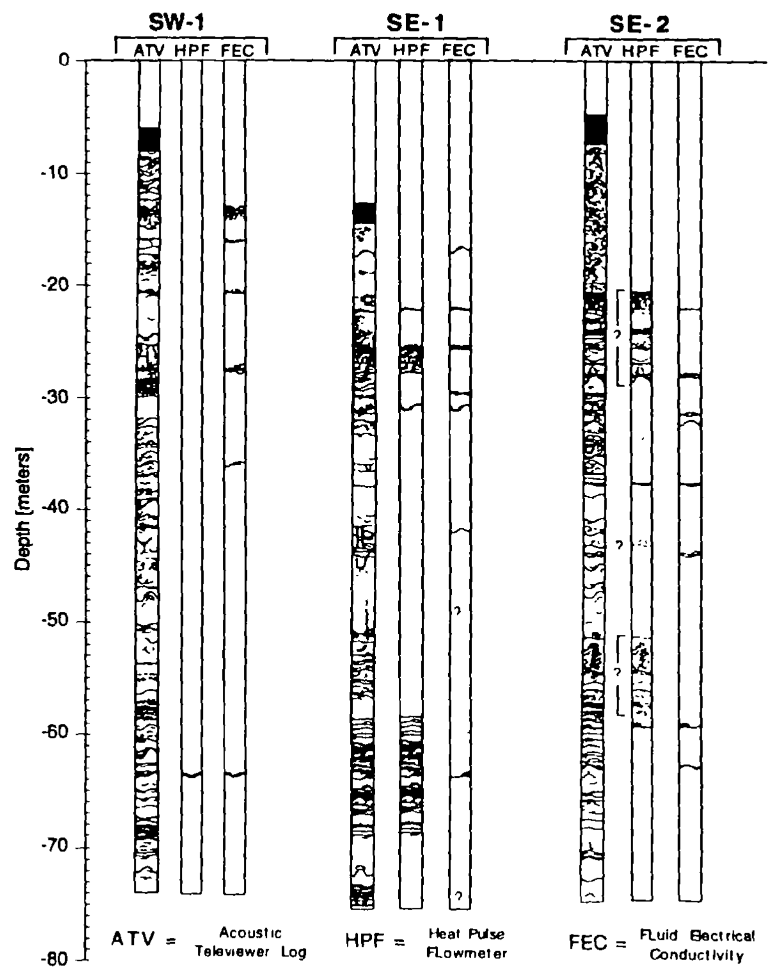

Reference from Cohen (1995)

Borehole flow logs

- Impeller flowmeter
  - Water in the borehole flows past the impeller
  - The flow rate (liters/minute) is calculated from the RPMs and the diameter of the borehole
  - Natural flow rates are usually too low to turn the impeller so a pump and pressure transducer are placed near the top of the water surface to induce higher upward flow and to measure the drawdown
  - As the impeller is lower in the borehole the flow rate through the impeller will decrease as conductive fracture zones are passed

Borehole flow logs (cont'd.)

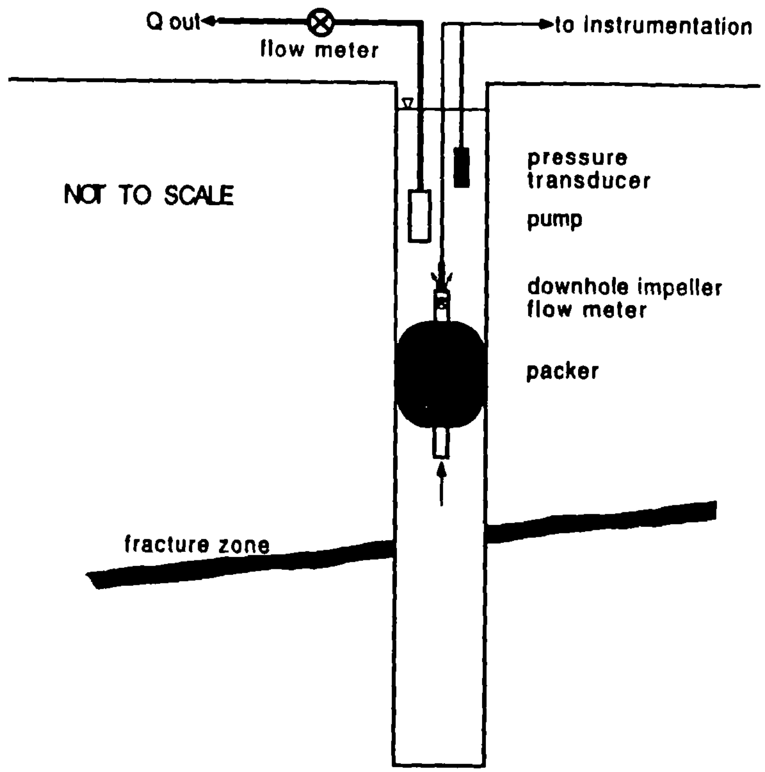

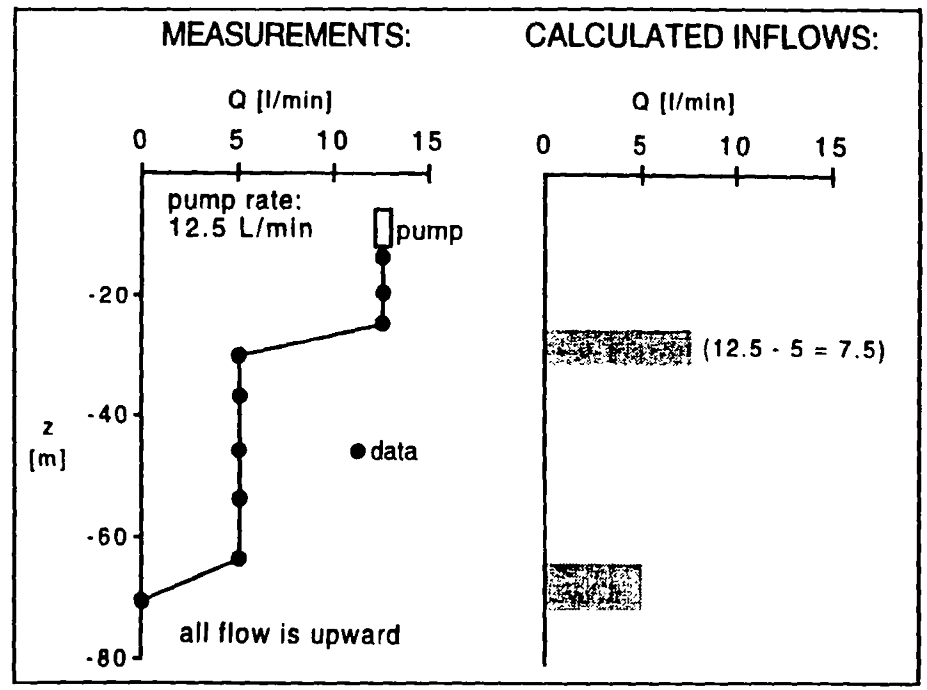

Schematic of impeller flowmeter test configuration. From Cohen (1995)

Example flow profile and calculation of wellbore inflows.
From Cohen (1993)

Borehole flow logs (cont'd.)

- The transmissivity (T) for the entire borehole interval is calculated from (Cohen, 1995)

$$T = \frac{2.3Q}{4\pi\left(\frac{\Delta s}{\text{log cycle}}\right)}$$

Q = Flow rate

Δs = Change in drawdown over one log cycle on drawdown(s) versus log time (t) plot (ft)

- The transmissivity for each conductive fracture internal (T_i) is calculated by

$$T_i = \frac{TQ}{Q}$$

Q_i = Flow rate for each conductive interval

- Relative conductivity for each interval is established by values of $\frac{Q}{Q}$

Borehole flow logs (cont'd.)

- Problems of impeller flowmeters:
  - Assume porous media equivalence — radial flow will may not be valid with some fracture geometries
  - Transmissivity values should be considered order of magnitude estimations. Cohen (1995)
  - Relative conductivity for each interval is established by values of $\frac{Q_i}{Q}$
  - Near the bottom of the borehole flow can decrease below the stall rate of the impeller giving the appearance of no flow
  - If the rock formation being tested has a low yield the water level will drop below the pump or conducting fractures

Borehole flow logs (cont'd.)

- Thermal — pulse flowmeter
  - Used in observations wells while another well is pumped
  - A pulse of heat is generated by a heat grid
  - Sensors above and below the heat grid detect the time it takes the heat to flow to one or the other sensor giving the flow rate and direction of flow (up and down)
  - Can measure lower flow rates than the impeller type so natural flow may be measured
  - Interval transmissivity is calculated with the same method as the impeller method

Borehole flow logs (cont'd.)

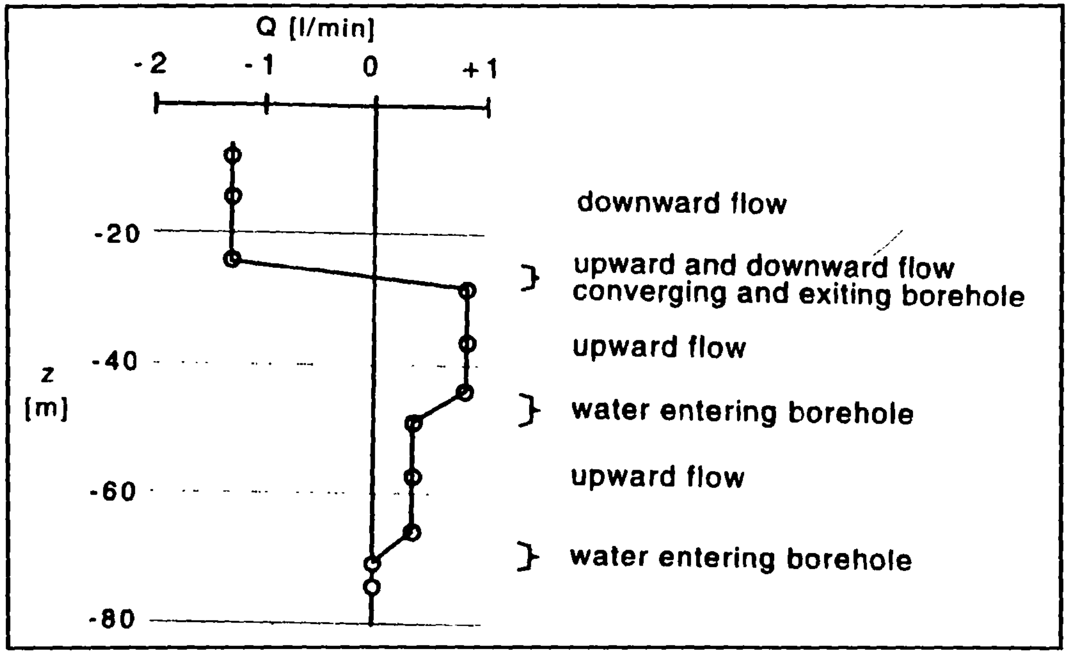

Hypothetical flow profile in a well during pumping in an adjacent well
From Cohen (1993)

- Problems of thermal — pulse flowmeter:
  - Same as impeller method but sensitivity of thermal pulse flowmeter detects turbulence, eddies and changes in the flow field that develop over time

Displaying the fractures

- Histogram graphical display of frequency distribution

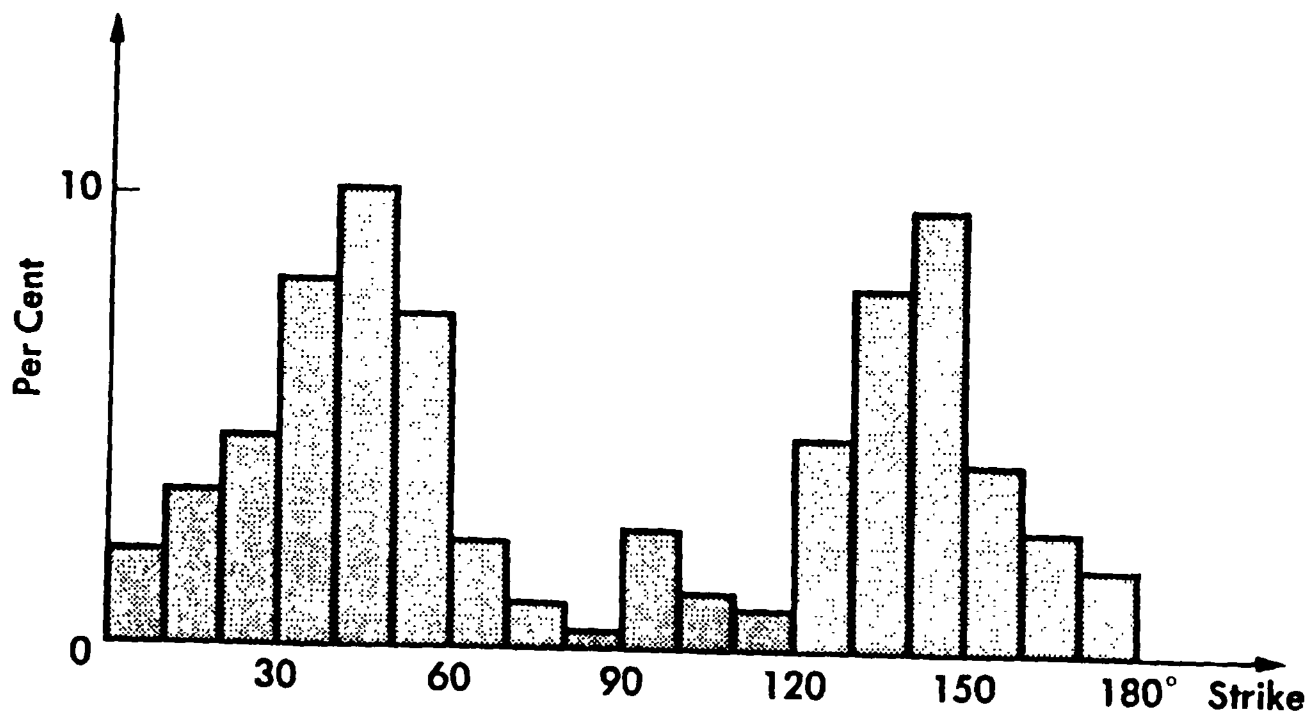

From Dennis (1972)

Displaying the fractures (cont'd.)

- Rose diagram
  - A specific type of histogram with circular or semi-circular shape for displaying a frequency distribution in relation to compass bearings

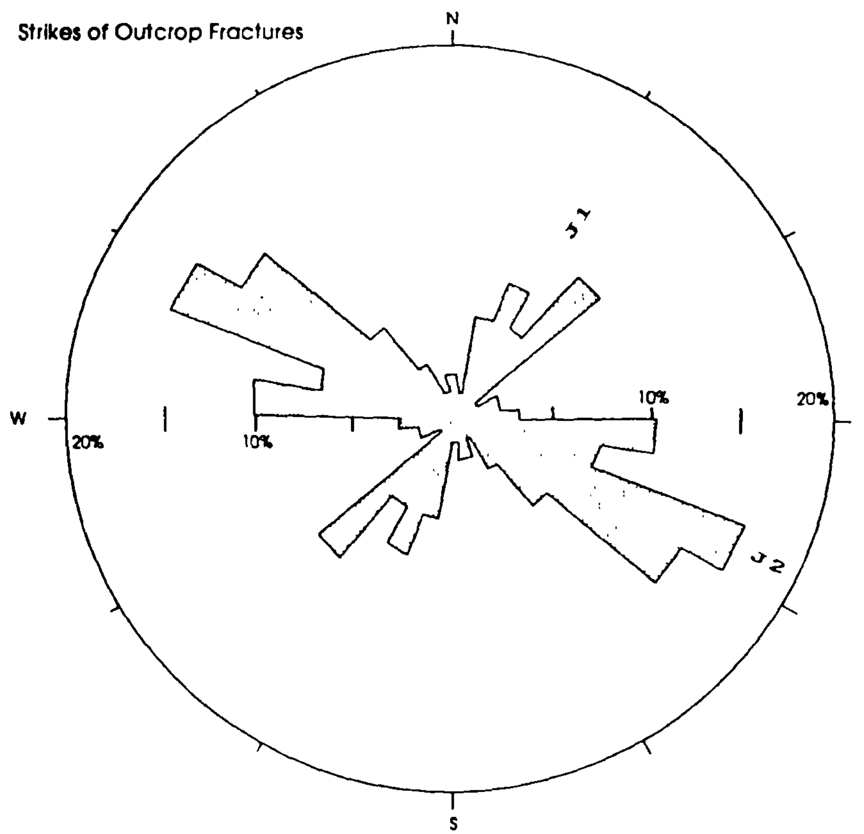

From Alfano (1993)

Displaying the fractures (cont'd.)

- Rose diagrams represent 2 dimensional features
- Stereonets allow the representation of features in 3 dimensions

Stereonet

- There are equal area (Schmidt) and equal angle (Wulff) stereonets

- The equal area stereonet is used for fracture analysis

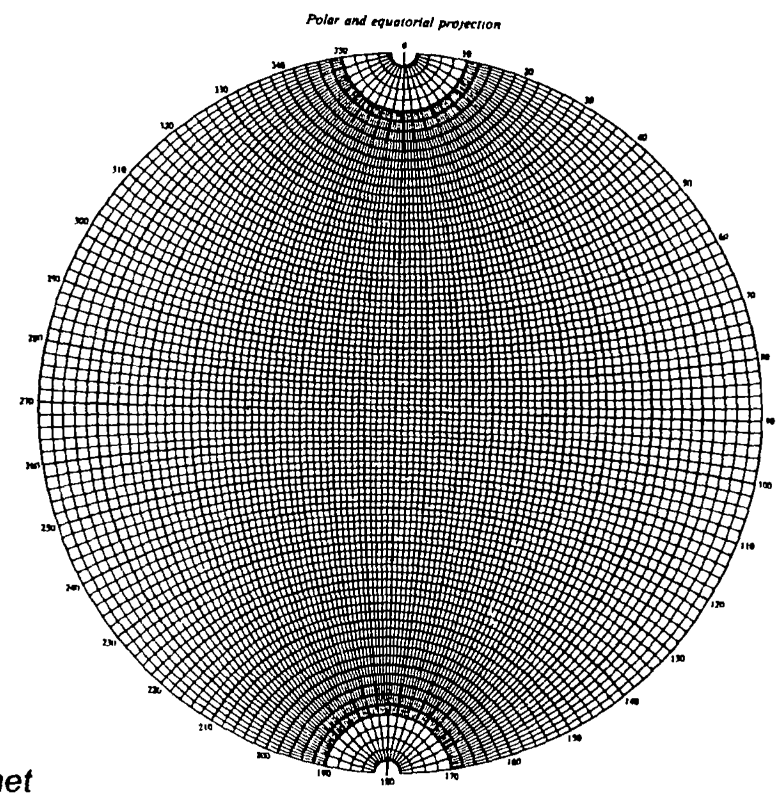

Equatorial equal -angle net

Stereonet (cont'd.)

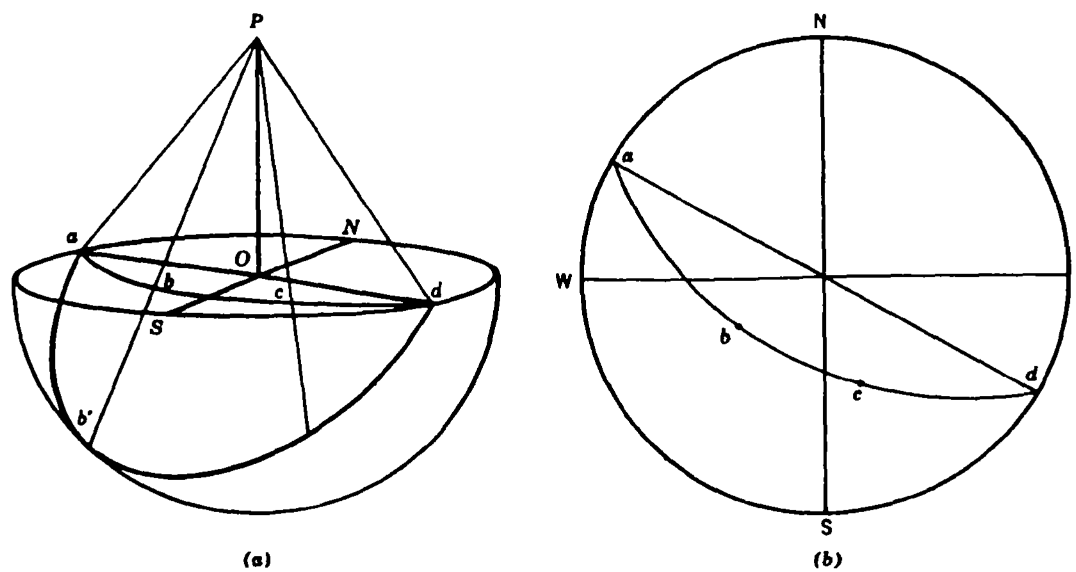

Stereographic projection of an inclined plane. (a) Projection to the horizontal equatorial plane. (b) Corresponding stereogram. (After Phillips, 1971. From Ragan, 1973)

- Planes (fracture, bedding planes, foliation) are represented as curved lines

Stereonet (cont'd.)

- When there are a lot of fracture it is convenient to plot the "poles" to the fractures
- Poles are a line perpendicular to the fracture plane. When the pole is projected on the stereonet it is represented by a point
- The pole is 90^0 from the curved line representing the fracture

Stereonet (cont'd.)

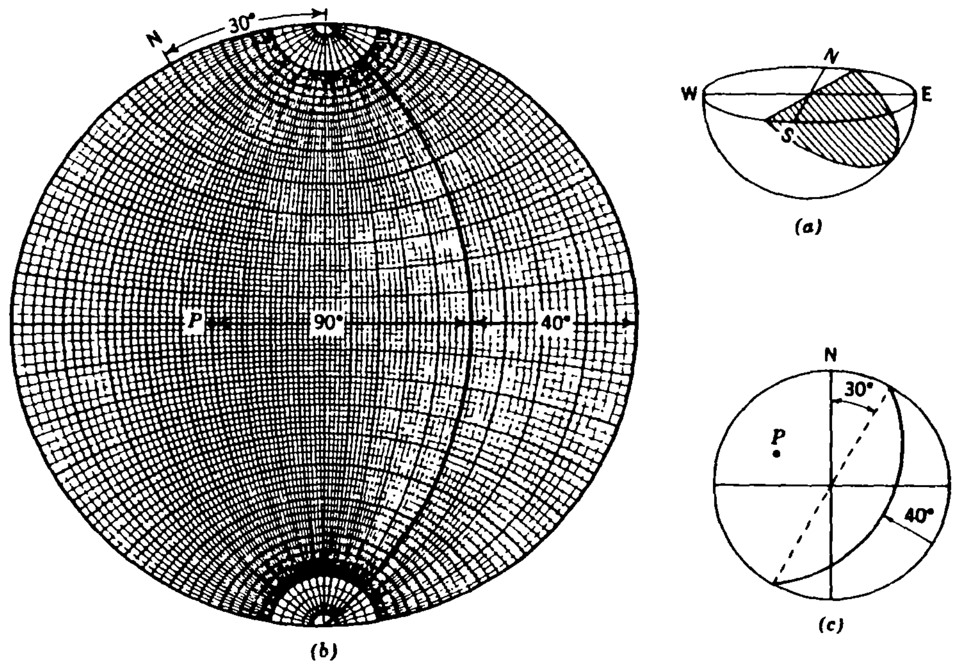

From Ragan (1973)

Stereonet (cont'd.)

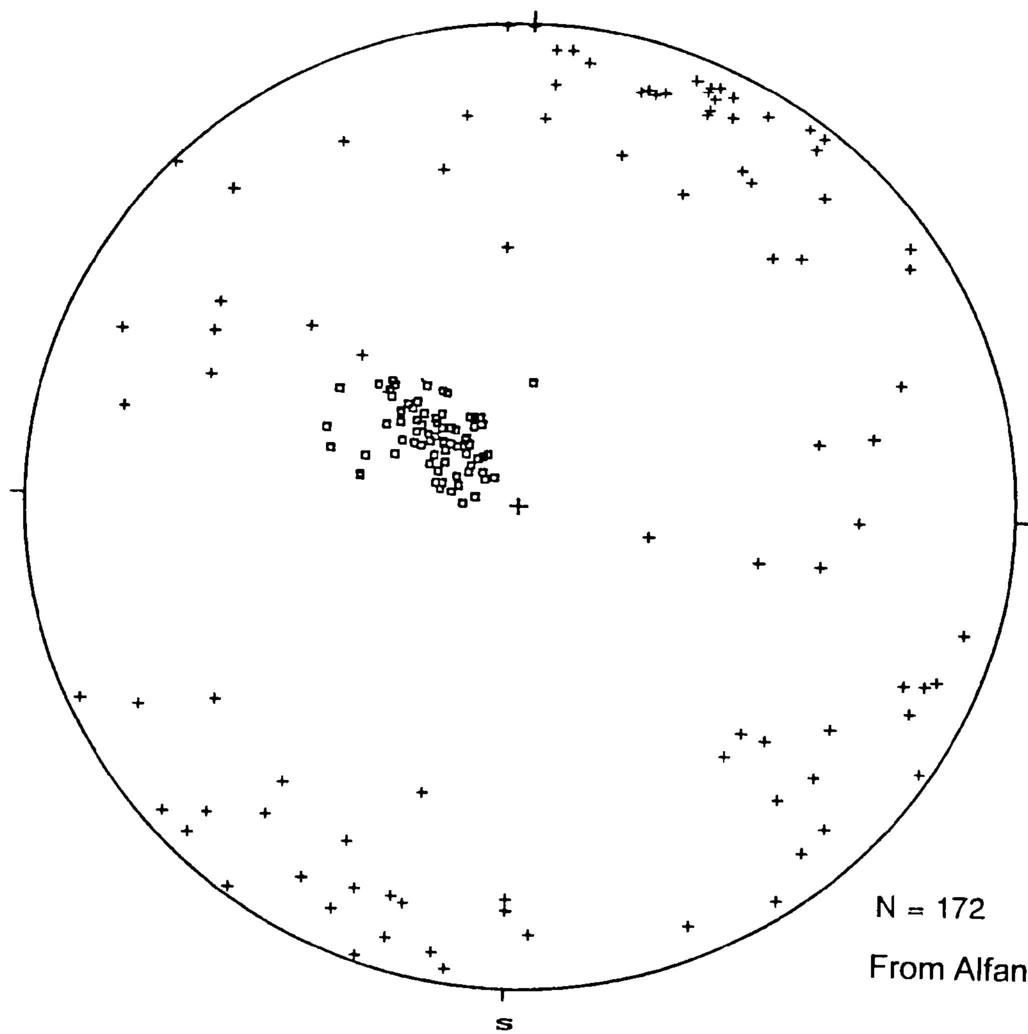

N = 172

From Alfano (1993)

Stereonet (cont'd.)

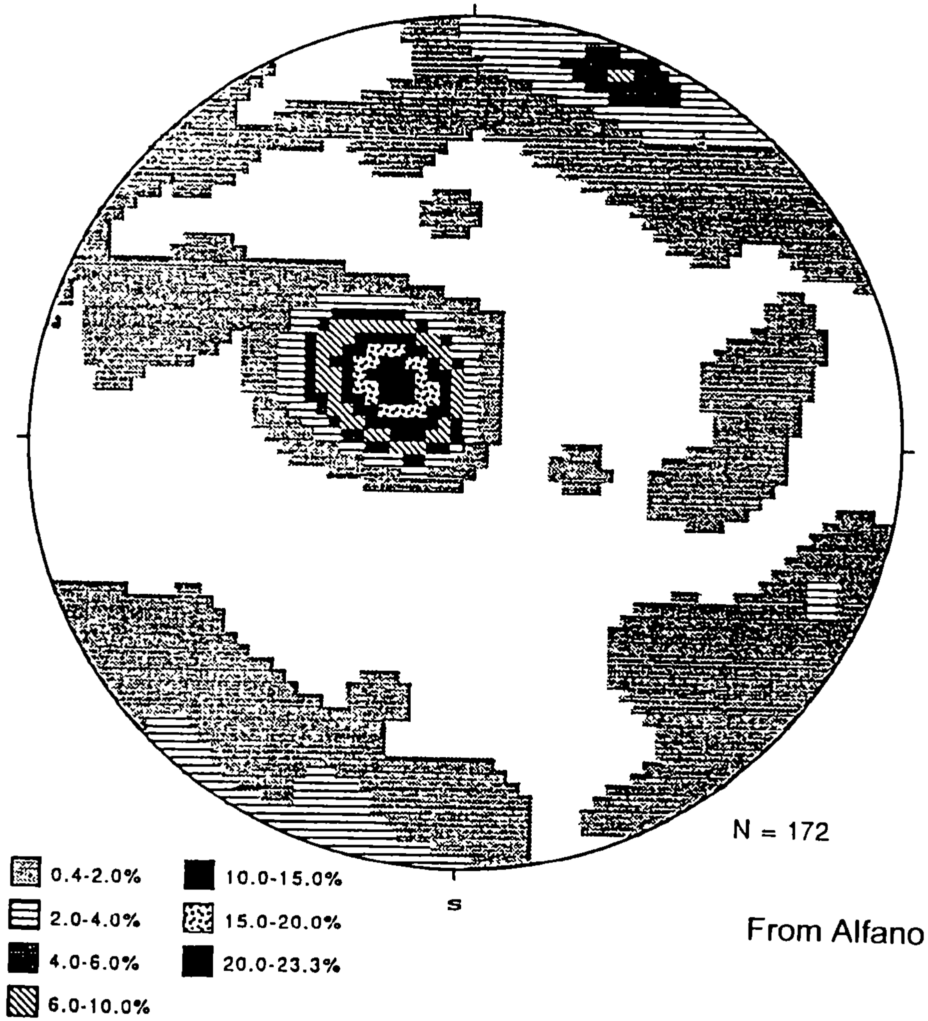

From Alfano (1993)

- Use a Kalsbeek counting net for contouring

Stereonet (cont'd.)

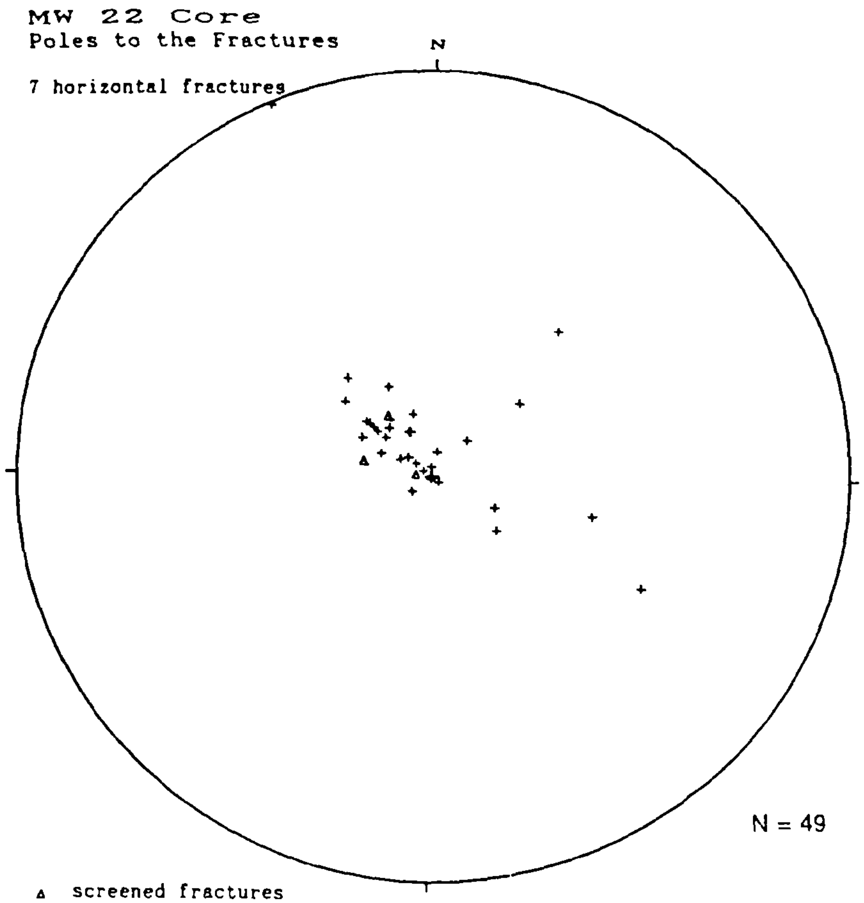

From Alfano (1993)

Stereonet (cont'd.)

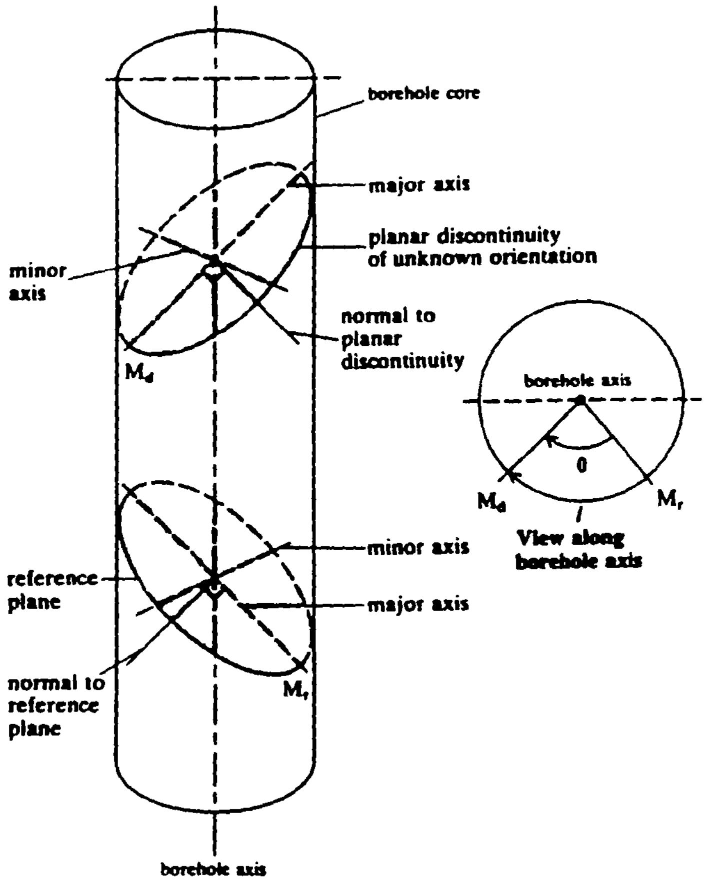

From Priest (1985)

Stereonet (cont'd.)

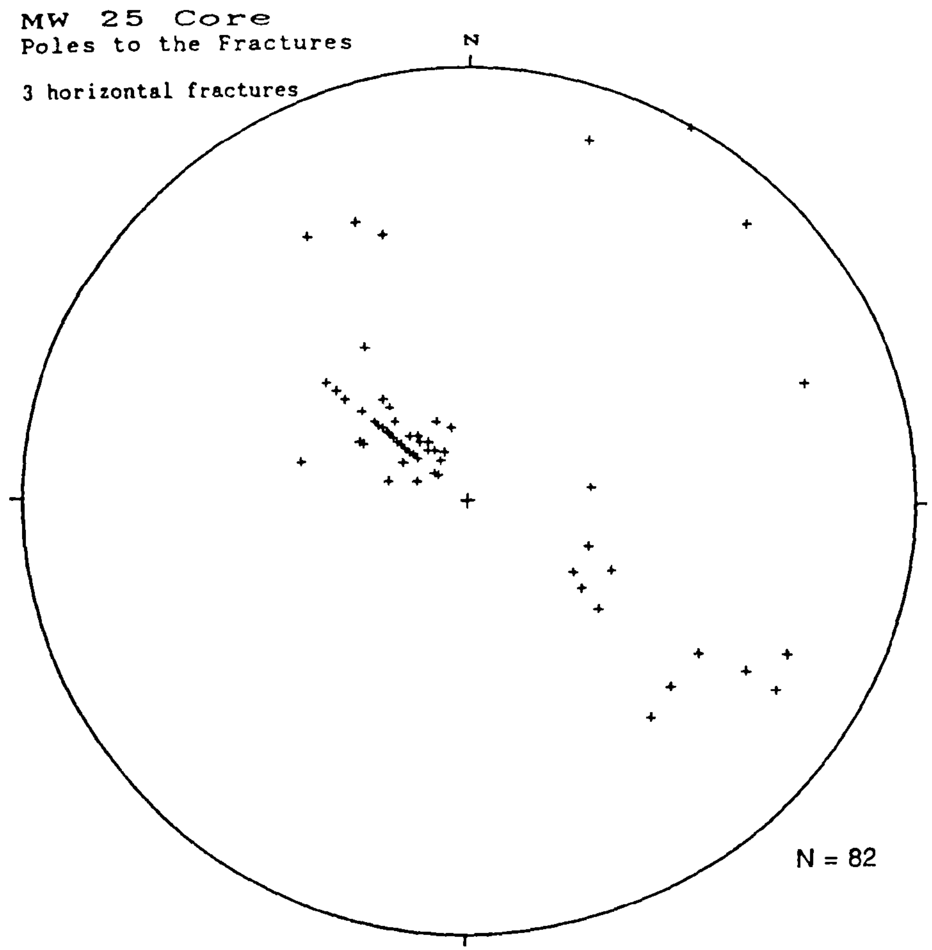

From Alfano (1993)

Stereonet (cont'd.)

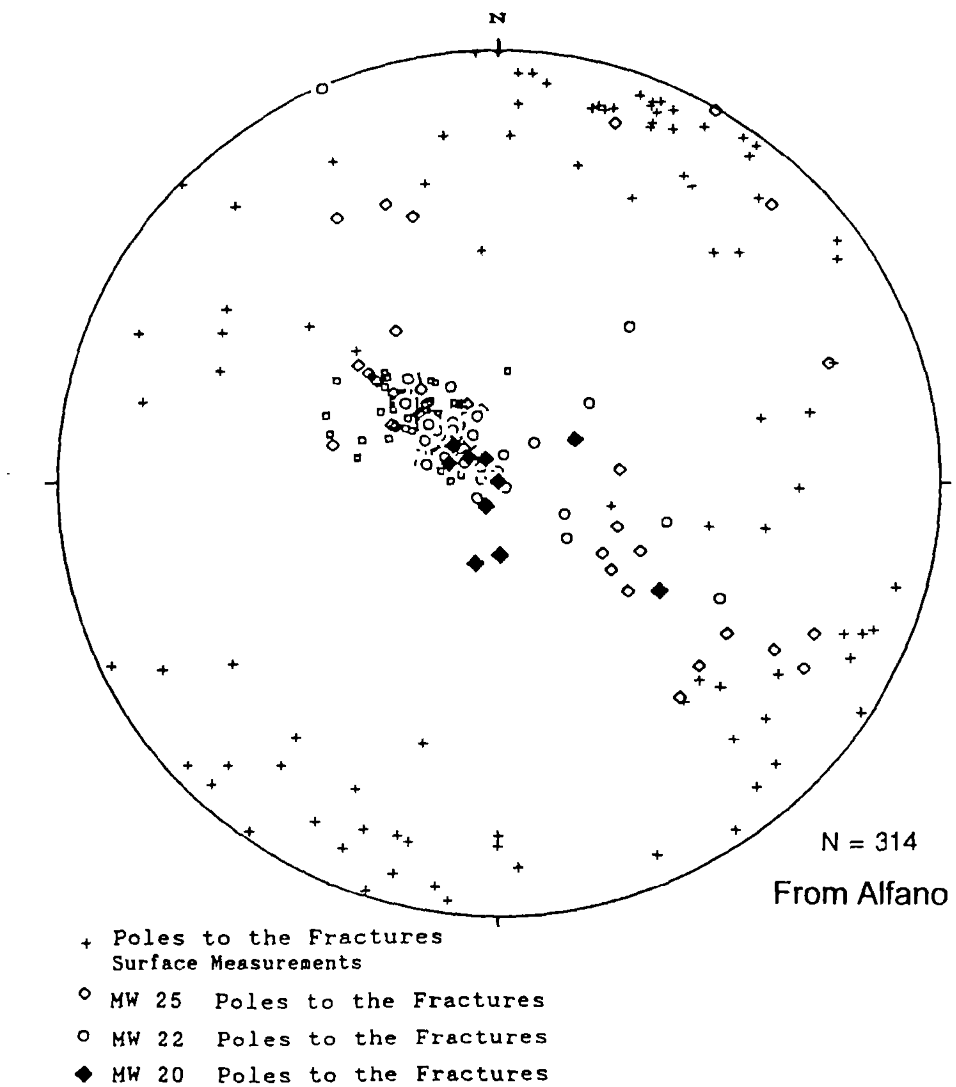

From Alfano (1993)

Hydrogeology

Fractured rock aquifer systems

- Fractured rock aquifer systems can have three or more layers with different hydraulic characteristics (e.g. hydraulic conductivity, storage, porosity)

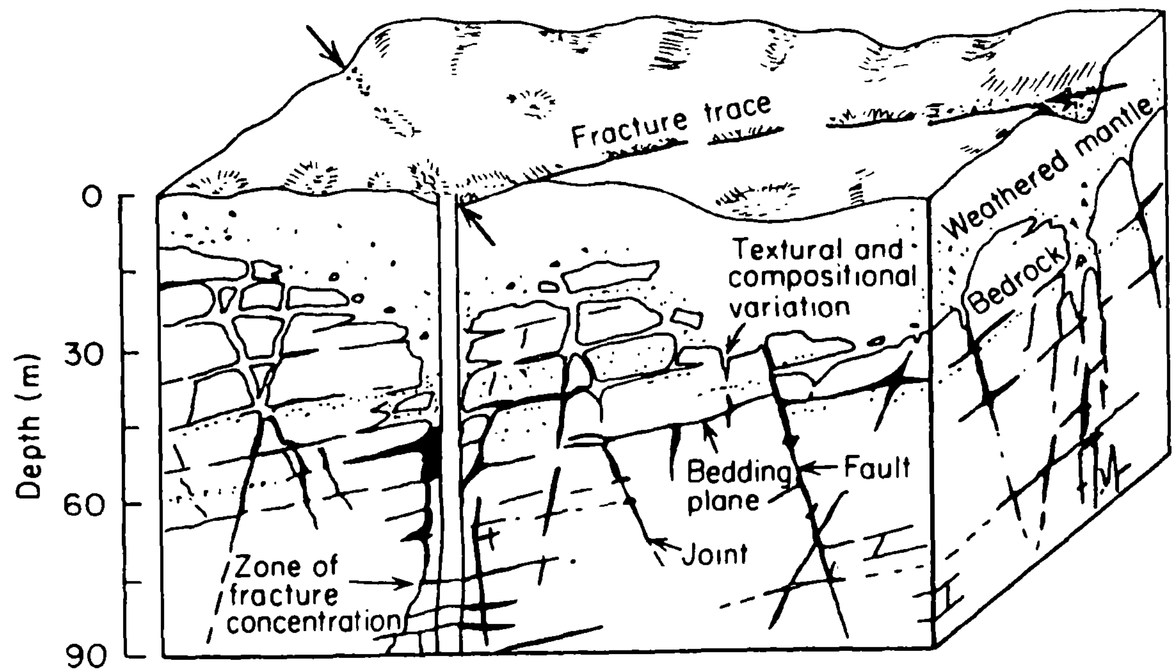

(After Lattman and Parizek, 1964. From Freeze and Cherry, 1979)

Fracturedrock aquifer systems (cont'd.)

- Shales, metamorphic and igneous rocks are impermeable for all practical purposes unless they are fractured
- Sandstone and limestones can have primary porosity
- Fracture density and size typically increase as you approach the bedrock surface

Fractured rock aquifer systems (cont'd.)

- Bedrock transitions into the partially weathered rock (PWR) which is typically highly fractured and has increased rock matrix porosity from weathering

- PWR zone is usually the thinnest layer but can be the most permeable

Fractured rock aquifer systems (cont'd.)

- The PWR grades into the weathered residual soil (residuum)
- The weathered residuum from igneous and metamorphic rock is called saprolite when it retains the original rock fabric (layering)

Fractured rock aquifer systems (cont'd.)

- The transition from bedrock to PWR or PWR to saprolite is more abrupt if associated with a horizontal (low angle) fracture zone
- Boulders of competent bedrock are found in the weathered residuum — floaters

Fractured rock aquifer systems (cont'd.)

- Monitoring wells are needed in all layers of a fractured rock aquifer system to determine the hydraulic interaction of the layers
- Upward or downward hydraulic gradients can exist between them

Fractured rock aquifer systems (cont'd.)

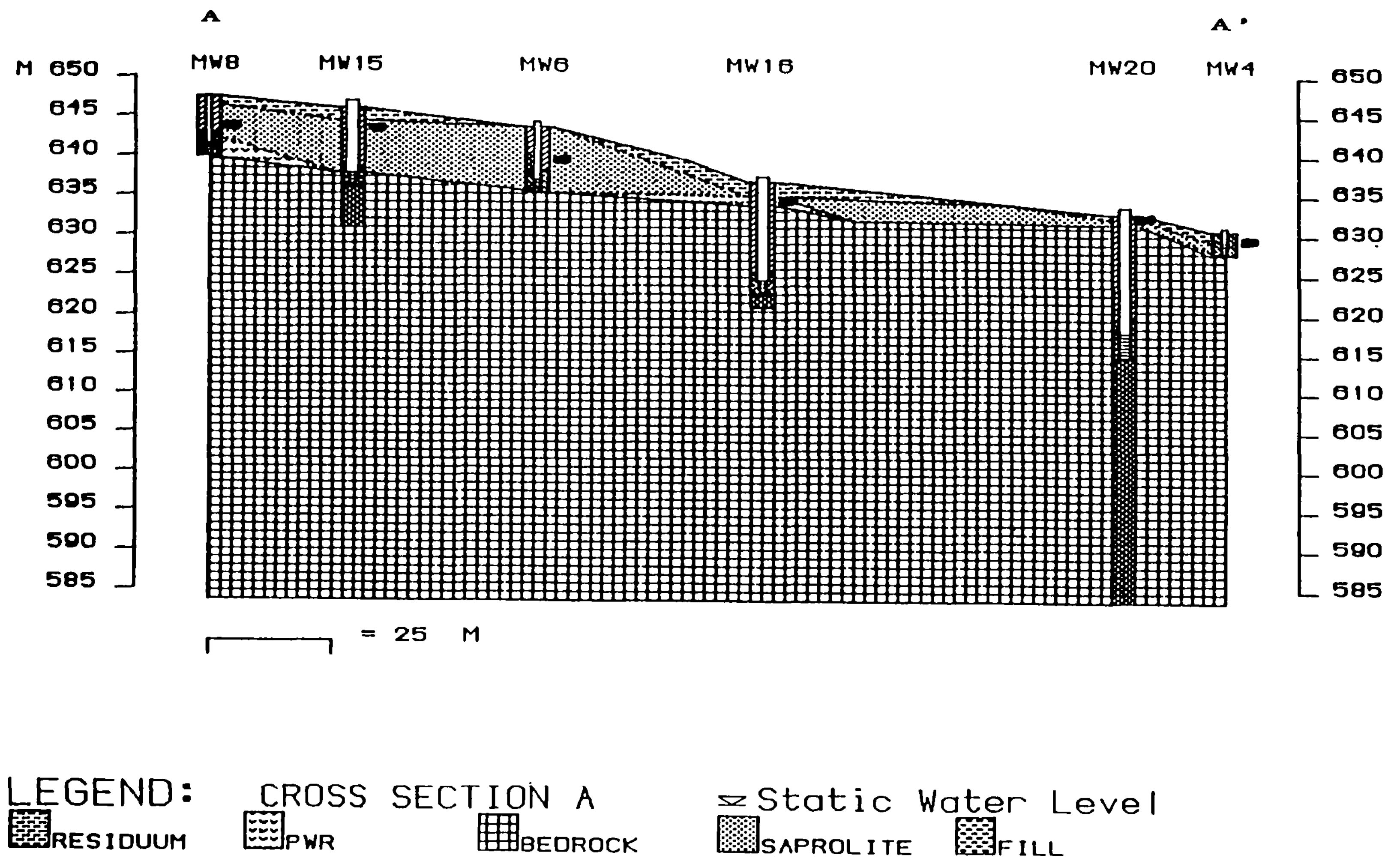

From Alfano (1993)

Fractured rock aquifer systems (cont'd.)

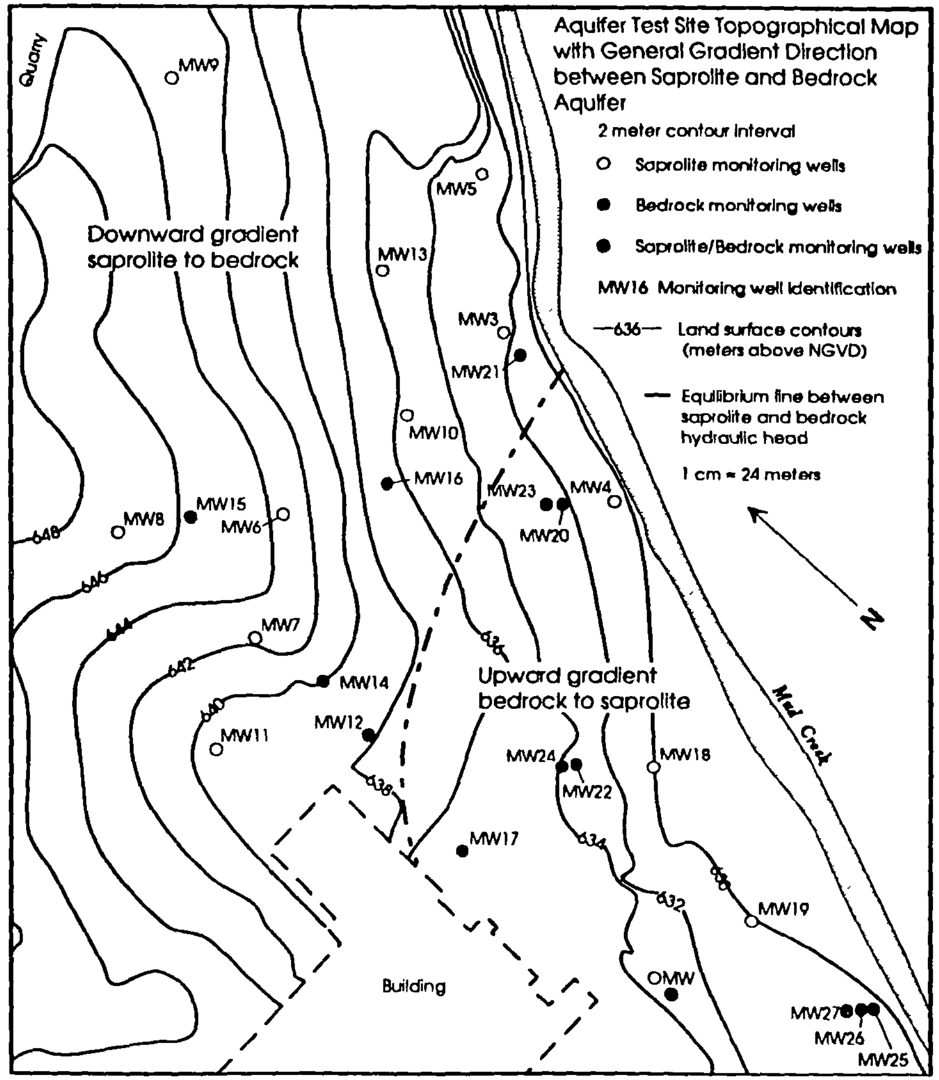

From Alfano (1993)

Where to locate monitoring wells

- In lineaments identified from aerial photographs
- Bedrock surface maps and overburden thickness maps are useful for locating depressions in the bedrock surface that can indicate a high angle fracture zone (joints)

Where to locate monitoring wells (cont'd.)

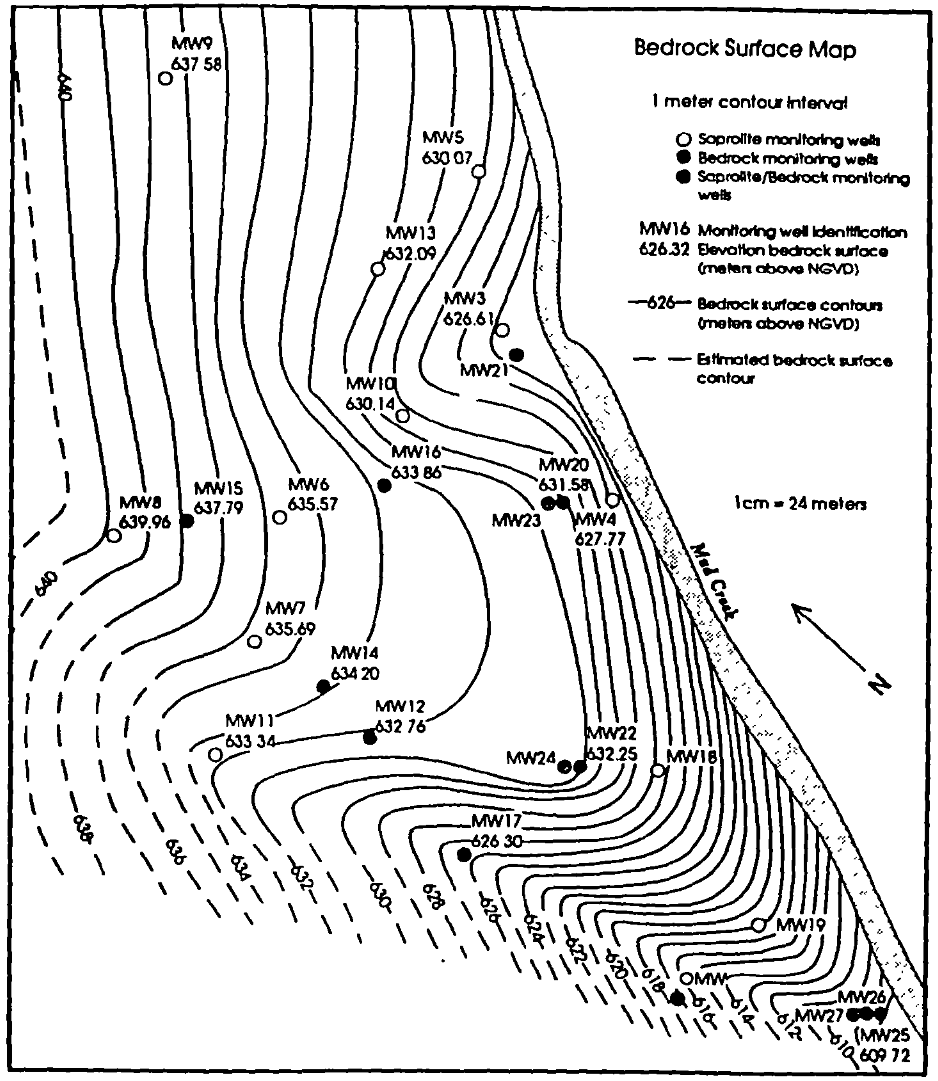

From Alfano (1993)

Where to locate monitoring wells (cont'd.)

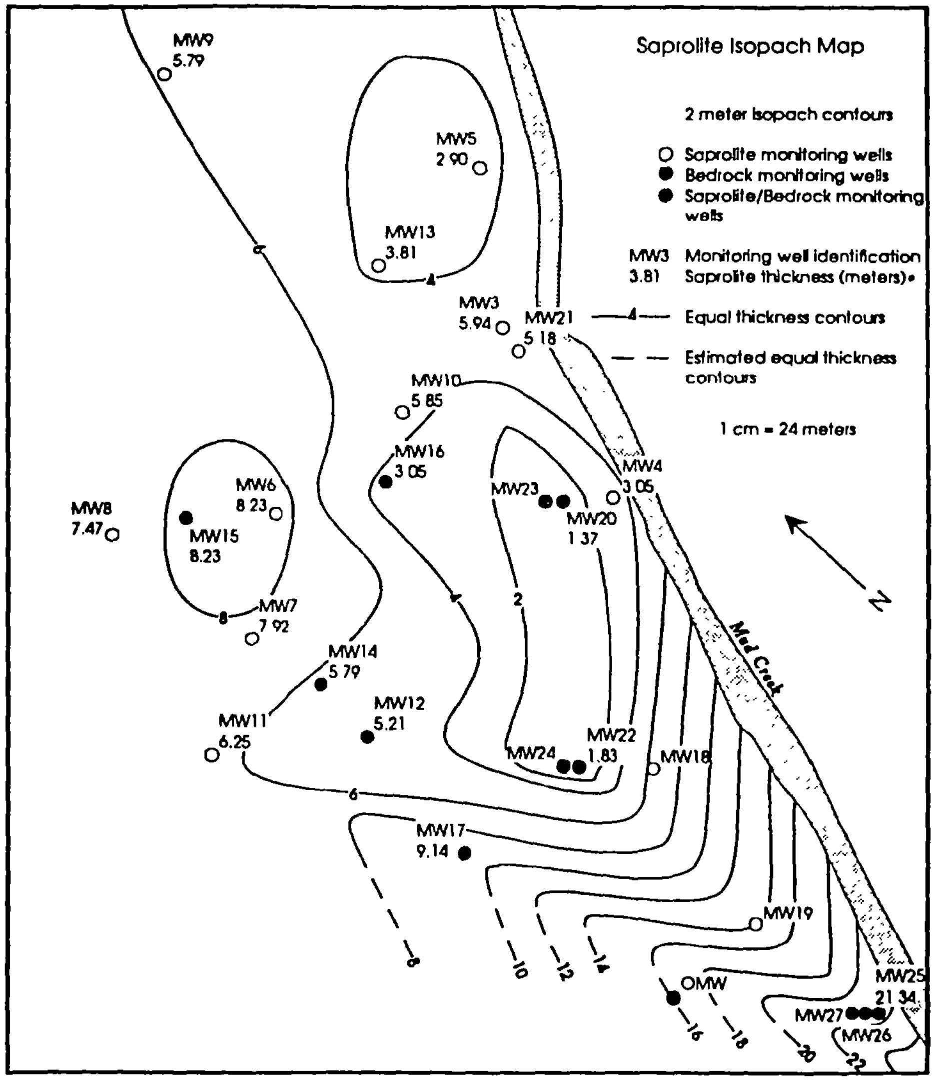

From Alfano (1993)

Where to locate monitoring wells (cont'd.)

- Extrapolation from nearby outcrops. Good for high angle and low angle fractures

- Horizontal (low angle) fracture are much easier to hit with a borehole

Potentiometric surface maps

- Only monitoring wells screened entirely in the fractured bedrock are used to produce a potentiometric surface map and *only* if it is proved that they are interconnected

- Pump a bedrock well and observe the response in the other bedrock monitoring wells

- Separate fracture systems are treated as separate flow systems

- Open borehole bedrock wells run the risk of connecting formerly unconnected fracture systems allowing contamination or DNALPs into uncontaminated portion of the bedrock aquifer

Potentiometric surface maps (cont'd.)

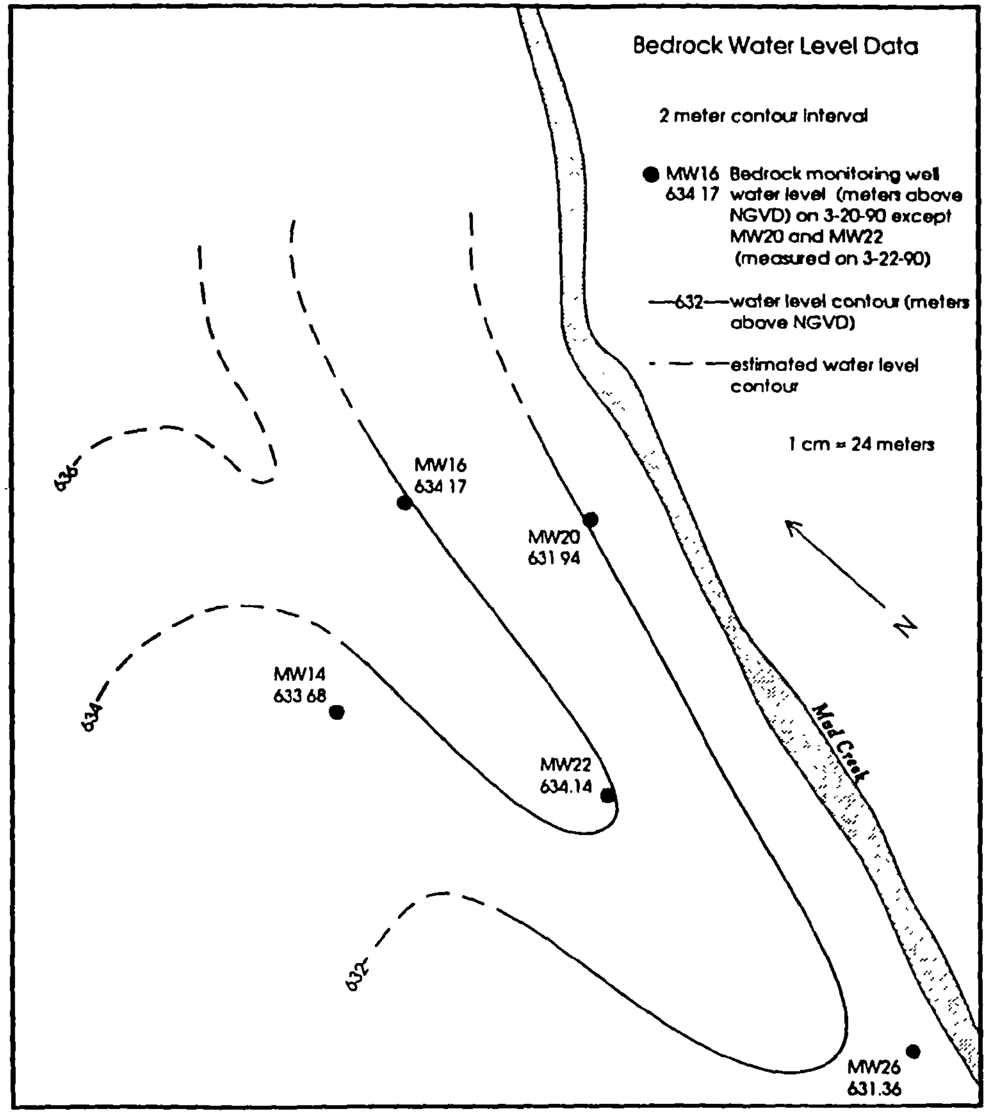

From Alfano (1993)

Potentiometric surface maps (cont'd.)

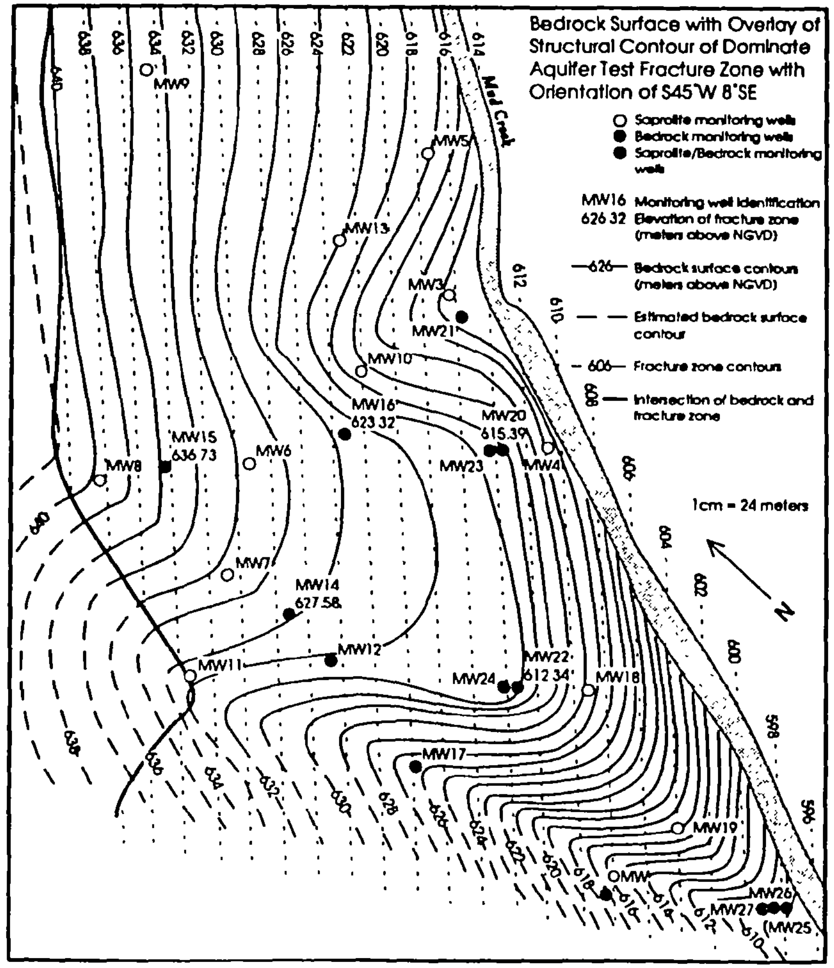

From Alfano (1993)

Potentiometric surface maps (cont'd.)

- Strictly speaking, a potentiometric surface map represents horizontal flow only so wells used to produce it should be screened at approximately the same elevation

- Monitoring wells located along a dipping fracture zone are not measuring horizontal flow but flow along a fracture zone. This information is useful but not a potentiometric surface map by definition

- Know what the water level measurements in fractured rock aquifer are showing you

- Distinguish between true horizontal flow and flow through discrete fracture zones

Anisotropy in fractured rock aquifers

- Weathered overburden aquifers are typically considered homogeneous isotropic so that groundwater flow (q) is in the same direction as hydraulic gradient (J)

Anisotropy in fractured rock aquifers (cont'd.)

- Fractured bedrock aquifers are often anisotropic so flow is usually not in the same direction as hydraulic gradient

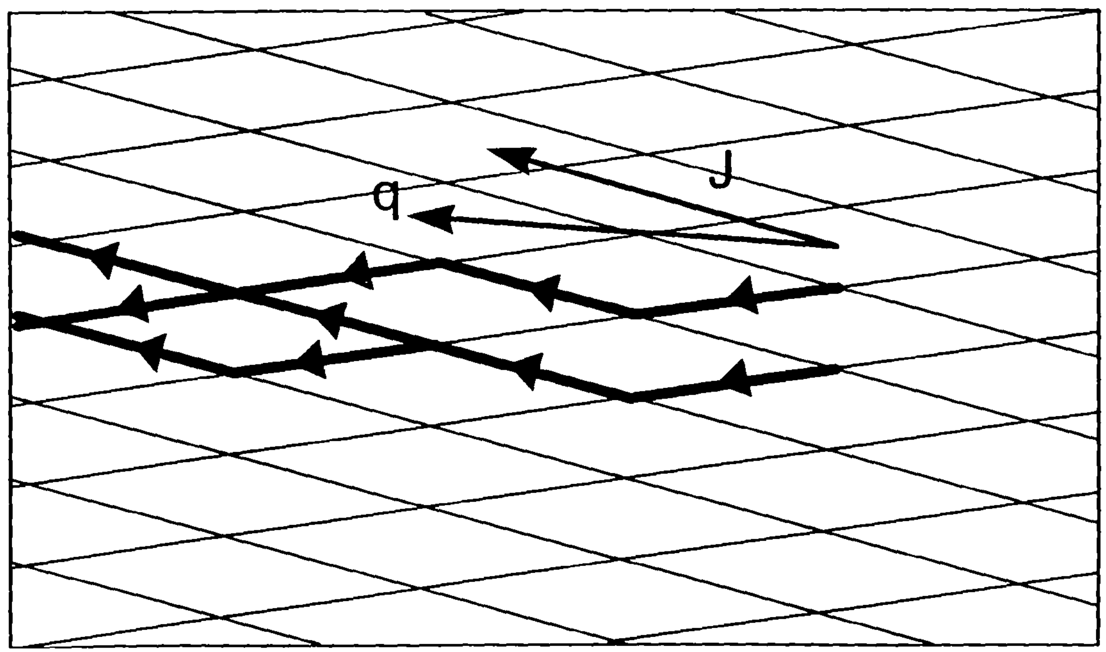

Anisotropy in fractured rock aquifers (cont'd.)

- When a single well is pumped in a homogenous isotropic aquifer the cone of depression forms a circle

- When a single well is pumped in an anisotropic aquifer the cone of depression forms an ellipse

Directional transmissivity

- A vector has magnitude and direction

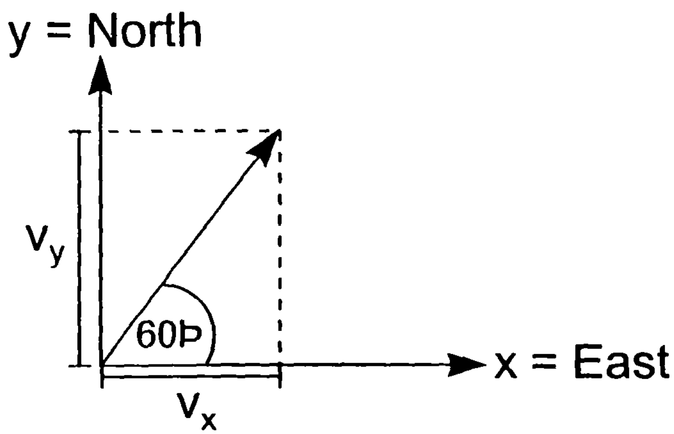

$\bar{v}$ direction N 30° E
$|\bar{v}|$ magnitude 5.0 m/sec.

$$v_x = |\bar{v}| \cos\theta$$
$$v_y = |\bar{v}| \sin\theta$$

$$v_x = 5 \cos 60^0 = 2.5 \text{ m/sec}$$
$$v_y = 5 \sin 60^0 = 4.3 \text{ m/sec}$$

$$|\bar{v}| = \begin{bmatrix} v_x \\ v_y \end{bmatrix} = \begin{bmatrix} |\bar{v}| \cos 60^0 \\ |\bar{v}| \sin 60^0 \end{bmatrix} = \begin{matrix} 2.5 \text{ m/sec} \\ 4.3 \text{ m/sec} \end{matrix}$$

Directional transmissivity (cont'd.)

θ = angle counterclockwise from x-axis

$\theta = \arctan \frac{v_y}{v_x}$ if θ lies in quadrants 1 and 4

$\theta = \arctan \frac{v_y}{v_x} + 180$ if θ lies in quadrants 2 and 3

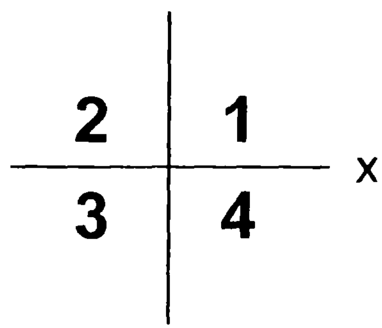

Directional transmissivity (cont'd.)

- Magnitude of vector is

$$|\bar{v}| = \sqrt{v_x^2 + v_y^2}$$

$$|\bar{v}| = \sqrt[3]{v_x^2 + v_y^2 + v_z^2}$$

- Unit vector (e)

$$e = \frac{\bar{v}}{|\bar{v}|} = \begin{bmatrix} \cos\theta \\ \sin\theta \end{bmatrix}$$

$$e = \frac{\bar{v}}{|\bar{v}|} = \frac{\text{Magnitude and direction}}{\text{Magnitude}}$$

e = Magnitude at 1 and direction

Directional transmissivity (cont'd.)

- Anisotropic aquifer — groundwater flow $\bar{q}$ is not in the same direction as the hydraulic gradient $\bar{J}$ except in the direction of the Principal Hydraulic Conductivity Directions

- $T_d(\theta)$ is the ratio between the magnitude of the groundwater flow to the component of hydraulic conductivity J in the direction of q

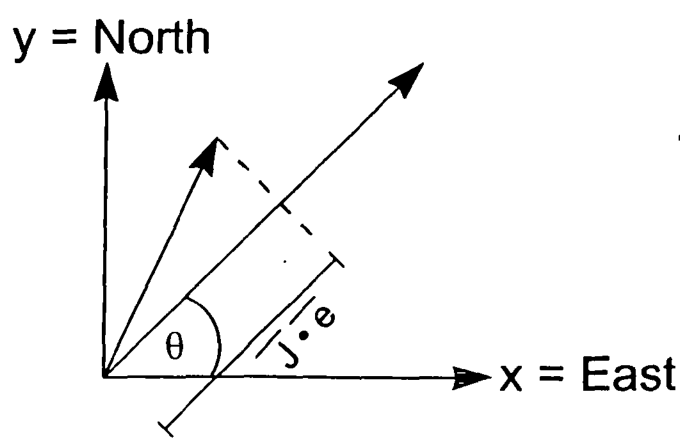

$$T_d\,(\theta) = \frac{|\bar{q}|}{\bar{J} \bullet \bar{e}}$$

Directional transmissivity (cont'd.)

- A unit vector $\overline{e}$ in the direction of $\overline{q}$ is

$$e = \begin{bmatrix} \cos\theta \\ \sin\theta \end{bmatrix}$$

- Groundwater flow $\overline{q}$ can be written

$$\frac{\overline{q}}{|\overline{q}|} = \begin{bmatrix} \cos\theta \\ \sin\theta \end{bmatrix}$$

$$\overline{q} = \underbrace{|\overline{q}|}_{\text{Magnitude}} \; \underbrace{\overline{e}}_{\text{Unit vector}} = |\overline{q}| \begin{bmatrix} \cos\theta \\ \sin\theta \end{bmatrix}$$

Directional transmissivity (cont'd.)

- The component of the hydraulic gradient $\bar{J}$ in the direction of the gradient flow $\bar{q}$ is the dot product of $\bar{J}$ with unit vector $\bar{e}$

$$\bar{J} \bullet \bar{e} = \begin{bmatrix} J_x \\ J_y \end{bmatrix} \bullet \begin{bmatrix} \cos\theta \\ \sin\theta \end{bmatrix} = J_x \cos\theta + J_y \sin\theta$$

θ = angle between x-axis and $\bar{q}$

Directional transmissivity (cont'd.)

$$T_d(\theta) = \frac{\left|\bar{q}\right|}{\bar{J} \bullet \bar{e}}$$

$$T_d(\theta) = \frac{\left|\bar{q}\right|}{J_x \cos\theta + J_y \sin\theta}$$

Directional transmissivity (cont'd.)

- Another way to write the directional transmissivity is as a tensor

$$\bar{q} = \begin{bmatrix} T_{xx} & T_{xy} \\ T_{yx} & T_{yy} \end{bmatrix} \bar{J}$$

symmetrical tensor

$T_{xy} = T_{yx}$

$$\underline{\begin{matrix} q_x \\ q_y \end{matrix}} = \begin{bmatrix} T_{xx} & T_{xy} \\ T_{yx} & T_{yy} \end{bmatrix} \begin{bmatrix} J_x \\ J_y \end{bmatrix}$$

Directional transmissivity (cont'd.)

- Values for Txx, Tyy, Txy are obtained from aquifer testings

$$\bar{T} = \begin{bmatrix} 7 & 5 \\ 5 & 3 \end{bmatrix}$$

$T_{xx} = 7$ m/sec

$T_{yy} = 3$ m/sec

$T_{xy} = T_{yx} = 5$ m/sec

Directional transmissivity (cont'd.)

- You know hydraulic gradient ($\bar{J}$) from potentiometric surface map can find groundwater flow

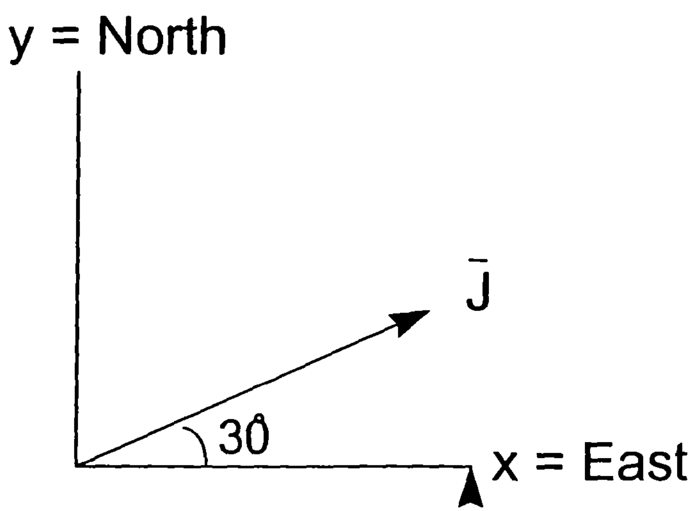

$\bar{J}$ = N 60 E or $\theta = 30°$

$|\bar{J}|$ magnitude is gradient $= .5$

$J_x = |\bar{J}| \cos 30°$ $\qquad$ $J_y = |\bar{J}| \sin 30°$

$J_x = .5 \cos 30°$ $\qquad$ $J_y = .5 \sin 30°$

$J_x = .43$ $\qquad$ $J_y = .25$

$$\bar{J} = \begin{bmatrix} J_x \\ J_y \end{bmatrix} = \begin{bmatrix} .43 \\ .25 \end{bmatrix}$$

Directional transmissivity (cont'd.)

- Groundwater flow discharge per unit width $\bar{q}$ induced by the hydraulic gradient $\bar{J}$ is

$$\frac{q_x}{q_y} = \begin{bmatrix} T_{xx} & T_{xy} \\ T_{yx} & T_{yy} \end{bmatrix} \begin{bmatrix} J_x \\ J_y \end{bmatrix}$$

Directional transmissivity (cont'd.)

- Matrix multiplication

$$\begin{bmatrix}7 & 5\\ 5 & 3\end{bmatrix}\begin{bmatrix}.43\\ .25\end{bmatrix} = \begin{bmatrix}7(.43)+5(.25\\ 5(.43)+3(.25\end{bmatrix}$$

$2 \times 2 \quad 2 \times 1$

can do

$$= \begin{bmatrix}3.01+1.25\\ 2.15+.75\end{bmatrix}$$

$$= \begin{bmatrix}4.3\\ 2.9\end{bmatrix}$$

Directional transmissivity (cont'd.)

$$\bar{q} = \bar{T}\bar{J}$$

$$\bar{q} = \begin{bmatrix} \bar{q}x \\ qy \end{bmatrix} = \begin{bmatrix} 4.3 \\ 2.9 \end{bmatrix} \begin{matrix} m/se \\ m/se \end{matrix}$$

$$|\bar{q}| = \sqrt{(4.3)^2 + (2.9)^2}$$

$$|\bar{q}| = \sqrt{26.9}$$

$$|\bar{q}| = 5.2 m/sec$$

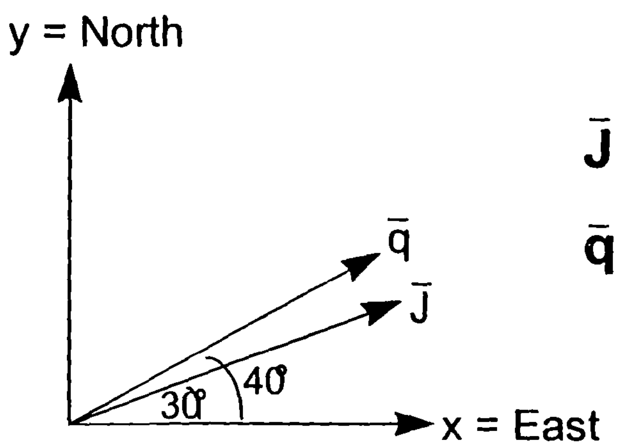

Direction:

$$\theta = \arctan\frac{q_y}{q_x}$$

$$\theta = \arctan\frac{2.9}{4.3}$$

$$\theta = 40^{\circ}$$

$\bar{J}$ = 0.5 @ N 60^0 E

$\bar{q}$ = 5.2 m/sec @ N 50^0 E

Graphical method to estimate difference between groundwater flow (q) and hydraulic gradient (J)

From Freeze and Cherry (1979)

K_x = maximum hydraulic conductivity axis

K_z = minimum hydraulic conductivity axis

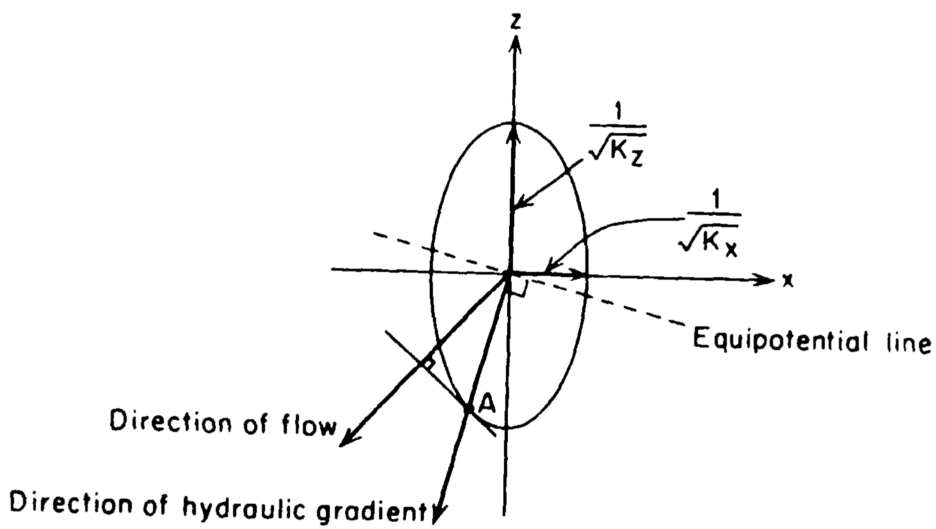

Determination of direction of flow in an anisotropic region with K_x/K_z = 5. Freeze and Cherry (1979)

Does groundwater and contaminants flow under the stream?

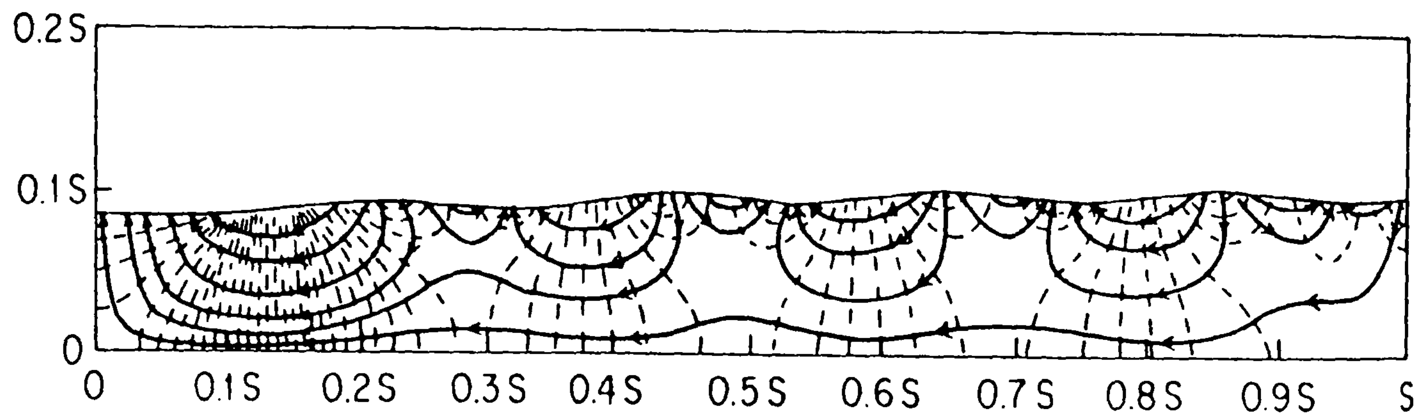

Regional and local flow. Freeze and Cherry (1979)

Does groundwater and contaminants flow under the stream (cont'd.)?

- Most likely to occur in area of regional faulting where significant fracture zones exist at depth

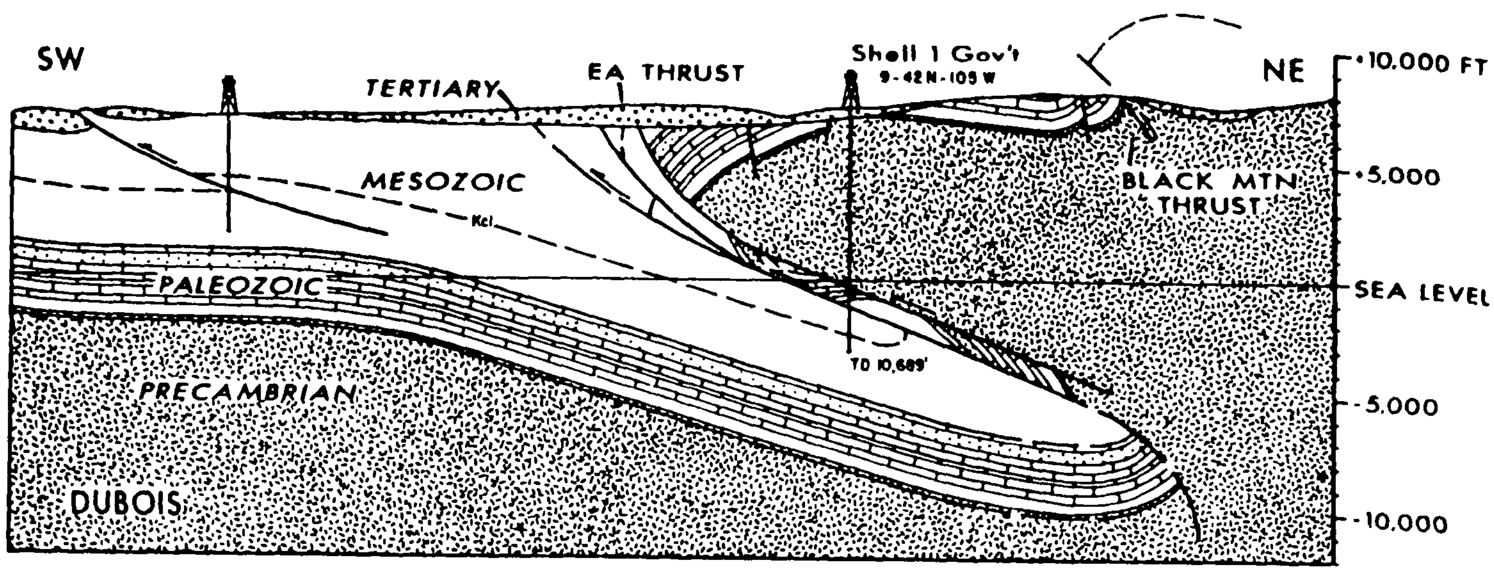

From Berg, 1962 & Dennis, 1972

Mathematical Models for Determining the Hydraulic Properties of Fractures and Fractured Rock Bodies

- Two approaches:
  - Discrete modeling
  - Equivalent porous medium modeling

Discrete model

- The equation for one-dimensional flow through a single fracture is:

$$q = K_f \frac{dh}{dx}$$

q = volume of flow per unit of time per unit length of the cross-sectional area of the fracture (b x w) with w = 1, (L/T)

K_f = hydraulic conductivity of the fracture, (L/T)

dh/hx = hydraulic head gradient, (no units)

Cubic law

$$\frac{Q}{bw} = \frac{b^2 \rho g}{12\,\mu}\frac{dh}{dx}$$

$$\frac{Q}{w} = \frac{b^3 \rho g}{12\,\mu}\frac{dh}{dx}$$

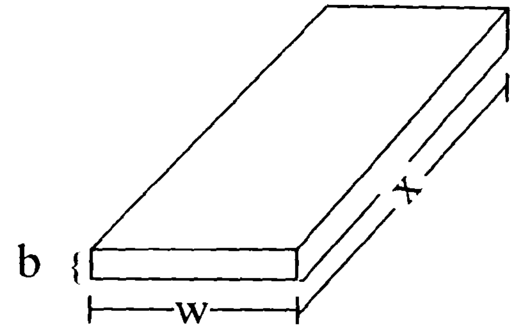

$$q^1 = \frac{b^3 \rho g}{12\,\mu}\frac{dh}{dx}$$

- The hydraulic conductivity of the fracture (K_f) with units of length/time is given by

$$K_f = \frac{b^2 \rho g}{12\,\mu}$$

$$k_f = \frac{b^2}{12}$$

Cubic law (cont'd.)

Q = volume of flow per unit of time, (L^3/T)
q^1 = volume of flow per unit of time per unit width of the fracture (L^2/T)
K = hydraulic conductivity of the fracture, (L/T)
k = permeability of fracture (L^2)
dh/dx = hydraulic head gradient, (no units)
w = unit width of the fracture, (L)
b = thickness of the fracture aperature, (L)
ρ = density of water, (M/L^3)
μ = dynamic viscosity of water, (M/TL)
g = acceleration due to gravity (L/T^2)

Discrete fractures

- For a number (n) of parallel fractures with equal aperture (b) the discharge per unit width is

$$q_1 = Knb\frac{dh}{dx}$$

$$K = n\frac{b^3}{12}\frac{\rho g}{\mu}$$

Discrete fractures (cont'd.)

- If the aperture varies the hydraulic conductivity can be written for the average aperture (b^1)

$$(b^1)^3 = \frac{1}{n}\sum_{i=1}^{n}(b_i)^3$$

$$K = \frac{(b^1)^3}{12}\frac{\rho g}{\mu}$$

Rock mass permeability

- The formulation of a fractured rock mass permeability was produced by Romm and Pozinenko (1963), Snow (1965, 1969), and Bianchi and Snow (1969). The permeability of a rock mass with continuous fractures is described by a second rank tensor. Snow (1969) defined this tensor in relation to a sampling line designated by (D) by

$$k_{ij} = \frac{2}{3} \Sigma \frac{b^3}{|P_i D_i|} (\delta_{ij} - m_{ij})$$

k_{ij} = permeability tensor, (L^2)

b = fracture apertures, (L)

p_i = direction cosines of normal to the fracture planes

D_i = direction cosines of the sampling line

$m_{ij} = p_i p_j$, matrix formed by the direction cosines of the normal to the fractured planes

δ_{ij} = Kronecker's delta which is 1 when i = j and 0 when i not = j

Rock mass permeability (cont'd.)

- The permeability of a rock mass along several sampling lines is determined by summing the permeability tensors of each sampling line.

- Once the permeability tensor is determined, the principal permeability axes are parallel to the eigenvectors and the values of the principal permeability are equal to the eigenvalues

Problems with the discrete model

- These mathematical formulations of fractured rock mass permeability and flow are limited by the assumption of infinite (in relation to the test area) fractures that are continuous in their own plane. In reality, these conditions are only found in small test areas

- The discrete formulae are also limited by the dependence of these equations on the knowledge of fracture aperatures (b). Real fractures do not have constant aperatures and are in contact in some areas and open in others. The aperature values would have to reflect the effective aperature, that is the aperature that allows the passage of water

Problems with the discrete model (cont'd.)

- Fracture apertures are extremely difficult to define in the field. Even measurements of fracture apertures from down-hole televiewers may not represent aperatures away from the borehole
- Not all fractures are interconnected
- Not all fractures conduct water
- Fracture aperature is effected by changes in stress
- Numerical computer models with statistical packages are being developed for these types of analysis

Porous media equivalent models

- SINGLE POROSITY models created for porous granular aquifers
- Theis solutions for confined transient radial flow and modifications for unconfined, leaky confined, and anisotropic aquifers
- DOUBLE POROSITY models for two overlapping continuum. Barenblatt and others (1969)
- Hydraulic conductivity and storage values for the fracture systems
- Different values for the rock matrix blocks

Porous media equivalent models (cont'd.)

- Porous media equivalent models are valid within a representative elemental volume
- The volume of aquifer for which a single value for a parameter (hydraulic conductivity, porosity) is measured with an increase in volume

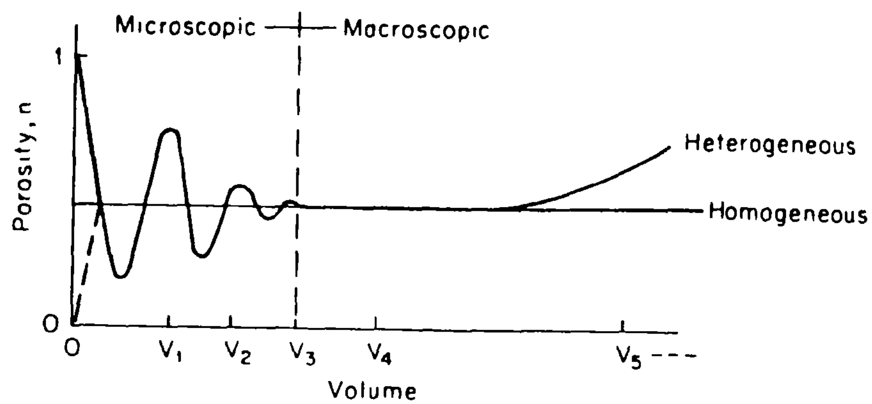

Microscopic and macroscopic domains and the representative elementary volume V3 (after Hubbert, 1956; Bear, 1972)

From Freeze and Cherry (1979)

Fractured rock aquifers as porous media

- Long and others (1982) determined that fractured crystalline rock aquifers behave more like porous media when:
  - The fracture density increases
  - Aperatures are constant rather than distributed
  - Orientations are variable rather than constant
  - Large volumes of rock are tested

- Long and Witherspoon (1985) investigated the influence of fracture length using two-dimensional computer models
  - Fracture length is more important than fracture frequency in the ability of the fracture system to behave like a porous medium
  - Increase in the fracture lengths increase the interconnection of the fracture system

Fractured rock aquifers as porous media (cont'd.)

- The porous behavior of a fracture set is determined by a polar coordinate plot of the square root of the directional hydraulic conductivity $(K(\theta))^{1/2}$
- If $(K(\theta))^{1/2}$ plots as an approximate ellipse then the fracture system is behaving as an equivalent porous medium (Long and Witherspoon, 1985)

Porous media equivalent models (cont'd.)

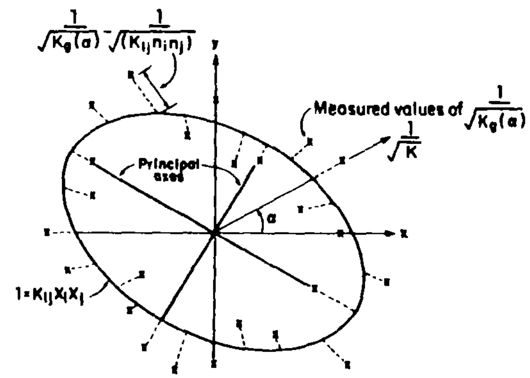

Plot of the measured values of $1/(Kg)^{1/2}$, and the corresponding "best fit" ellipse

From Long and Witherspoon (1985)

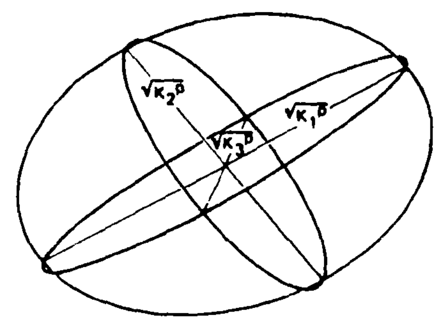

Directional hydraulic conductivity ellipsoid. The semiaxes of the ellipsoid are the square roots of the principal hydraulic conductivities K_1^P, K_2^P and K_3^P

From Hsieh and others (1985)

Porous media equivalent models (cont'd.)

- An equivalent porous medium is described by a symmetrical hydraulic conductivity (K) or transmissivity (T) tensor

$$\bar{q} = K\,\bar{J}$$

$$\begin{bmatrix} q_x \\ q_y \\ q_z \end{bmatrix} = \begin{bmatrix} K_{xx} & K_{xy} & K_{xz} \\ K_{yx} & K_{yy} & K_{yz} \\ K_{zx} & K_{yz} & K_{zz} \end{bmatrix} \begin{bmatrix} J_x \\ J_y \\ J_z \end{bmatrix}$$

- In a symmetrical tensor $K_{yx} = K_{xy}$
  $K_{xz} = K_{xz}$
  $K_{zy} = K_{yz}$

- There are six unknowns in a 3D symmetrical tensor

Single porosity models

- Developed for primary porosity aquifer

  or

- Secondary porosity (fracture) only when matrix permeability is negligible compared to fracture permeability (fractured crystalline rock or shale)

Single porosity models (cont'd.)

Theis assumptions

1. Aquifer is confined by impermeable layers
2. Flow is laminar not turbulent
3. Aquifer is horizontal and only horizontal flow occurs
4. Aquifer is of infinite extent (large in relation to tested area)
5. Pumping well is fully penetrating and fully screened (ensures horizontal flow)

Single porosity models (cont'd.)

Theis assumptions (cont'd.)

6. Pumping well diameter is small (no significant wellbore storage)

7. Aquifer is pumped at a constant rate (Q is constant)

8. Aquifer is of constant thickness

9. Aquifer is Homogeneous and Isotropic

   Homogeneity = Transmissivity or transmissivity tensor is the same everywhere in the aquifer

   Isotropy = Transmissivity value is the same in all three directions

Single porosity models (cont'd.)

- Conditions of horizontal laminar flow in a homogeneous equal thickness aquifer is problematic in fractured rock aquifers
- At best, porous media equivalence solution gives an order of magnitude estimate of aquifer properties
- Use with other methods of investigation (geochemical, geological, and qualitative data)

Fracture system as porous media equivalent

- Confined radial flow — Theis solution log drawdown(s) versus log time (t)

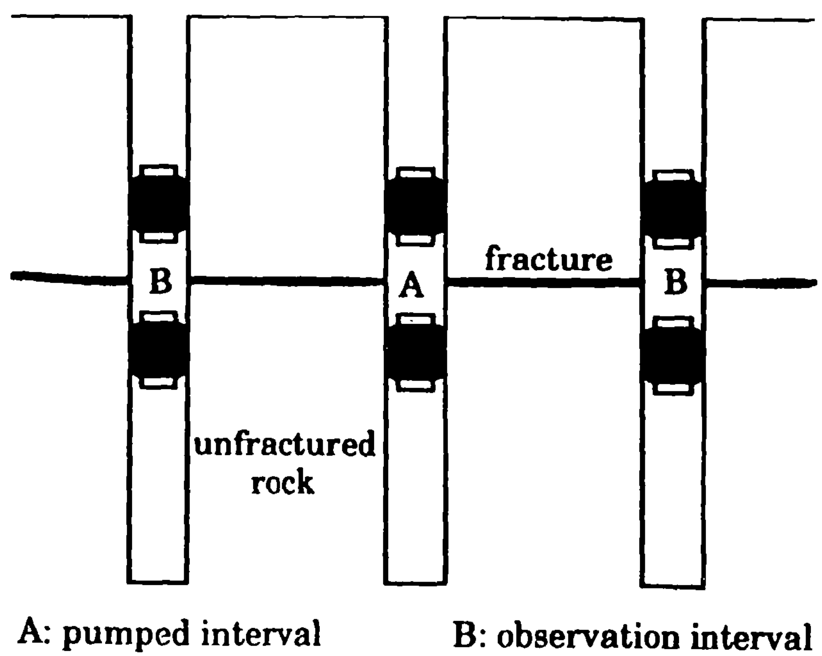

From National Research Council (1996)

Fracture system as porous media equivalent (cont'd.)

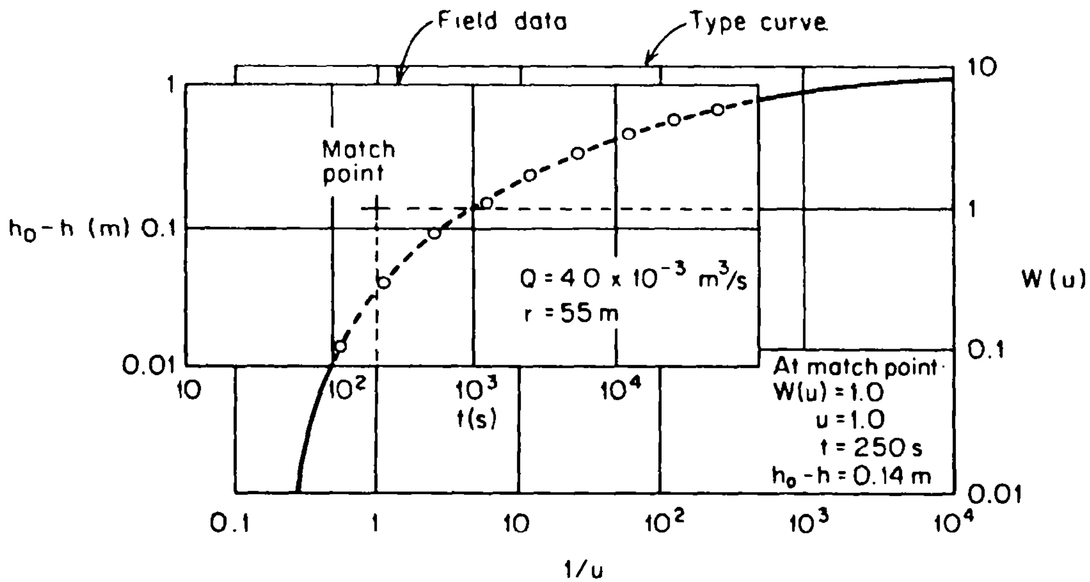

$$T = \frac{QW(u)}{4\pi(h_0-h)} = \frac{(4.0 \times 10^{-3})(1.0)}{(4.0)(3.14)(0.14)} = 0.0023\ \text{m}^2/\text{s}\ \ (15{,}700\ \text{U.S. gal/day/ft})$$

$$S = \frac{4uTt}{r^2} = \frac{(4.0)(1.0)(0.0023)(250)}{(55.0)^2} = 7.5 \times 10^{-4}$$

Determination of T and S from h_0 — h versus t data using the log-log curve-matching procedure and the W(u) versus 1/u-type curve

From Freeze and Cherry (1979)

Fracture system as porous media equivalent (cont'd.)

- Cooper-Jacob straight-line method (1946) drawdown(s) versus log time (t)

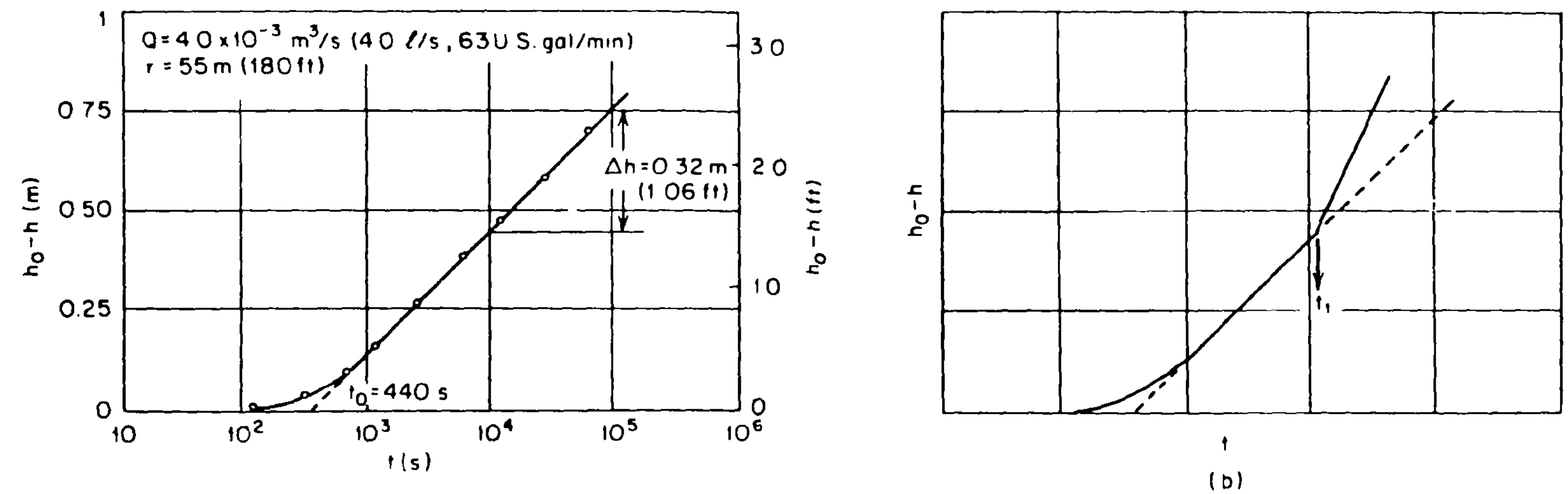

$$T = \frac{2.3Q}{4\pi\Delta h} = \frac{(2.3)(4.0\times10^{-3})}{(4)(3.14)(0.32)} = 0.0023\ m^2/s$$

$$S = \frac{2.25Tt_0}{r^2} = \frac{(2.25)(0.0023)(440)}{(55)^2} = 7.5\times10^{-4}$$

(a)

(a) Determination of T and S from h_0 — h versus t data using semilog method; (b) semilog plot in the vicinity of an impermeable boundary . From Freeze and Cherry (1979)

Fracture system as porous media equivalent (cont'd.)

- A good fall-back method for fractured rock
  - Several porous media equivalent solutions exhibit this behavior including anisotropic and double porosity models

- Change in the slope of the line indicates possible hetergeneities or boundaries
  - Increase in slope
    - Impermeable boundary — closing of fracture system
  - Decrease in slope
    - Recharge boundary — increase in permeability of fracture system

Fracture system as porous media equivalent (cont'd.)

- Problem:

- No all straight lines on the drawdown versus log time plot in fracture systems is actually laminar radial flow

- The following method is used to determine if the values calculated with the straight line method are valid. Sen (1995)

Fracture system as porous media equivalent (cont'd.)

- Using the T and S value calculated from the straight line method plot values of dimensionless time (u_f) and dimensionless drawdown (w_f) on semi-log graph paper from the following equations

$$u_f = \frac{r^2 S}{4 t_f T}$$

and

$$w_f = \frac{4 \pi T s_f}{Q}$$

- Plot the dimensionless time on the log x-axis and dimensionless drawdown on the y-axis. Graph paper must have same scale as original straight-line plot

Fracture system as porous media equivalent (cont'd.)

- The field drawdown (s_f) and time (t_f) values for the above equation are obtained from the original field data with the drawdown corresponding to several arbitrarily picked times

- The semi-log plot of dimensionless drawdown (w_f) versus log dimensionless time (u_f) must have approximately the same slope as the original drawdown versus log time field data plot for the calculated T and S values to be valid

Fracture system as porous media equivalent (cont'd.)

Semi-confined (leaky) aquifers

- Hantush (1960)
  - Includes water released from storage from confining layers
  - Not a good assumption for impermeable rock matrix like crystalline rock

- Hantush and Jacob (1955) and Hantush (1956)
  - Water just passes through confining layers (K values only)
  - Better assumption for fractured impermeable rock

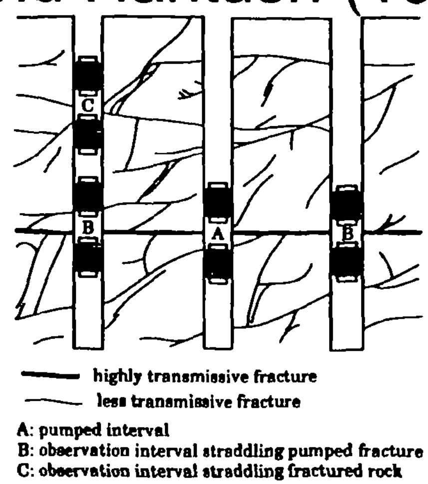

From National Research Council(1996)

Fracture system as porous media equivalent (cont'd.)

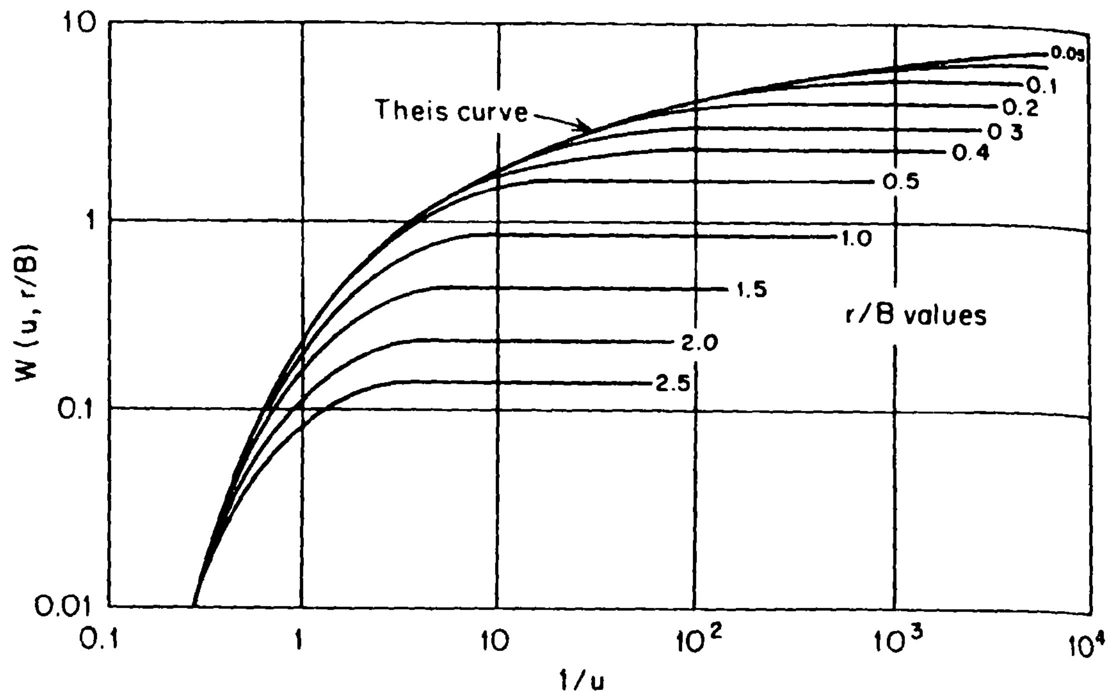

Theoretical curves of W (u, r/B0 versus 1/u for a leaky aquifer (after Walton, 1960)

From Freeze and Cherry(1979)

Fracture system as porous media equivalent (cont'd.)

- Multiple Aquifer System
  - Neuman and Witherspoon (1969)
  - Hantush (1967)

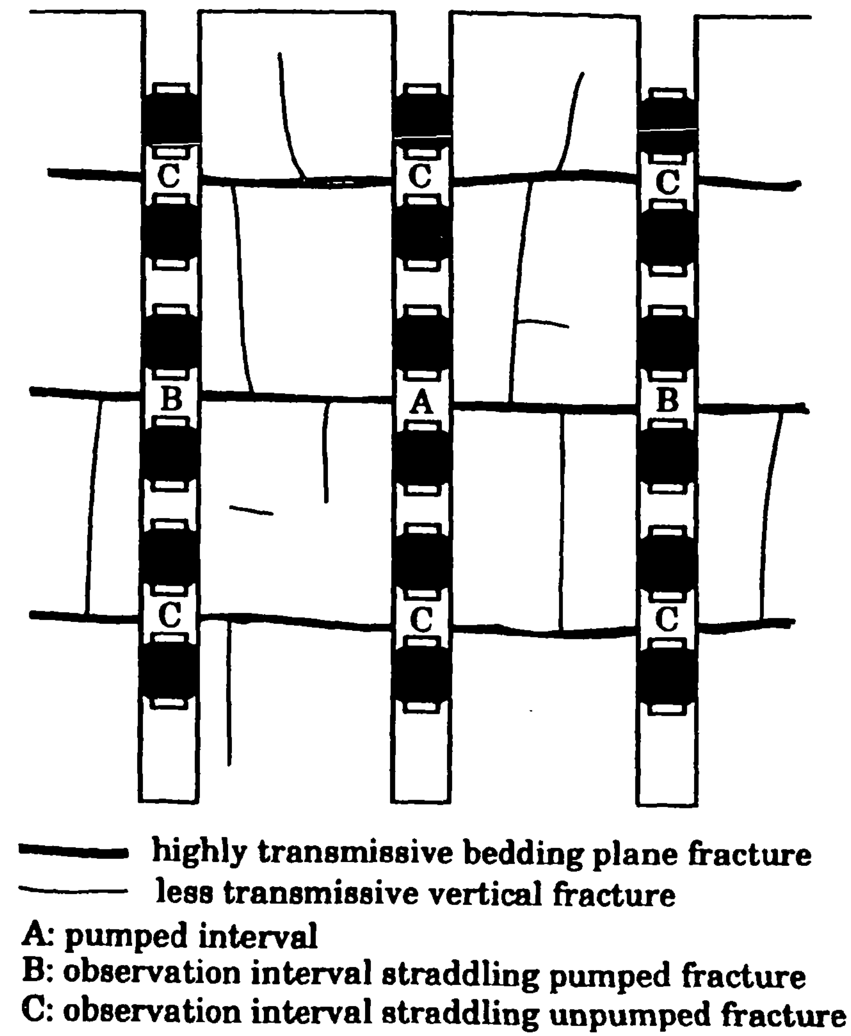

From National Research Council (1996)

Fracture system as porous media equivalent (cont'd.)

- Complex Fracture Systems
  - Beyond simple analytical models
  - Numerical computer modeling

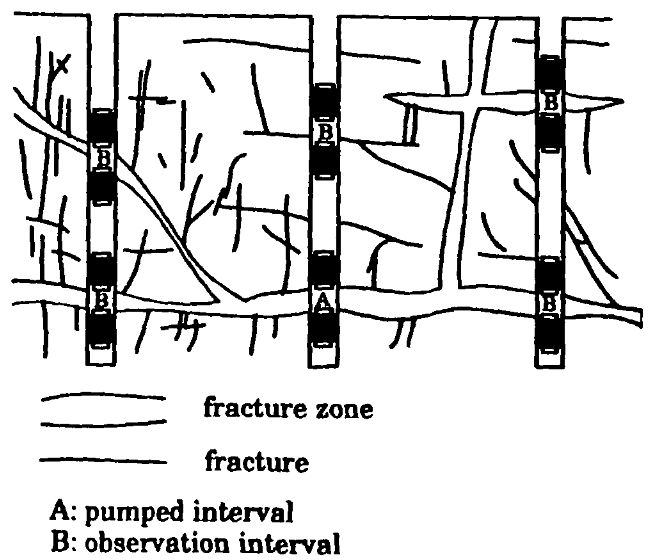

From National Research Council (1996)

Fracture-induced anisotropy

- All porous media equivalent models discussed so far are isotropic models
- Fractures often induce preferred directions of flow — anisotrophy
- K and T values obtained from isotropic models are the effective K or effective T value of an anisotropic aquifer
  - $K_{effective} = \sqrt{K_x K_y}$ 2 dimensions
  - $T_{effective} = \sqrt[3]{T_x T_y T_z}$ 3 dimensions

Fracture-induced anisotropy (cont'd.)

- Isotropic values are the geometric mean of the directional values
- The maximum transmissivity value will be larger than the calculated effective (isotropic) value

Fracture induced anisotrophy (cont'd.)

- Anisotropic aquifers
  - An elliptical cone of depression is created when an anisotropic aquifer is pumped
  - The long axis of the ellipse is in the direction of the maximum transmissivity
  - The short ellipse axis is the minimum transmissivity (90° from the maximum T) direction

Fracture induced anisotrophy (cont'd.)

- Directional transmissivity $T_d\ (\theta)$
  - Two dimensional $T_d\ (\theta)$ is written in the form (Popadopulous, 1965)

$$T_d\ (\theta) = \frac{D}{T_{yy} \cos^2 \theta + T_{xx} \sin^2 \theta - 2\, T_{xy} \cos \theta \sin \theta}$$

  - D is the determinant of the transmissivity tensor

Fracture induced anisotrophy (cont'd.)

$$D \text{ of } \begin{bmatrix} T_{xx} & T_{xy} \\ T_{yx} & T_{yy} \end{bmatrix} = T_{xx} T_{yy} - T_{xy} T_{yx}$$

- Symmetrical tensor so $T_{xy} = T_{yx}$

$$D = T_{xx} T_{yy} - (T_{xy})^2$$

Fracture induced anisotrophy (cont'd.)

- When $T_d\,(\theta)$ is calculated for different angles (θ) a polar coordinate plot of $\sqrt{T_d\,(\theta)}$ versus direction (θ) yields an ellipse

- The long axis of the ellipse is equal to the square root of the maximum transmissivity ($\sqrt{T_{max}}$) and the short axis is equal to the square root of the minimum transmissivity ($\sqrt{T_{min}}$)

Anisotropic aquifer methods

- Popadopulous Method (1965)
  - All Theis assumptions except anisotropic
  - Must have one pumping well and at least three observation wells. More are better
  - Three approaches
    - Type curve matching to Theis type curve
    - Straight-line, semi-log based on Cooper-Jacob method
    - Modified graphical approach using polar plot of $\sqrt{T_d}\,(\theta)$ versus direction (θ). Easiest method

- Problems with the Popadopulous Method
  - Aquifer must be confined (no leakage)
  - Only deals with two dimensional horizontal flow

Anisotropic aquifer methods (cont'd.)

- Hantush (1966) and Hantush-Thomas (1966)
  - Same assumptions as Theis method except anisotropic and can be a leaky aquifer
  - Need one pumping well and at least three observation wells
  - Uses values of (T/S) from abundant isotropic methods. S = storage

- Problems with the Hantush-Thomas method
  - Method assumes that T_d (θ) versus direction (θ) is an ellipse and calculates values of T_d (θ) accordingly
  - Cannot check if aquifer is behaving as a homogeneous anisotropic aquifer unlike the Popadopulous method

Anisotropic aquifer methods (cont'd.)

- Problem with all porous media equivalent homogeneous anisotropic methods when applied to fractured rock aquifers
  - Hetergencities can make aquifer behave as an anisotropic aquifer making the calculated directions and values incorrect (National Research Council, 1996)
  - If observation wells are screened in areas of higher (more or larger fractures) or lower (less or smaller fractures) transmissivity the discharge (Q) is not constant throughout the test area
  - Anisotropic calculation is invalid

Anisotropic aquifer methods (cont'd.)

- Three dimensional anisotropy
  - In fractured rock systems, the third principal transmissivity axis may not be vertical (perpendicular to horizontal flow)

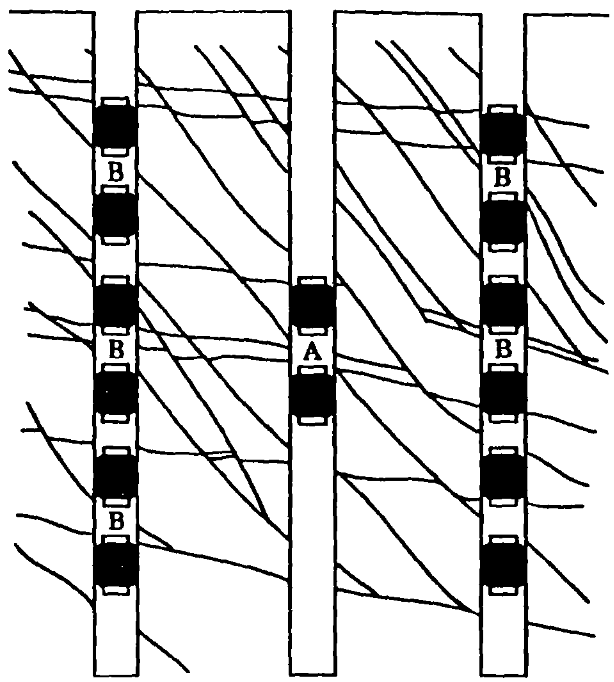

A: pumped interval
B: observation interval

From National Research Council (1996)

Anisotropic aquifer methods (cont'd.)

- Hsieh-Neuman Cross-hole method (1985)
  - Can calculate the three-dimensional transmissivity ellipsoid if fractured rock system behaves as homogeneous anisotropic aquifer
  - Move packers to obtain at least six measurements from at least three boreholes that do not lie in a plane
  - Simplest approach to the method is for packer intervals that are small compared to the distance between the boreholes

Anisotropic aquifer methods (cont'd.)

$$\Delta h_{PD} = \mathrm{erfc}\left(\sqrt{\frac{1}{4t_D}}\right)$$

Δh_{PD} = dimensionless head

t_D = dimensionless time

erfc = complimentary error function

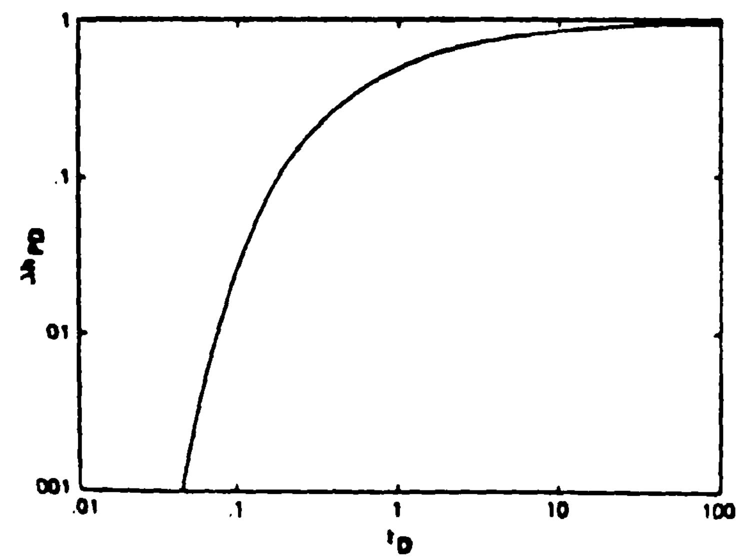

Log-log plot of ²h_{pd} versus t_d. From Hsieh and Neuman (1985)

Anisotropic aquifer methods (cont'd.)

- Develop at least six (six unknowns) simultaneous equation to determine the three dimensional conductivity tensor

- The degree to which an ellipsoid is formed is the degree to which the rock is an anisotropic porous medium equivalent

Double porosity models

- Used when there is primary (rock matrix) and secondary (fracture) porosity (fractured limestone or sandstone)
- Barenblatt and others (1960) developed the double porosity concept
- A homogeneous isotropic porous rock matrix continuum overlaps a homogeneous isotropic fracture system continuum
- The fractures have high transmissivity and low storage. The rock blocks have low transmissivity and high storage
- Water is pumped from the fractures lowing the pressure in the fractures. The rock matrix then releases water from storage into the fractures

Double porosity models (cont'd.)

- Warren and Root model (1963) — for pumping well only
  - Fracture system is idealized as orthogonal system with cubic rock blocks (homogeneous isotropic)

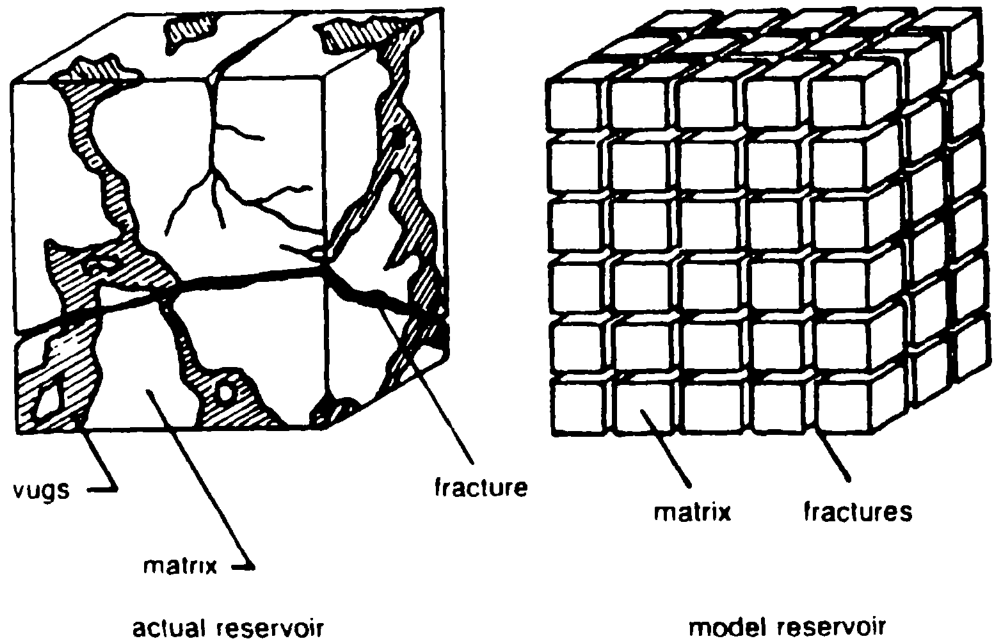

After Warren and Root . From Aquilera (1980)

Double porosity models (cont'd.)

- The log-log type curve resembles the unconfined aquifer type curve. The geology of the aquifer must be known to distinguish which behavior is being observed

- The semi-log plot of dimensionless pressure (P_D) versus log dimensionless time (t_D) clearly shows the three parts of the double porosity model

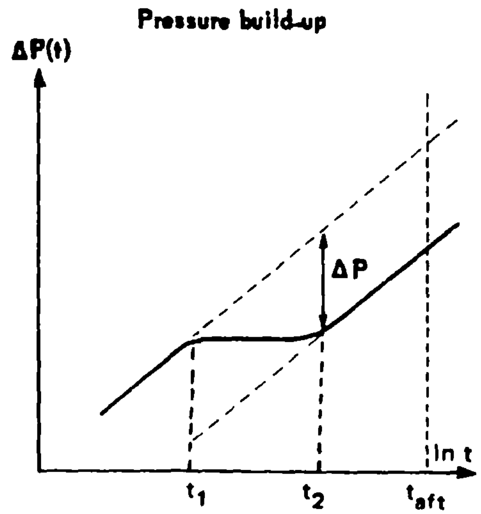

Transient pressure behavior according to Warren and Root. From Reiss (1980)

Double porosity models (cont'd.)

- First straight line segment (early time)
  - Radial flow through the fracture system. Storage from fracture system only. Can analyze with Cooper-Jacob straight line method

- Flat segment (intermediate time)
  - Water released from storage from the rock matrix
  - The length of this segment depends on the difference in the storage in the rock matrix and the fracture system (w)

- Second straight line segment (late time)
  - Radial flow through fracture system
  - Same slope as first straight line segment (same transmissivity)
  - Storage is combined fracture system and rock matrix storage

Double porosity models (cont'd.)

- Double porosity models have variables to represent the interaction of the fracture system and the rock matrix

Permeability contrast ratio

$$\lambda = \propto r_w^2 \frac{k_m}{k_f}$$

k_m = permeability of rock matrix

k_f = permeability of fractures

r_w = radius of pumping well

Coefficient of block surface

$$\propto = \frac{4n(2n+1)}{L^2}$$

n = number of fracture planes

L = length of block (cubes)

Double porosity models (cont'd.)

- Specific storage ratio (w)

$$w = \frac{S_f}{S_f + S_m}$$

S_f = specific storage in fractures

S_m = specific storage in rock matrix

As S_f -> 0 then w -> 0 purely rock matrix porosity

As S_m -> 0 then w-> 1 purely fracture porosity (blocks impermeable)

$w \cong \frac{t_1}{t_2}$ from semi leg plot

Double porosity models (cont'd.)

- Kazemi model - For observation well
  - Fracture system idealized as horizontal fractures with slab of homogeneous isotropic rock

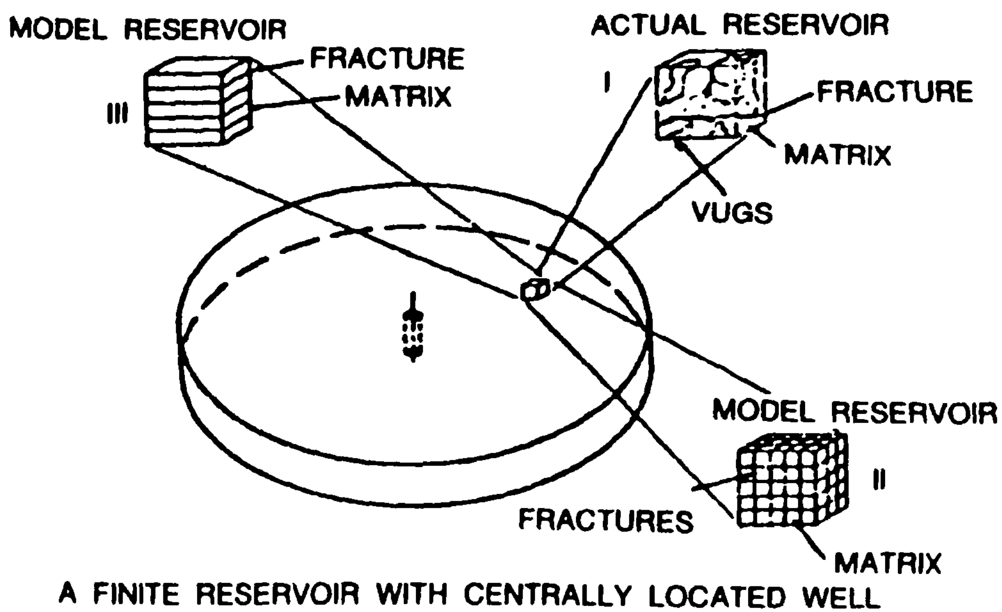

Idealization of naturally fractured porous medium. II, Warren-Root model; III, Kazemi model (after Kazemi). From Aquilera (1980)

Double porosity models (cont'd.)

- Kazemi model (cont'd.)
  - If there is not a large contrast between hydraulic properties (K and S) of the fractures and rock matrix, or
  - If observation well is far from the pumping well:
    - The first straight line segment will be missing
    - The flat intermediate segment will be short or missing
    - The third straight line segment is analyzed with the Cooper-Jacob straight line method

- More details on the solution to double porosity models are in "Applied Hydrogeology for Scientists and Engineers" by Zekai Sen (1995)

Vertical Fracture Model - Not a double porosity model

- Vertical fracture in a homogeneous isotropic porous aquifer
  - Gringarten and others (1974)
  - Gringarten and Witherspoon (1972)
  - The vertical fracture is of finite size with the pumping well in the middle of the fracture
  - The pumping well and any observation wells screened in the fracture will have a 1/2 unit slope on a log drawdown versus log time plot
  - At a late time in the pumping well or for an observation well far from the pumping well (within the equivalent porous medium part of the system), the aquifer will behave like horizontal radial flow (Cooper-Jacob) straight line method when plotted on drawdown versus log time graph

Horizontal Fracture Model - Not a double porosity model

- Horizontal fracture in a homogeneous isotropic porous aquifer
  - Gringarten and Ramey (1974)
  - The pumping well is in the middle of a horizontal fracture surrounded by an equivalent porous medium aquifer
  - The initial response can be the 1/2 unit slope on the log drawdown versus log time plot but altered by a dimensionless head factor (H_D)

$$H_D = \frac{h}{r_f}\sqrt{\frac{k_f}{k_m}}$$

h = thickness of equivalent porous medium
r_f = half the length of the fracture
k_f = fracture permeability
k_m = equivalent porous medium permeability

Summary of characteristic well responses

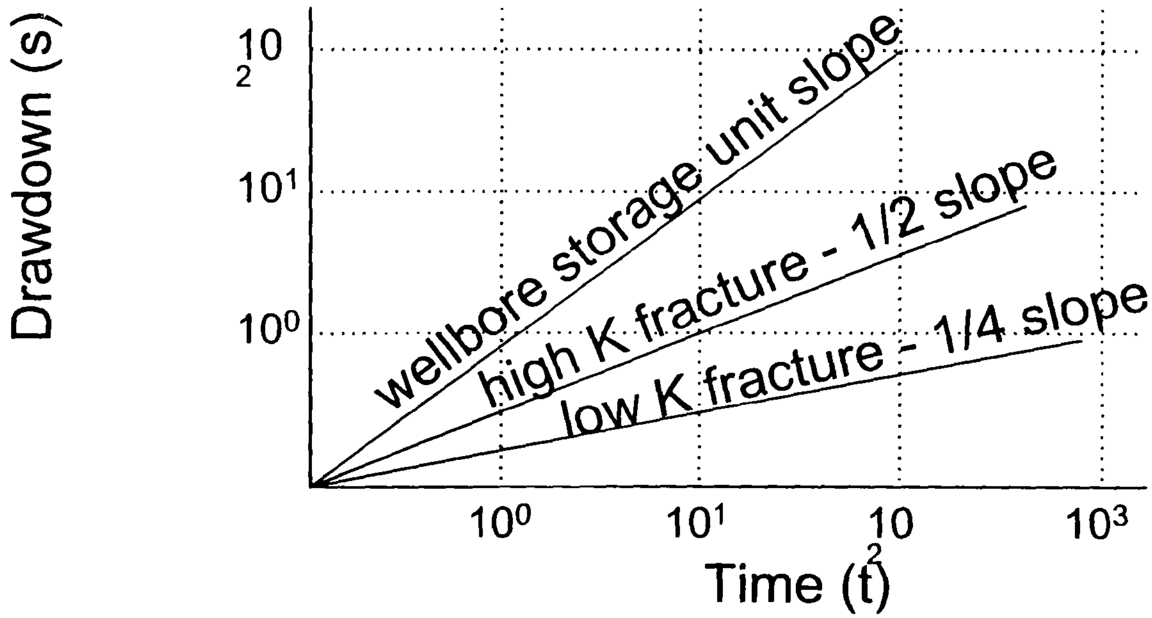

- Log drawdown versus log time plot
  - Wellbore storage — unit slope (45°)

- Linear flow
  - High conductivity fracture — 1/2 slope
  - Low conductivity fracture — 1/4 slope

Summary of characteristic well responses (cont'd.)

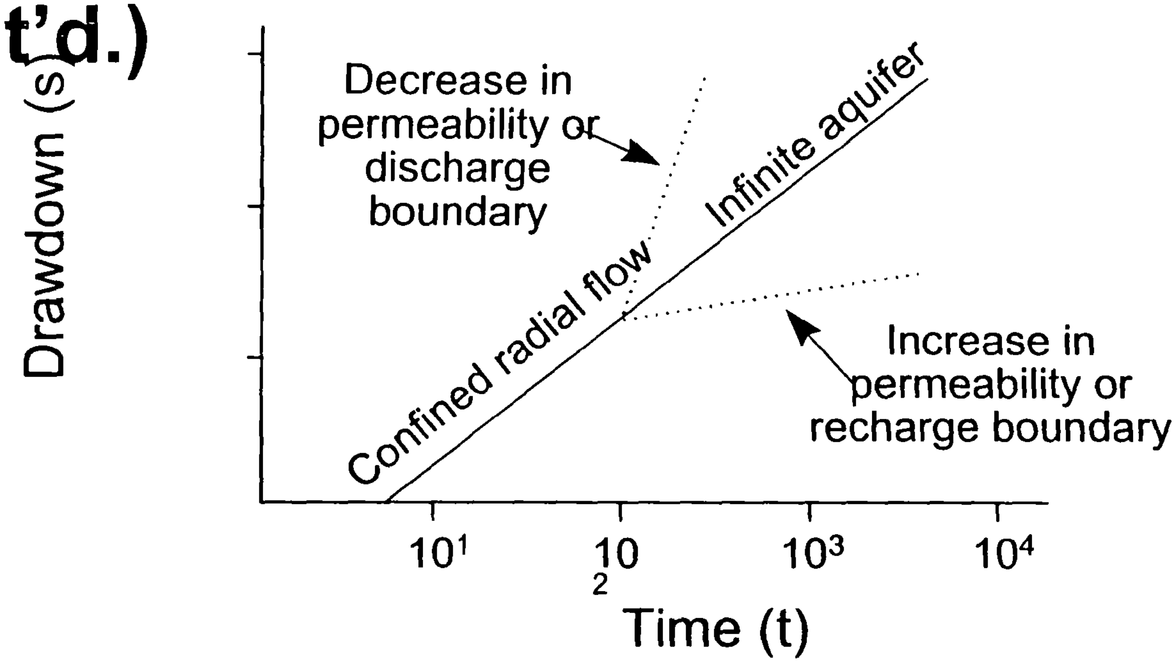

- Drawdown versus log time plot (semi-log)

- Radial flow — transmissivity inversely proportional to the slope of the straight line

$$T = \frac{2.3\,Q}{4\pi(\Delta s / \log \text{cycle})}$$

Packer Test

- Packer test
  - Zanger (1953)
  - U.S. Dept of Interior (1977)

- Have been used for years in geotechnical engineering to determine the hydraulic conductivity of discrete fracture zones

- Problems
  - Increase in pressure during injection test can open fractures, causing an increase in conductivity during testing

Packer Tests (cont'd.)

- Must be careful to measure pressure changes above and below packer interval that may be caused by "short circuiting" or bad seal on the borehole wall

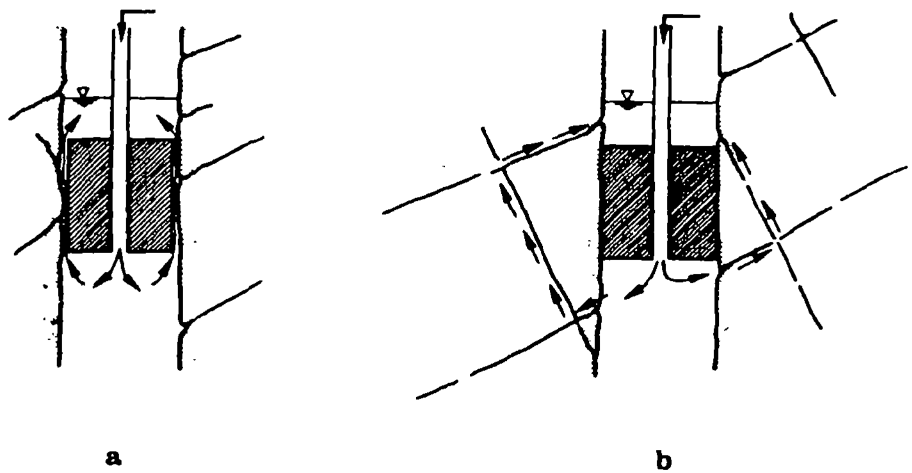

Invalidation of test results: a) leakage at the packer; b) flow around the packer

From Wittke (1990)

Problems with porous media equivalent aquifer test methods — Cohen (1995)

- Glosses over detail to give you the composite behavior of the aquifer
  - There can be features (fractures) within the system with a order of magnitude higher hydraulic conductivities than calculated with porous media equivalent models
- For pumping well
  - Well bore storage and skin effects (damaged or enhanced conditions caused by the drilling or development of well) can mask important early time data
- For observation well
  - Results may not be from the area of the system you are interested in

REFERENCES

Alfano, J., 1993, M.S. Thesis, Hydrogeological Evaluation of a Fractured Crystalline Rock Aquifer, Hendersonville, North Carolina: Geology Department, Georgia State University.

Armstrong, R.L., and Dick, H.J.B., 1974, A model for the development of thin overthrust sheets of crystalline rock: Geology, January, p. 35-40.

Arnold, M.D., Gonzalez, H.J., and Crawford, P.B., 1962, Estimation of reservoir anisotropy From production data: Journal of Petroleum Technology, August, p. 909-912.

Atobrah, K., 1985. On the relationships of flow in crystalline rock aquifers, a solution to the fracture problem: Hydrogeology of Rocks of Low Permeability in Memoires of the International Association of Hydrogeologist, v. XVII, p. 527-537.

Barker, J.A., 1988, A generalized radial flow model for hydraulic tests in fractured rock: Water Resources Research, v. 24, n. 10, p. 1796-1804.

Berkowitz, B., Bear, J., and Braester, C., 1988, Continuum models for contaminant transport in fractured porous formations: Water Resources Research, v. 24, n. 8, p. 1225-1236.

Bianchi, L., and Snow, D.T., 1969, Permeability of crystalline rock interpreted from measured orientation and aperatures of fractures: Annals of Arid Zone, v. 8, n. 2, p. 231-245.

Blanchet, P.H., 1957, Development of fracture analysis as exploration method: Bulletin of the American Association of Petroleum Geologists, v. 40, n. 8, p. 1748-1759.

Boulton, N.S., and Streltsova-Adams, T.D., 1978, Unsteady flow to a pumped well in an unconfined fissured aquifer: Journal of Hydrology, v. 37, p. 349-363.

Boulton, N.S., and Streltsova, T.D., 1977, Unsteady flow to a pumped well in a two-layered water-bearing formation: Journal of Hydrology, v. 35, p. 245-254.

-----1977, Unsteady flow to a pumped well in a fissured water-bearing formation: Journal of Hydrology, v. 35, p. 257-269.

-----1975, New equations for determining the formation constants of a aquifer from pumping test data: Water Resources Research, v. 11, n. 1, p. 148-153.

Boulton, N.S., and Pontin, J.M.A., 1971, An extended theory of delayed yield from storage applied to pumping tests in unconfined anisotropic aquifers: Journal of Hydrology, v. 14, p. 53-65.

Boulton, N.S., 1973, The influence of delayed drainage on data from pumping tests in unconfined aquifers: Journal of Hydrology, v. 19, p. 157-169.

Boulton, N.S., 1970, Analysis of data from pumping tests in unconfined anisotropic aquifers: Journal of Hydrology, v. 10, p. 369-378.

-----1965, The discharge to a well in an extensive unconfined aquifer with constant pumping level: Journal of Hydrology, v. 3, p. 124-130.

-----1963, Analysis of data from non-equilibrium pumping tests allowing for delayed yield from storage: Proceedings of the Institution of Civil Engineers, v. 26, p. 469-482.

-----1955, Unsteady radial flow to a pumped well allowing for delayed yield from storage: Internation Association of Science, Hydrology Pubilication, v. 37, p. 472-477.

-----1954, The drawdown of the water-table under non-steady conditions near a pumped well in an unconfined formation: Proc. Instn. civ. Engrs, v. 6, p. 564-579.

Bourdet, D., Whittle, T.M., Douglas, A.A., and Pirard, Y.M., 1983, A new set of type curves simplifies well test analysis, May, p. 95-106.

Bouwer, H., and Rice, R.C., 1976, A slug test for determining hydraulic conductivity of unconfined aquifers with completed or partially penetrating wells: Water Resources Research, v. 12, n. 3, p. 423-428.

Brace, W.F., 1984, Permeability of crystalline rocks- new in situ measurements: Journal of Geophysical Research, v. 89, n. B6, p. 4327-4330.

Brace, W.F., 1980, Permeability of crystalline and argillaceous rocks: International Journal of Rock Mechanics, Mining Science and Geomechanical Abstracts, v. 17, p. 241-251.

Brook, G.A., 1988, Hydrogeological factors influencing well productivity in the crystalline rock regions of Georgia: Southeastern Geology, v. 29, n. 2, p. 65-80.

Chen, C., Serra, K., Reynolds, A.C., and Raghavan, R., 1985, Pressure transient analysis methods for bounded naturally fractured reservoirs: Society of Petroleum Engineers Journal, June, p. 451-464.

Cohen, A., 1995, Hydrogeologic characterization of fractured rock formations: A guide for groundwater remediators: Earth Sciences Division, Ernest Orlando Lawrence Berkeley National Laboratory, University of California, October, 144 pp.

Cooley, R.L., and Case, C.M., 1973, Effect of a water table aquitard on drawdown in an underlying pumped aquifer: Water Resources Research, v. 9, n. 2, p. 434-447.

Cooper, H.H., Jr., and Jacob, C.E., 1946, A generalized graphical method for evaluating formation constants and summarizing well field history: Tranactions of the American Geophysical Union, v. 27, p. 526-534.

Dagan, G., 1967, A method of determining the permeability and effective porosity of unconfined anisotropic aquifers: Water Resources Research, v. 3,n. 4, p. 1059-1071.

Dallmeyer, R.D., and Hatcher, R.D., 1985, The Alto allochthon; Part 2, geochronological constrints on tectonothermal evolution: Geological Society of America, Abstracts with Programs, v. 17, p. 86.

Davis, S.N., and Turk, L.J., 1964, Optimum depth of wells in crystalline rocks: Groundwater, v. 2, p. 6-11.

Dennis, J.G., 1972, Structural geology: The Ronald Press Company, 532 pp.

Domenico, P.A., and Schwartz, F.W., 1990, Physical and chemical hydrogeology: John Wiley & Sons, Inc., 824 pp.

Duguid, J.O., and Lee, P.C.Y., 1977, Flow in fractured porous media: Water Resources Research, 13(3), p. 558-566.

El-Hadidi, S.M., and Ritter, A.W., 1976, Interpretation of bottom-hole pressure build-up tests on fractured oil reservoirs: SPE Paper 6020 presented at the 51st Annual Fall Technical Conference of SPE of AIME, New Orleans, October 3-6.

Elkins, L.F., and Skov, A.M., 1960, Determination of fracture orientation from pressure interference: Transactions of the American Institution of Mineral Engineers, v. 219, p. 301-304.

Endo, H.K., and Witherspoon, P.A., 1985, Mechanical transport and porous media equivalence in anisotropic fracture network: Hydrogeology of Rocks of Low Permeability in Memoires of the International Association of Hydrogeologist, v. XVII, p. 527-537.

Endo, H.K., Long, J.C.S., Wilson, C.R., and Witherspoon, P.A., 1984, A model for investigating mechanical transport in fracture networks: Water Resources Research, v. 20, n. 10, p. 1390-1400.

Gale, J.E., 1982, Assessing the permeability characteristics of fractured rock: Geological Society of America, Special Paper 189, p. 163-181.

Gale. J.E., 1975, A numerical, field, and laboratory study of flow in rocks with deformable fractures [Ph.D. dissertation]: Berkeley, University of California, 255 p.

Gangi, A.F., 1981, The variation of mechanical and transport properties of cracked rock with pressure: Proceedings of the 22nd US Symposium on Rock Mechanics, Massachusetts Institute of Technology, p. 91-95.

Gordon, M.J., 1986, Dependence of effective porosity on fracture continuity in fractured media: Ground Water, v. 24, n. 4, p. 446-452.

Gringarten, A.C., 1982, Flow-test evaluation of fractured resevoirs: Geological Society of America, Special Paper 189, p. 237-263.

Gringarten, A.C., and Ramey, H.J., 1974, Unsteady-state pressure distributions created by a well with a single horizontal fracture, partial penetration, or restricted entry: Society of Petroleum Engineers Journal, August, p. 413-426.

Gringarten, A.C., Ramey, H.J., and Raghavan, R., 1974, Unsteady-state pressure distributions created by a single infinite-conductivity vertical fracture: Society of Petroleum Engineers Journal, August, p. 347-360.
Hantush, M.S., and Jacob, C.E., 1954, Plane potential flow of groundwater with linear leakage: Trns of American Geophysical Union, v. 35, p. 917-936.
Hantush, M.S., and Jacob, C.E., 1955, Non-steady radial flow in an infinite leaky aquifer: Transactions of the American Geophysical Union, v. 36, n. 1, p. 95-100.
Hantush, M.S., and Thomas, R.G., 1966, A method for analyzing a drawdown test in anisotropic aquifers: Water resources Research, v. 2, n. 2, p. 281-285.
Hantush, M.S., 1967, Flow of groundwater in relatively thick leaky aquifers: Water Resources Research, v. 3, n. 2, p. 583-590.
-----1966a, Wells in homogeneous anisotropic aquifer: Water resources Research, v. 2, no. 2, p. 273-279.
-----1966b, Analysis of data from pumping tests in anisotropic aquifers: Journal of Geophysical Research, v. 71, n. 2, p. 421-426.
-----1964a, Drawdown around wells of variable discharge: Journal of Geophysical Research, v. 69, n. 20, p. 4221-4235.
-----1964b, Hydraulics of wells: Advances in Hydroscience, v. 1, p. 281-432.
-----1962, Aquifer tests on partially penetrating wells: Transactions of the American Society of Civil Engineers, v. 127, p. 284-308.
-----1960, Modification of the theory of leaky aquifers: Journal of Geophysical Research, v. 65, n. 11, p. 3713-3725.
-----1956, Analysis of data from pumping tests in leaky aquifers: Tins of American Geophysical Union, v. 37, p. 702-714.
Haxby, W.F., and Turcotte, D.L., 1976, Stresses induced by the addition or removal of overburden and associated thermal effects: Geology, March, p. 181-184.
Hsieh, P.A., Neuman, S.P., Stiles, G.K., and Simpson, E.S., 1985, Field determination of the three-dimensional hydraulic conductivity tensor of anisotropic media; Theory: Water Resources Research, v. 21, no. 11, p. 1655-1665.
Hsieh, P.A., Neuman, S.P., Stiles, G.K., and Simpson, E.S., 1985, Field determination of the three-dimensional hydraulic conductivity tensor of anisotropic media; Methodology and application to fractured rocks: Water Resources Research, v. 21, no. 11, p. 1667-1676.
Huitt, J.L., 1956, Fluid flow in simulated fractures: Journal AICHE, v. 2, p. 259.

Huntoon, P.W., 1981, Fault controlled ground-water circulation under the Colorado river, Marble Canyon, Arizona: Ground Water, v. 19, n. 1, p. 20-27.

Iwai, K., 1976, Fundamental studies of fluid flow through a single fracture (Ph.D. dissertation): Berkeley, University of California, 208 p.

Jacob, C.E., 1963, Determining the permeability of water-table aquifers: USGS Water Supply Paper 1536-I; Methods of Determining Permeability, Transmissivity, and Drawdown, p. 245-271.

Jacob, C.E., 1963, Correction of drawdowns caused by a pumped well tapping less than the full thickness of an aquifer: USGS Water Supply Paper 1536-I; Methods of Determining Permeability, Transmissivity, and Drawdown, p. 272-282.

Jones, F.O., 1975, A laboratory study of the effects of confining pressure on fracture flow and storage capacity in carbonate rocks: Journal of Petroleum Technology, Jan, p. 21-27.

Karasaki, K., Long, J.C.S., and Witherspoon, P.A., 1988, Analytical models for slug tests: Water Resources Research, v. 24, no. 1, p. 115-126.

Karasaki, K., 1986, Well analysis in fractured media: Ph.D. Thesis, Earth Sciences Division, Lawrence Berkeley Laboratory, University of California.

Kazemi, H., Seth, M.S., and Thomas G.W., 1969, The interpretation of interference tests in naturally fractured reservoirs fracture distribution: Society of Petroleum Engineers Journal, Dec., p. 463-472.

King, P.B., 1971, Systematic pattern of triassic dikes in the Appalachian region-second report: USGS Professional Paper 750D, p. D84-D88.

King, P.B., 1961, Systematic pattern of triassic dikes in the Appalachian region: USGS Professional Paper 424A, p. B93-B95.

Kranz, R.L., Frankel, A.D., Engelder, T., and Scholz, C.H., 1979, The permeability of whole and jointed Barre granite: International Journal of Rock Mechanics, Mining Science and Geomachanical Abstracts, v. 16, p. 225-234.

Krothe, N.C., and Bergeron, M.P., 1981, The relationship between fracture traces and joints in a tertiary basin, southwest Montana: Ground Water, March - April, p. 138-143.

Kruseman, G.P., and DeRidder, N.A., 1983, Analysis and evaluation of pumping test data: Bulletin 11, International Institute for Land Reclamation and Improvement, The Netherlands, 200 p.

LaPointe, P.R., and Hudson, J.A., 1985, Characterization and interpretation of rock mass joint patterns: Geological Society of America Special Paper 199, p. 3-25.

Lattman, L.H., and Nickelsen, R.P., 1958, Photogeologic fracture-trace mapping in Appalachian plateau: American Association of Petroleum Geology, v. 42, part II, n. 9, p. 2238-2245.

LeGrand, H.E., 1979, Evaluation techniques of fractured-rock hydrology: Journal of Hydrology, v. 43, p. 333-346.

LeGrand, H.E., 1967, Groundwater of the Piedmont and Blue Ridge provinces in the southeastern states, U.S.Geological Survey Circular 538, 11 p.

Lindholm, R.C., 1978, Triassic-Jurassic faulting in eastern North America- a model based on pre-Triassic structures: Geology, v. 6, p. 365-368.

Lohman, S.W., 1972, Groundwater Hydraulics: U.S. Geological Survey Professional Paper 708, 70 p.

Lomize, G.M., 1951, Fluid flow in fractured rocks: Goseneroizdat, Moscow (in Russia).

Long, J.C.S., Remer, C.R., Wilson, P.A., and Witherspoon, P.A., 1982, Porous media equivalents for networks of discontinuous fractures: Water Resources Research, v. 18, no. 3, p. 645-658.

Long, C.S., and Witherspoon, P.A., 1985, The relationship of the degree of interconnection to permeability in fracture networks: Journal of Geophysical Research, v. 90, n. B4, p. 3087-3098.

Losch, F., 1960, Tables of Higher Functions, McGraw-Hill Book Company, 318 p.

Maasland, M., 1957, Theory of fluid flow through anisotropic media: Drainage of Agricultural Lands, ed. Luthin, J.N., American Society of Agronomy, Madison, Wis.

Marine, I.W., 1981, Comparison of laboratory, in situ, and rock mass measurements of the hydraulic conductivity of metamorphic rock at the Savannah river plant near Aiken, South Carolina: Water Resources Research, v. 17, n. 3, p. 637-640.

-----1980, Determination of the location and connectivity of fractures in metamorphic rock with in-hole tracers: Groundwater, v. 18, n. 3, p. 252-261.

-----1966, Hydraulic correlation of fracture zones in buried crystalline rock at the Savannah River Plant near Aiken, South Carolina: United States Geological Survey Professional Paper 550-D, p. D223-D227.

Marshak, S., and Mitra, G., 1988, Basic methods of structural geology: Prentice-Hall Inc., Engle Cliff, N.J., p. 131-143.

May, P.R., 1971, Pattern of Triassic-Jurassic diabase dikes around the North Atlantic in the context of predrift position of the continents: Geological Society of America Bulletin, v. 82, p. 1285-1292.

McConnell, C.L., 1993, Double porosity well testing in fractured carbonate rocks of the Ozarks: Gound Water, v. 31, n. 1, p. 75-83.

McSween, H.Y., and Abbott, R.N., and Raymond, L.A., 1989, Metamorphic conditions in the Ashe metamorphic suite, North Carolina Blue Ridge: Geology, v. 17, p. 1140-1143.
Moench, A.F., 1984, Double-porosity for a fissured groundwater reservoir with fracture skin: Water Resources Research, v. 20, n. 7, p. 831-846.
Moench, A.F., and Ogata, A., 1984, Analysis of constant discharge wells by numerical inversion of Laplace transform solutions: Groundwater Hydraulics, Water Resouces Monograph Series 9, America Geophysical Union, p. 146-170.
Moench, A.F., and Prickett, T.A., 1972, Radial flow in an infinite aquifer undergoing conversion from artesian to water table conditions: Water Resources Research, v. 8, n. 2, p. 494-499.
Moran, J.H., and Finklea, E.E., 1962, Theoretical analysis of pressure phenomena associated with the wireline formation tester: Society of Petroleum Engineers Journal, August, p. 899-907.
Mundi, E.K., and Wallace, J.R., 1973, On the permeability of some fractured crystalline rocks: Bulletin of the Association of Engineering Geologists, v. 10, n. 4, p.299-312.
National Research Council, 1996, Rock fractures and fluid flow, Contempory understanding and applications: Committee on Fracture Characterization and Fluid Flow, National Academy Press, 551 pp.
Neuman, S.P., Walter, G.R., Bentley, H.W., Ward, J.J., and Gonzalez, D.D., 1984, Determination of horizontal aquifer anisotropy with three wells: Ground Water, v. 22, no. 1, p. 66-72.
Neuman, S.P., and Witherspoon, P.A., 1972, Field determination of the hydraulic properties of leaky multiple aquifer systems: Water Resources Research, v. 8, p. 1284-1298.
-----1969a, Theory of flow in a confined two-aquifer system: Water Resources Research, v. 5, p. 803-816.
-----1969b, Applicability of current theories of flow in leaky aquifers: Water Resources Research, v. 5, p. 817-829.
Neuman, S.P., 1987, On methods of determining specific yield: Groundwater, v. 25, n. 6, p. 679-683.
-----1982, Statistical characterization of aquifer heterogeneities; An overview, Geological Society of America- Special Paper 189, p. 81-87.
-----1979, Perspective on delayed yield: Water Resources Research, v. 15, n. 4, p. 899-908.
----1975, Analysis of pumping test data from anisotropicunconfined aquifers considering delayed gravity response: Water Resources Research, v. 11, n. 2, p. 329-342.

Neuman, S.P., 1974, Effect of partial penetration on flow in unconfined aquifers considering delayed gravity response: Water Resources Research, v. 10, n. 2, p. 303-312.
-----1973, Supplementary comments on 'Theory of flow in unconfined aquifers considering delayed response of water table: Water Resources Research, v. 9, n. 4, p. 1102-1103.
-----1972, Theory of flow in unconfined aquifers considering delayed response of the water table: Water Resources Research, v. 8, n. 4, p. 1031-1045.
Neuzil, C.E., and Tracy, J.V., 1981, Flow through fractures: Water Resources Research, v. 17, no. 1, p. 191-199.
Novakowski, K.S., 1990, Analysis of aquifer tests conducted in fractured rock; a review of the physical background and the design of a computer program for generating type curves: Ground Water, v. 28, n. 1, p. 99-107.
Odom, A.L., and Fullagar P.D., 1973, Geochronologic and tectonic relationships between the Inner Piedmont, Brevard zone, and Blue Ridge belts , North Carolina: American Journal of Science, v. 273-A, p. 133-149.
Parsons, R.W., 1966, Permeability of idealized fractured rock: Society of Petroleum Engineers Journal, v. 10, p. 126-136.
Passchier, C.W., 1991, Geometric constraints on the development of shear bands in rocks: Geologie en Mijnbouw, v. 70, p. 203-211.
Popadopulos, I.S., 1967, Non-steady flow to a well in an infinite anisotropic aquifer: Proceedings, Dubrovnik Symposium on Hydrology of Fractured Rocks: International Association of Scientific Hydrology, v. 1, n. 23, p. 21-31.
Pratt, H.R., Swolfs, H.S., Brace, W.F., Black, A.D., and Handin, J.W., 1977, Elastic and transport properties of an in-situ jointed granite: International Journal of Rock Mechanics and Mineral Science, v. 14, p. 35-45.
Press, F., and Siever, R., 1978, Earth, W.H. Freeman and Company, 649 pp.
Prickett, T.A., 1965, Type-curve solution to aquifer tests under water-table conditions: Ground water, v. 3, p. 5-14.
Priest, S.D., 1993, Discontinuity analysis for rock engineering: St. Edmundsbury Press, Ltd., Great Britain, 473 pp.
Priest, S.D., 1985, Hemispherical projection in rock mechanics: George Allen and Unwin, London, p. 26-50.
Priest, S.D., and Hudson, J.A., 1975, Discontinuity spacings in rock: International Journal of Rock Mechanics, Mining Sciences and Geomechanical Abstracts, v. 13, p. 135-148.
Ragan, D.M., 1973, Structural geology: An introduction to geometrical techniques, John Wiley and Sons,p. 121-129

Raghavan, R., and Clark, K.K., 1975, Vertical permeability from limited entry flow tests in thick formations: Society of Petroleum Engineers Journal, Febuary, p. 65-73.
Ramsay, J.G., 1980, Shear zone geometry; a review: Journal of Structural Geology, v. 2, n. 1/2, p. 83-99.
Reed, J.C., Jr., and Bryant, B.H., 1964, Evidence for strike-slip faulting along the Brevard Zone in North Carolina: Geological Society of America Bulletin, v. 75, p. 1177-1196.
Reed, J.C., Jr., and Bryant, B.H., 1960, A major topographic lineament in western North Carolina and its possible structural significance: United States Geological Survey Professional Paper 400-B, p. B195-B197.
Reed, J.C., Jr., Johnson, H.S., Jr., Bryant, B.H., Bell, H., and Overstreet, W.C., 1961, The Brevard zone in North and South Carolina: United States Geological Survey Professional Paper 424-C, p. C67-C70.
Reiss, L.H., 1980, The reservoir engineering aspects of fractured formations: Gulf Publishing Company, 108 pp.
Romm, E.S., 1972, Fluid flow in fractured rocks, Translated by Blake, W.R., Phillips Petroleum Company.
Romm, E.S., and Pozinenko, B.V., 1963, Investigation of seepage in fractured rocks: Trudy VNIGRI, 214, (in Russia).
Roper, P.J., and Justus, P.S., 1973, Polytectonic evolution of the Brevard zone: American Journal of Science, v. 273-A, p. 105-132.
Roper, P.J., and Dunn, D.E., 1973, Superposed deformation and polymetamorphism, Brevard zone, South Carolina: Geological Society of America, v. 84, p. 3373-3385.
Sagar, B., and Runchal, A., 1982, Permeability of fractured rock; effect of fracture size and data uncertainties: Water Resources Research, v. 18, n. 2, p. 266-274.
Sauveplane, C., 1984, Pumping test analysis in fractured aquifer formations, State of the art and some perspectives: Groundwater Hydraulics, Water Resources Monograph Series 9, America Geophysical Union, p. 171-206.
Secor, D.T., Snoke, A.W., and Dallmeyer, R.D., 1986, Character of the Alleghanian orogeny in the southern Appalachians; part III. regional tectonic relations: Geological Society of America Bulletin, v. 97, p. 1345-1353.
Sen, Z., 1995, Applied hydrogeology for scientist and engineers: CRC Press, Inc., 444 pp.
Sen, Z., 1986, Aquifer test analysis in fractured rocks with linear flow pattern: Ground Water, v. 24, n. 1, p. 72-78.

Smith, B.M., Reynolds, S.J., Day, H.W., and Bodnar, R.J., 1991, Deep-seated fluid involvement in ductile-brittle deformation and mineralization, South Mountains metamorphic core complex, Arizona: Geological Society of America Bulletin, v. 103, April, p. 559-569.

Smith, W.A., 1987, Paleomagnetic results from a crosscutting system of northwest and north-south trending diabase dikes in the North Carolina Piedmont: Tectonophysics, v. 136, p. 137-150.

Snow, D.T., 1970, The frequency and aperatures of fractures in rock: Int. Journal of Rock Mechanics, Mining Sciences: V. 7, p. 23-40.

-----1969, Anisotropic permeability of fractured media: Water Resources Research, v. 5, no. 6, p. 1273-1289.

-----1968, Rock fracture spacing, openings, and porosity: Journal of Soil Mechanics and Foundation Division, V. 94, p. 73-91.

-----1968, Fracture deformation and changes of permeability and storage upon changes of fluid pressure: Colorado School of Mines Quarterly, v. 63, no. 1, p. 201-244.

-----1965, A parallel plate model of fractured permeable media (Ph.D. dissertation): Berkeley, University of California, 331 p.

Spencer, E.W., 1977, Introduction to the structure of the earth: McGraw-Hill Book Company, 640 pp.

Stallman, R.W., 1965, Effects of water table conditions on water level changes near pumping wells: Water Resources Research, v. 1, n. 2, p. 295-312.

-----1961, Relation between storage changes at the water table and observed water-level changes: USGS Professional Paper 424, p. B39-B40

-----1961, The significance of vertical flow components in the vicinity of pumping wells in unconfined aquifers: USGS Professional Paper 424, B41-B43.

-----1961, Boulton's integral for pumping-test analysis: USGS Professional Paper 424, p. C25-C29.

Steward, J.W., 1964, Infiltration and permeability of weathered crystalline rock, Georgia nuclear laboratory, Dawson County, Georgia: USGS Bulletin 1133-D, p. D1-D57.

Stirewalt, G.L., and Dunn, D.E., 1973, Mesoscopic fabric and structural history of Brevard zone and adjacent rocks, North Carolina: Geological Society of America Bulletin, v. 84, p. 1629-1650.

Streltsova, T.D., 1988, Well Testing in Heterogeneous Formations, An Exxon Monograph, John Wiley and Sons, 413 p.

-----1976a, Hydrodynamics of groundwater flow in a fractured formation: Water Resources Research, v. 12, no. 3, p. 405-414.

-----1976b, Analysis of aquifer-aquitard flow: Water Resources Research, v. 12, n. 3, p. 415-422.

Streltsova, T.D., 1972, Unsteady radial flow in a unconfined aquifer: Water Resources Research, v. 8, n. 4, p. 1059-1066.

Streltsova-Adams, T.D., 1978, Well hydraulics in heterogeneous aquifer formations: Advances in Hydroscience, Academic Press, v. 11. p. 357-423.

Tchalenko, J.S., 1970, Similarities between shear zones of different magnitudes: Geological Society of America Bulletin, v. 81, June, p. 1625-1640.

Thorpe, R.K., 1981, An example of fracture characterization in granitic rock: Proceedings of the 22nd US Symposium on Rock Mechanics, Massachusetts Institute of Technology, p. 497-502.

Tsang Y.W., and Tsang, C.F., 1987, Channel model of flow through fractured media: Water Resources Research, v. 23, no. 3, p. 467-479.

Tullis, J., and Yund, R.A., 1987, Transition from cataclastic flow to dislocation creep of feldspar, mechanisms and microstructure: Geology, v. 15, July, p. 606-609.

Uhl, V.W., and Sharma, G.K., 1978, Results of pumping tests in crystalline rock aquifers: Ground Water, v. 16, no. 3, p. 192-203.

United States Department of the Interior, 1981, Ground Water Manual, 480 p.

United States Geological Survey Water-Supply Paper 1536 A-J, 1960-1963, 366 p.

Van Golf-Racht, T.D.., 1982, Fundamentals of Fractured Reservoir Engineering, Elsevier Scientific Publishing, 709 p.

Wallis, P.F., and King, M.S., 1980, Discontinuity spacings in a crystalline rock: International Rock Mechanics, Mining Sciences and Geomechanical Abstracts, v. 17, p. 63-66.

Warren, J.E., and Root, P.J., 1963, The behavior of naturally fractured reservoirs: Transactions, AIME, v. 228, p. 245-255.

Way, S., and McKee, C.R., 1982, In-situ determination of three dimensional aquifer permeabilities: Ground Water, v. 20, n. 5, p. 594-603.

Weeks, E.P., 1969, Determining the ratio of horizontal to vertical permeability by aquifer-test analysis: Water Resources Research, v. 5, n. 1, p. 196-214

Wehr, F., and Glover, L., 1985, Stratigraphy and tectonics of the the Virginia-North Carolina Blue Ridge; evolution of a late Proterozoic-early Paleozoic hinge zone: Geological Society of America Bulletin, v. 96, March, p. 285-295.

Wilson, C.W., and Witherspoon, P.A., 1974, Steady state flow in rigid networks of fractures: Water Resources Research, v. 10, n. 2, p. 328-335.

Wilson, C.W., and Witherspoon, P.A., 1970, An investigation of laminar flow in fractured rocks: Geotechnical Report No. 70-6, University of California, Berkeley.

Witherspoon, P.A., and Neuman, S.P., 1967, Evaluating a slightly permeable caprock in aquifer gas storage; I. caprock of infinite thickness, Society of Petroleum Engineers Journal, July, p. 949-955.

Witherspoon, P.A., and Tsang, Y.W., 1981, New approaches to problems of fluid flow in fractured rock masses: Proceedings of the 22nd US Symposium on Rock Mechanics, Massachusetts Institute of Technology, p. 3-22.

Wittke, W., 1990, Rock Mechanics- Theory and applications with case histories, Springer-Verlag, 1066 p.

Zanger, C.N., 1953, Theory and problems of water percolation: US Department of the Interior, Bureau of Reclamation.

APPENDIES

Table A1.1 Definitions, Dimensions, and SI Units for Basic Mechanical Properties

Property	Symbol	Definition	SI unit	SI symbol	Dimension of unit: Derived	Basic
Mass	M		kilogram	kg		kg
Length	l		meter	m		m
Time	t		second	s		s
Area	A	$A = l^2$				m^2
Volume	V	$V = l^3$				m^3
Velocity	v	$v = l/t$				m/s
Acceleration	a	$a = l/t^2$				m/s^2
Force	F	$F = Ma$	newton	N	N	$kg \cdot m/s^2$
Weight	w	$w = Mg$	newton	N	N	$kg \cdot m/s^2$
Pressure	p	$p = F/A$	pascal	Pa	N/m^2	$kg/m \cdot s^2$
Work	W	$W = Fl$	joule	J	$N \cdot m$	$kg \cdot m^2/s^2$
Energy		Work done	joule	J	$N \cdot m$	$kg \cdot m^2/s^2$
Mass density	ρ	$\rho = M/V$				kg/m^3
Weight density	γ	$\gamma = w/V$			N/m^3	$kg/m^2 \cdot s^2$
Stress	σ, τ	Internal response to external p	pascal	Pa	N/m^2	$kg/m \cdot s^2$
Strain	ϵ	$\epsilon = \Delta V/V$				Dimensionless
Young's modulus	E	Hooke's law			N/m^2	$kg/m \cdot s^2$

Table A1.2 Definitions, Dimensions, and SI Units for Fluid Properties and Groundwater Terms

Property	Symbol	Definition	SI unit	SI symbol	Dimensions of unit: Derived	Basic
Volume	V	$V = l^3$	liter ($= m^3 \times 10^{-3}$)	ℓ	ℓ	m^3
Discharge	Q	$Q = l^3/t$			ℓ/s	m^3/s
Fluid pressure	p	$p = F/A$	pascal	Pa	N/m^2	$kg/m \cdot s^2$
Head	h					m
Mass density	ρ	$\rho = M/V$				kg/m^3
Dynamic viscosity	μ	Newton's law	centipoise ($= N \cdot s/m^2 \times 10^{-3}$)	cP	cP, $N \cdot s/m^2$	$kg/m \cdot s$
Kinematic viscosity	ν	$\nu = \mu/\rho$	centistoke ($= m^2/s \times 10^{-6}$)	cSt	cSt	m^2/s
Compressibility	α, β	$\alpha = 1/E$			m^2/N	$m \cdot s^2/kg$
Hydraulic conductivity	K	Darcy's law			cm/s	m/s
Permeability	k	$k = K\mu/\rho g$			cm^2	m^2
Porosity	n					Dimensionless
Specific storage	S_s	$S_s = \rho g(\alpha + n\beta)$				1/m
Storativity	S	$S = S_s b$*				Dimensionless
Transmissivity	T	$T = Kb$*				m^2/s

*b, thickness of confined aquifer

From Freeze and Cherry (1979)

b = thickness of the fracture zone or interval being tested
s = drawdown = $h_{initial} - h_{final}$
r = distance from pumping well to observation well
r_w = radius of pumping well
K' = hydraulic conductivity of the confining layer
b' = thickness of the confining layer
$T_{14}, T_{16}, T_{20} = T_d(\theta)$ = directional transmissivity in the direction of monitoring wells 14, 16 and 20

APPENDIX A

THE BOULTON (1954, 1963) UNCONFINED AQUIFER METHOD

$$s = \frac{Q}{4\pi T} W(u_A, u_B, \frac{r}{B}) \qquad (22)$$

$$u_A = \frac{r^2 S}{4Tt} \qquad (23)$$

$$u_B = \frac{r^2 S_y}{4Tt} \qquad (24)$$

$$\frac{r}{B} = \frac{r}{\sqrt{\frac{T}{\alpha S_y}}} \qquad (25)$$

<u>Using the Early Time A-curves</u>

<u>MW-14</u>

$Q = 15150.50$ cm^3/min

$r = 10668.00$ cm

$b = 3048.00$ cm

<u>Match Point Coordinates</u>

$W(u_A, r/B) = 10.00$

$1/u_A = 1.00$

$s = 240.00$ cm

$t = 30.00$ min

$r/B = .40$

Use Equation (22) to solve for transmissivity (T).

Use Equation (23) to solve for storativity (S).

MW-16

$Q = 15150.50\ cm^3/min$

$r = 13563.60$ cm

$b = 3048.00$ cm

Match Point Coordinates

$W(u_A, r/B) = 10.00$

$1/u_A = 1.00$

$s = 560.00$ cm

$t = 14.00$ min

$r/B = .30$

Use Equation (22) to solve for transmissivity (T).

Use Equation (23) to solve for storativity (S).

MW-20

$Q = 15150.50\ cm^3/min$

$r = 10668.00$ cm

$b = 3048.00$ cm

Match Point Coordinates

$W(u_A, r/B) = 10.00$

$1/u_A = 1.00$

$s = 30.50$ cm

$t = 10.50$ min

$r/B\ \ .10$

Use Equation (22) to solve for transmissivity (T).

Use Equation (23) to solve for storativity (S).

APPENDIX B

THREE POINT SOLUTION TO DETERMINE THE ORIENTATION OF THE FRACTURE ZONE

$$\overline{AD} = \frac{Elevation\ D - Elevation\ A}{Elevation\ C - Elevation\ A}\,(\overline{AC}) \qquad (26)$$

$$\tan\theta = \frac{Elevation\ B - Elevation\ A}{\overline{AD}} \qquad (27)$$

θ = amount of the dip angle

Calculate the length of line AD from Equation (26).

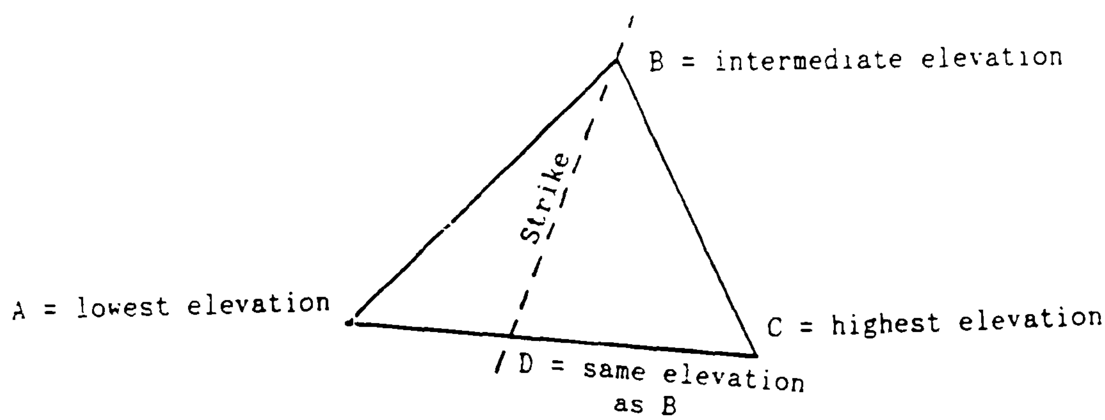

The strike of the fracture zone is determined graphically by the orientation of a line connecting the intermediate fracture zone well and the point with the same elevation along the AC line. This point with the same elevation as the intermediate well fracture zone is determined by the length of AD.

Calculate the dip angle amount by Equation (27).

Using MW-14, MW-15, and MW-16

A = MW-16 fracture zone elevation = 2045.00 ft

B = MW-14 fracture zone elevation = 2059.00 ft

C = MW-15 fracture zone elevation = 2089.00 ft

Fracture zone orientation = S47W 9.4SE

Using MW-14, MW-16, and MW-22

A = MW-22 fracture zone elevation = 2009.00 ft

B = MW-16 fracture zone elevation = 2045.00 ft

C = MW-14 fracture zone elevation = 2059.00 ft

Fracture zone orientation = S45W 8.1SE

Using MW-14, MW-16, and MW-20

A = MW-20 fracture zone elevation = 2019.00 ft

B = MW-16 fracture zone elevation = 2045.00 ft

C = MW-14 fracture zone elevation = 2059.00 ft

Fracture zone orientation = S38W 5.7SE

APPENDIX C

COOPER AND JACOB (1946) STRAIGHT LINE METHOD FOR A RADIAL FLOW AQUIFER

$$\Delta s = \frac{2.3\,Q}{4\pi T} \quad (28) \qquad S = \frac{2.25\,T t_0}{r^2} \quad (29)$$

Δs = change in drawdown per log cycle

t_0 = time at which the extended straight line intersects the time axis ($s = 0$)

<u>MW-14</u>

Q = 15150.50 cm^3/min

r = 10668.00 cm

b = 152.40 cm

Use Equation (28) to solve for transmissivity (T).

Use Equation (29) to solve for storativity (S).

First Straight Line Segment

Δs = 35.05 cm	T = 1.32 cm^2/sec
t_0 = 26.00 min	K = 8.65 X 10^{-3} cm/sec
	S = 4.07 X 10^{-5}

Second Straight Line Segment

$\Delta s = 3.66$ cm

t_0 = negligibly small

$T = 12.63\ cm^2/sec$

$K = 8.29 \times 10^{-2}$

S = negligibly small

MW-16

$Q = 15150.50\ cm^3/min$

$r = 13563.60$ cm

$b = 152.4$ cm

Use Equation (28) to solve for transmissivity (T).

Use Equation (29) to solve for storativity (S).

First Straight Line Segment

$\Delta s = 87.17$ cm

$t_0 = 13.00$ min

$T = 5.30 \times 10^{-1}\ cm^2/sec$

$K = 3.48 \times 10^{-3}$ cm/sec

$S = 5.06 \times 10^{-6}$

Second Straight Line Segment

$\Delta s = 2.44$ cm

t_0 = negligibly small

$T = 75.76\ cm^2/sec$

$K = 4.97 \times 10^{-1}$

S = negligibly small

MW-20

$Q = 15150.50\ cm^3/min$

$r = 10668.00\ cm$

$b = 152.4\ cm$

Use Equation (28) to solve for transmissivity (T).

Use Equation (29) to solve for storativity (S).

First Straight Line Segment

$\Delta s = 5.94\ cm$ — $T = 7.78\ cm^2/sec$

$t_0 = 11.00\ min$ — $K = 5.10 \times 10^{-2}\ cm/sec$

$S = 1.01 \times 10^{-4}$

Second Straight Line Segment

$\Delta s = 3.37\ cm$ — $T = 3.37\ cm^2/sec$

$t_0 = 100.00\ min$ — $K = 2.21 \times 10^{-2}$

$S = 4.00 \times 10^{-4}$

APPENDIX D

HANTUSH (1956, 1960) METHOD FOR A SEMI-CONFINED AQUIFER

$$s = \frac{Q}{4\pi T} H(u, \beta) \qquad (30)$$

$$u = \frac{r^2 S}{4Tt} \qquad (31)$$

$$\beta^2 = \frac{r^2}{16b^2}\left(\frac{K' S_s'}{K S_s}\right) \qquad (32)$$

<u>MW-14</u> - Radial Flow Period 50-300 min

Q = 15150.50 cm^3/min

r = 10668.00 cm

<u>Match Point Coordinates</u>

β = 0.10

H(u, β) = 1.00

1/u = 1.00

s = 25.00 cm

t = 25.30

Use Equation (30) to solve for transmissivity (T).

Use Equation (31) to solve for storativity (S).

Use Equation (32) to solve for $K'S_s'$

MW-16 - Radial Flow Period 30-300 min

$Q = 15150.50\ cm^3/min$

$r = 13563.60\ cm$

Match Point Coordinates

$\beta = 0.30$

$H(u,\beta) = 1.00$

$1/u = 1.00$

$s = 86.00\ cm$

$t = 11.20$

Use Equation (30) to solve for transmissivity (T).

Use Equation (31) to solve for storativity (S).

Use Equation (32) to solve for $K'S_s'$

MW-20 - Radial flow Period 40-600 min

$Q = 15150.50\ cm^3/min$

$r = 10668.00\ cm$

Match Point Coordinates

$\beta = 0.20$

$H(u,\beta) = 1.00$

$1/u = 1.00$

$s = 5.00\ cm$

$t = 10.80$

Use Equation (30) to solve for transmissivity (T).

Use Equation (31) to solve for storativity (S).

Use Equation (32) to solve for $K'S_s'$

APPENDIX E

HANTUSH AND JACOB (1960) METHOD FOR A SEMI-CONFINED AQUIFER

$$s = \frac{Q}{4\pi T} L(u,v) \qquad (33)$$

$$u = \frac{r^2 S}{4Tt} \qquad (34)$$

$$\frac{K'}{b'} = 4T\frac{v^2}{r^2} = S\frac{\left(\frac{v^2}{u}\right)}{t} \qquad (35)$$

<u>MW-14</u> - Radial Flow Period 50-300 min

$Q = 15150.50$ cm^3/min	<u>Match Point Coordinates</u>
r = 10668.00 cm	v = 0.30
b = 152.40 cm	L(u,v) = 1.00
	1/u = 1.00
	s = 29.00 cm
	t = 34.00

<u>MW-14</u> - Extended Radial Flow Period 50-800 min

$Q = 15150.50$ cm^3/min	<u>Match Point Coordinates</u>
r = 10668.00 cm	v = 0.20
b = 152.40 cm	L(u,v) = 1.00
	1/u = 1.00

s = 23.50 cm

t = 29.00

Use Equation (33) to solve for transmissivity (T).

Use Equation (34) to solve for storativity (S).

Use Equation (35) to solve for K′

MW-16 - Radial Flow Period 30-300 min

Q = 15150.50 cm^3/min

r = 13563.60 cm

b = 152.40 cm

Match Point Coordinates

v = 0.20

L(u,v) = 1.00

1/u = 1.00

s = 63.00 cm

t = 16.00

MW-16 - Extended Radial Flow Period 30-650 min

Q = 15150.50 cm^3/min

r = 13563.60 cm

b = 152.40 cm

Match Point Coordinates

v = 0.20

L(u,v) = 1.00

1/u = 1.00

s = 64.00 cm

t = 16.20

Use Equation (33) to solve for transmissivity (T).

Use Equation (34) to solve for storativity (S).

Use Equation (35) to solve for K'

MW-20 - Radial Flow Period 40-600 min

$Q = 15150.50\ cm^3/min$	Match Point Coordinates
$r = 10668.00$ cm	$v = 0.10$
$b = 152.40$ cm	$L(u,v) = 1.00$
	$1/u = 1.00$
	$s = 3.48$ cm
	$t = 12.30$

Use Equation (33) to solve for transmissivity (T).

Use Equation (34) to solve for storativity (S).

Use Equation (35) to solve for K'

APPENDIX F

CALCULATION FOR MAPPING THE CONE OF DEPRESSION

HANTUSH (1966 a&b) AND

HANTUSH AND THOMAS (1966)

$$s = \frac{Q}{4\pi T_e} L(u,v) \qquad (36)$$

$$u = \frac{r^2}{4t}\frac{S}{T_n} \qquad (37)$$

<u>MW-14</u>

From the Hantush Anisotropic Method

T_e = 41.57 cm^2/min

T_{14}/S = 836810.50 cm^2/min

v = 0.30

Q = 15150.50 cm

Solve Equation (36) for L(u,v).

A value for "u" is found from Leaky Aquifer Type Curve or a table of L(u,v), v, u values.

For any given time (t) and any given drawdown (s) Equation (37) is solved for the distance (r).

$t = 200.00$ min

$s = 5.00$ cm $\quad$ $r = 28343.20$ cm $= 929.90$ ft

$s = 10.00$ cm $\quad$ $r = 21647.50$ cm $= 710.20$ ft

$s = 100.00$ cm $\quad$ $r = 258.70$ cm $= < 8.50$ ft

MW-16

From the Hantush Anisotropic Method

$T_e = 19.14\ cm^2/min$

$T_{16}/S = 2874550.70\ cm^2/min$

$v = 0.20$

$Q = 15150.50$ cm

Solve Equation (36) for $L(u,v)$.

A value for "u" is found from Leaky Aquifer Type Curve or a table of $L(u,v)$, v, u values.

For any given time (t) and any given drawdown (s) Equation (37) is solved for the distance (r).

$t = 200.00$ min

$s = 5.00$ cm $\quad$ $r = 64337.80$ cm $= 2110.82$ ft

$s = 10.00$ cm $\quad$ $r = 55303.90$ cm $= 1814.40$ ft

$s = 100.00$ cm $\quad$ $r = 14780.60$ cm $= 484.90$ ft

MW-20

From the Hantush Anisotropic Method

T_e = 388.92 cm^2/min

T_{20}/S = 2789368.20 cm^2/min

v = 0.05

Q = 15150.50 cm

Solve Equation (36) for L(u,v).

A value for "u" is found from Leaky Aquifer Type Curve or a table of L(u,v), v, u values.

For any given time (t) and any given drawdown (s) Equation (37) is solved for the distance (r).

t = 200.00 min

s = 5.00 cm	r = 14938.19 cm = 490.10 ft
s = 10.00 cm	r = 6680.56 cm = 219.18 ft
s = 100.00 cm	r = 0.0 cm = 0.0 ft

The calculated distances (r) are marked along the rays from the pumping well to the observation wells. The same drawdown value (s) along each ray are joined by an arc of an ellipse with the equipotential line forming an ellipse in a homogeneous anisotropic aquifer. The result is a map of the cone of depression for 200.00 minutes into the aquifer test.

APPENDIX G

HANTUSH (1966 a & b) AND HANTUSH-THOMAS (1966) METHOD FOR A HOMOGENEOUS ANISOTROPIC AQUIFER

The transmissivity determined from any radial flow solution is taken as the effective transmissivity (T_e).

$$T_e = \sqrt{T_x T_y} \qquad (38)$$

T_x = maximum transmissivity

T_y = minimum transmissivity

$$s = \frac{Q}{4\pi T_e} W(u') \qquad (39)$$

$$u' = \frac{r^2 S}{4 t T_n} \qquad (40)$$

T_n is the transmissivity in the direction (θ) of a ray (n) originating at the pumping well.

From Maasland (1957) and Hantush (1966)

$$T_n = T(\theta) = \frac{T_x}{\cos^2(\theta + \alpha) + \frac{T_x}{T_v}\sin^2(\theta + \alpha)} \qquad (41)$$

$$\frac{T_x}{T_y} = m = \left(\frac{T_e}{T_y}\right)^2 \qquad (42)$$

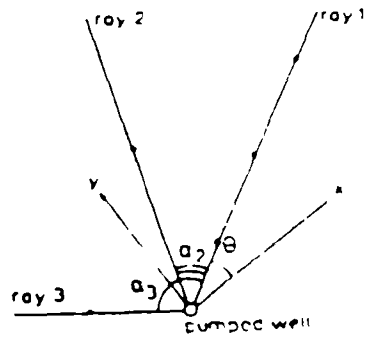

The illustration above shows the relationship of the rays (defined by a line from the pumping well to each observation well) to the x-axis (maximum transmissivity direction). θ is the angle from the x-axis to the first ray. Since α_1 is the angle from the first ray to another arbitrary ray $\alpha_1 = 0$. The angle from ray 1 to ray 2 is designated as α_2 and the angle from ray 1 to ray 3 is α_3 and so on. So the $(\theta + \alpha_n)$ term refers to the angle between the nth ray and the x-axis.

Since $\alpha_1 = 0$, it follows from Equation (41) that

$$T_1 = \frac{T_x}{\cos^2\theta + m\sin^2\theta} \qquad (43)$$

From Equations (41) and (43)

$$\frac{T_1}{T_n} = a_n = \frac{\cos^2(\theta + \alpha_n) + m\sin^2(\theta + \alpha_n)}{\cos^2\theta + m\sin^2\theta} \qquad (44)$$

so that a1 = 1

Solving Equation (44) for m yields

$$m = \frac{T_x}{T_y} = \left(\frac{T_e}{T_y}\right)^2 = \frac{a_n\cos^2\theta - \cos^2(\theta + \alpha_n)}{\sin^2(\theta + \alpha_n) - a_n\sin^2\theta} \qquad (45)$$

For three rays (observation wells), solving Equation (44) for θ yields

$$\tan(2\theta) = -2\,\frac{(a_3 - 1)\sin^2\alpha_2 - (a_2 - 1)\sin^2\alpha_3}{(a_3 - 1)\sin 2\alpha_2 - (a_2 - 1)\sin 2\alpha_3} \qquad (46)$$

From the Hantush (1956, 1960) semi-confined homogeneous isotropic method for the short radial flow period.

T_{e14}/S = 1124567.40 cm^2/min

T_{e16}/S = 4106501.00 cm^2/min

T_{e20}/S = 2634403.30 cm^2/min

From the geometry of the wells

$\alpha_2 = 39°$

$\alpha_1 = 0°$

$\alpha_3 = -30°$

Calculated with Equation (44)

$a_1 = 1.0000$

$a_2 = 3.6516$

$a_3 = 1.5588$

Calculated with Equation (46)

$\theta = 8.6135°$

Calculated with Equation (45)

$m = T_x/T_y = 6.715$

T_x and T_y are calculated with Equation (42).

T_{14}, T_{16}, and T_{20} are calculated with Equation (41).

S is calculated with the original values of T_{e14}/S, T_{e16}/S, T_{e20}/S and the calculated values of T_{14}, T_{16}, and T_{20}.

From the Hantush and Jacob (1955) semi-confined homogeneous isotropic method for the short radial flow period.

$T_{e14}/S = 836810.50\ cm^2/min$

$T_{e16}/S = 2874550.70\ cm^2/min$

$T_{e20}/S = 2313134.6\ cm^2/min$

From the geometry of the wells

$\alpha_2 = 39°$

$\alpha_1 = 0°$

$\alpha_3 = -30°$

Calculated with Equation (44)

$a_1 = 1.0000$

$a_2 = 3.4351$

$a_3 = 1.2427$

Calculated with Equation (46)

$\theta = 11.8°$

Calculated with Equation (45)

$m = T_x/T_y = 6.31$

From the Hantush and Jacob (1955) semi-confined homogeneous isotropic method for the extended radial flow period.

T_{c14}/S = 981088.10 cm^2/min

T_{c16}/S = 2839062.40 cm^2/min

T_{c20}/S = 2313134.6 cm^2/min

From the geometry of the wells

$\alpha_2 = 39°$

$\alpha_1 = 0°$

$\alpha_3 = -30°$

Calculated with Equation (44)

$a_1 = 1.0000$

$a_2 = 2.894$

$a_3 = 1.227$

Calculated with Equation (46)

$\theta = 11.2°$

Calculated with Equation (45)

$m = T_x/T_y = 4.94$

T_x and T_y are calculated with Equation (42).
T_{14}, T_{16}, and T_{20} are calculated with Equation (41).
S is calculated with the original values of T_{e14}/S, T_{e16}/S, T_{e20}/S and the calculated values of T_{14}, T_{16}, and T_{20}.

For a system to be considered truly homogeneous and anisotropic the values of T_e and S from all observation wells should be about the same.

Appendix H

Parameters for Appendix H

s = s = drawdown
P = pressure = $\rho g h$
ΔP = change in pressure = $\rho g \Delta h$ = Δh because ρg is constant
T = transmissivity
S = Storage
t = time
ϕ_m = Porosity of matrix
C_m = Compressibility of matrix
$\phi_m C_m$ = Specific Storage of matrix
ϕ_f = Porosity of fractures
C_f = Compressibility of fractures
$\phi_f C_f$ = Specific Storage of fractures
μ = dynamic viscosity for water → 1 centipoise
β_o = formation volume factor = 1
k_m = permeability of matrix
k_f = permeability of fracture
X = x coordinate of observation well
Y = y coordinate of observation well
ω = storage contrast ratio (double porosity)
λ = permeability contrast ratio (double porosity)

Flow Test Methods

Homogeneous and Anisotropic:

Papadopulos: (1965)

Confined aquifer
Homogeneous and Anisotropic
Three observation wells

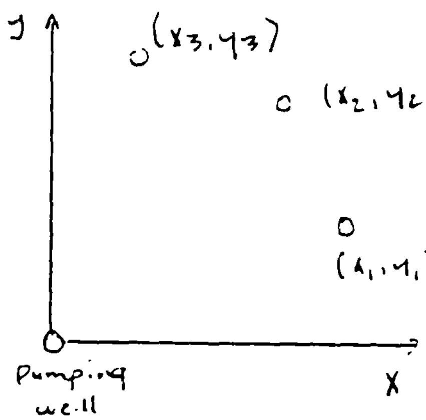

$$T = \begin{bmatrix} T_{xx} & T_{xy} \\ T_{yx} & T_{yy} \end{bmatrix}$$

Determinant of Transmissivity

$$D = T_{xx} T_{yy} - T_{xy}^2$$

$$s = \frac{Q}{4\pi (T_{xx} T_{yy} - T_{xy}^2)^{1/2}} W(u, x, y) \qquad (1)$$

$$u_{xy} = \frac{S}{4t} \left(\frac{T_{xx} y^2 + T_{yy} x^2 - 2 T_{xy} x^2 y^2}{T_{xx} T_{yy} - T_{xy}^2} \right) \qquad (2)$$

Match field curve ($\log s$ vs $\log t$) to Theis type curve ($\log W(u_{xy})$ vs $\log \frac{1}{u_{xy}}$)

Calculate value of determinant from eq 1
Will get a determinant value for each observation well.
Chose best single value for D.

From eq 2 determine equation for all observation well of the form

$$a\,ST_{xx} + b\,ST_{yy} - 2c\,ST_{xy} = A$$

Solve for ST_{xx}, ST_{yy}, and ST_{xy} by simultaneous equations

Solve for S by $T_{xx}T_{yy} - T_{xy}^2 = D$ by substituting

$$T_{xx} = \frac{d}{S}, \quad T_{yy} = \frac{e}{S}, \quad T_{xy} = \frac{f}{S}$$

Then solve for T_{xx}, T_{yy}, and T_{xy}

<u>Papadopulos</u>: (1965)
Straight line method (Semi log method)

$$W(u_{xy}) = 2.30 \log_{10} \frac{2.25\,Tt}{r^2 S} \qquad (3)$$

$$s = \frac{2.30\,Q}{4\pi (T_{xx}T_{yy} - T_{xy}^2)^{1/2}} \log_{10}\left[\frac{2.25t}{S}\;\frac{T_{xx}T_{yy} - T_{xy}^2}{T_{xx}y^2 + T_{yy}x^2 - 2T_{xy}xy}\right] \quad ($$

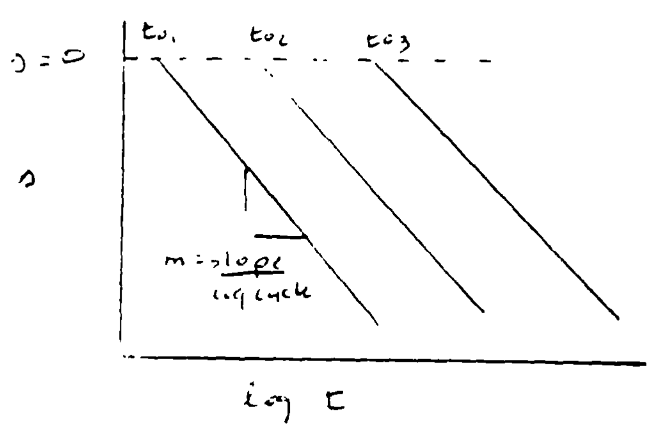

slope $= m = \dfrac{\Delta s}{\text{one log cycle}}$

Determine $T_{xx}T_{yy} - T_{xy}^2$ from

$$m = \frac{2.30\,Q}{4\pi (T_{xx}T_{yy} - T_{xy}^2)^{1/2}} \qquad (5)$$

Will calculate a $T_{xx}T_{yy} - T_{xy}^2$ value for each pumping well. Choose best one value.

If $s = 0$, $t = t_0$

$$0 = \log_{10} \frac{2.25 t}{S} \cdot \frac{T_{xx} T_{yy} - T_{xy}^2}{T_{xx} y^2 + T_{yy} x^2 - 2 T_{xy} xy}$$

$$\log^{-1} 0 = \log^{-1} \log_{10} \frac{2.25 t}{S} \cdot \frac{T_{xx} T_{yy} - T_{xy}^2}{T_{xx} y^2 + T_{yy} x^2 - 2 T_{xy} xy}$$

$$1 = \frac{2.25}{S} \cdot \frac{T_{xx} T_{yy} - T_{xy}^2}{T_{xx} y^2 + T_{yy} x^2 - 2 xy xy} \qquad (6)$$

Solve by simultaneous equation derived from eq. 6 for ST_{xx}, ST_{yy}, ST_{xy}

Find S by substituting

$$T_{xx} = \frac{d}{S} \quad T_{yy} = \frac{e}{S} \quad T_{xy} = \frac{f}{S}$$

into $T_{xx} T_{yy} - T_{xy}^2 = D$

Then solve for T_{xx}, T_{yy}, and T_{xy}

<u>Papadopulos Modified Method:</u>

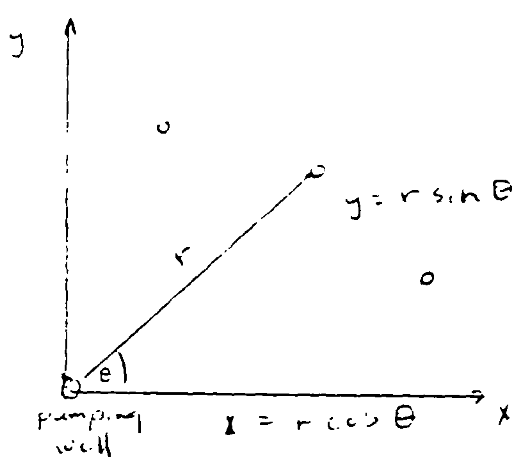

$$s = \frac{Q}{4\pi (T_{xx} T_{yy} - T_{xy}^2)^{1/2}} \, w(u_{xy}) \qquad (7)$$

$$u_{xy} = \frac{r^2 S}{4t \, T_d(\theta)} \qquad (8)$$

$$T_d(\theta) = \frac{T_{xx} T_{yy} - T_{xy}^2}{T_{yy} \cos^2\theta + T_{xx} \sin^2\theta - 2 T_{xy} \cos\theta \sin\theta} \qquad (9$$

$$u_{xy} = \frac{r^2 S \, (T_{xx} \sin^2\theta + T_{yy} \cos^2\theta - 2 T_{xy} \cos\theta \sin\theta}{4t \, (T_{xx} T_{yy} - T_{xy}^2)} \qquad (10)$$

From matching curves obtain s, t, $w(u_{xy})$, u_{xy}

θ, $\cos\theta$, $\sin\theta$, r are known

Find $T_{xx}T_{yy} - T_{xy}^2$ from eq. 7

Find $\frac{Td(\theta)}{S}$ for each observation well from eq 8

Plot $\sqrt{\frac{Td(\theta)}{S}}$ vs. θ on polar graph to determine transmissivity ellipse.

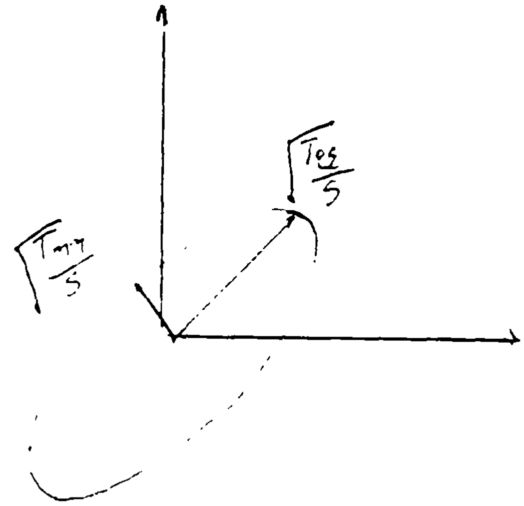

Determinant is now

$D = T_{\xi\xi}T_{\eta\eta}$

$$\sqrt{\frac{T_{\xi\xi}}{S}}\sqrt{\frac{T_{\eta\eta}}{S}} = \frac{D^{1/2}}{S} \qquad (11)$$

Solve for S by eq. 11.

Gringarten and others: (1974)

Single Vertical Fracture - Infinite homogeneous matrix with pumping well intersecting a vertical fracture

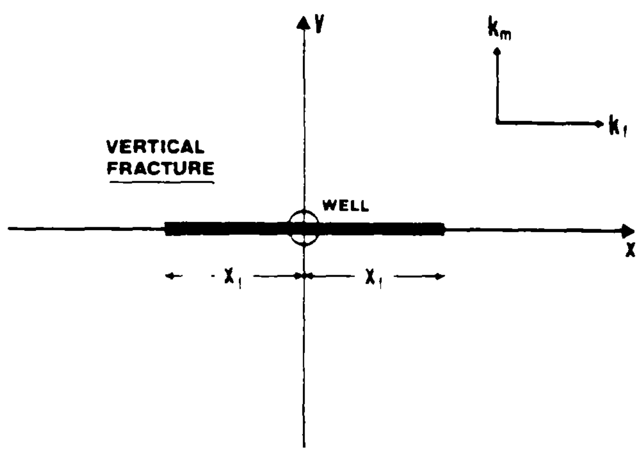

F.gure ertical fracture model.

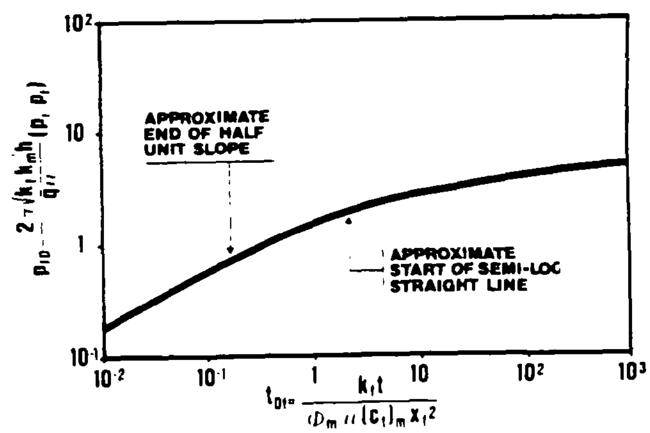

Figure Type curve for vertical-fracture

log-log method

Match field curve with Gringarten's type curve and obtain Δp, t, P_{fD}, t_D

Can calculate mean conductivity $\sqrt{k_f k_m}$ from

$$P_{fD} = \frac{2\pi \sqrt{k_f k_m}}{q \, \eta} \left(P_i - P_{f,m,l} \right) \qquad (12)$$

If radius of fracture is known can find storage $\phi_m C_m$ from

$$t_D = \frac{k_f t}{\phi_m C_m \eta \, x_f^2} \qquad (13)$$

At observation wells

$$t_D = \frac{t}{\phi_m C_m \eta} \cdot \frac{k_f k_m}{\sqrt{\left[k_f y^2 + (x + x_f)^2 k_m\right]\left[k_f y^2 + (x - x_f)^2 k_m\right]}} \qquad (14$$

$$r_D = \frac{1}{x_f} \sqrt{x^2 + y^2 \frac{k_f}{k_m}} \qquad (15)$$

If observation wells are used a type curve that contains curves for varying r_D values is needed

At $r_D \geq 5.0$

Problem is solved by Papadopulos method.

<u>Gringarten and Ramey:</u> (1974)

Single Horizontal Fracture - Pumping well intersects horizontal fracture at the midpoint.

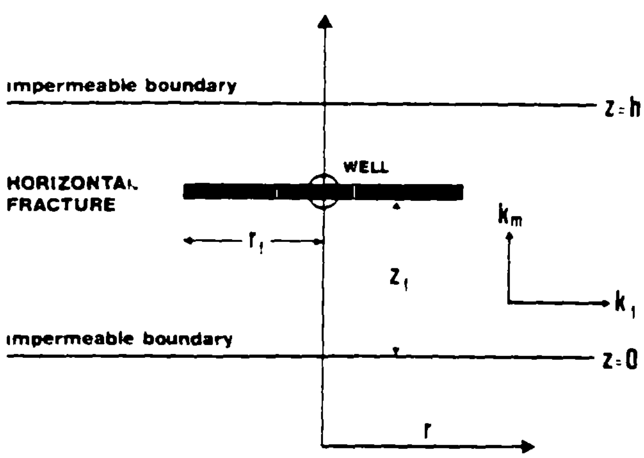

Figure Horizontal fracture model.

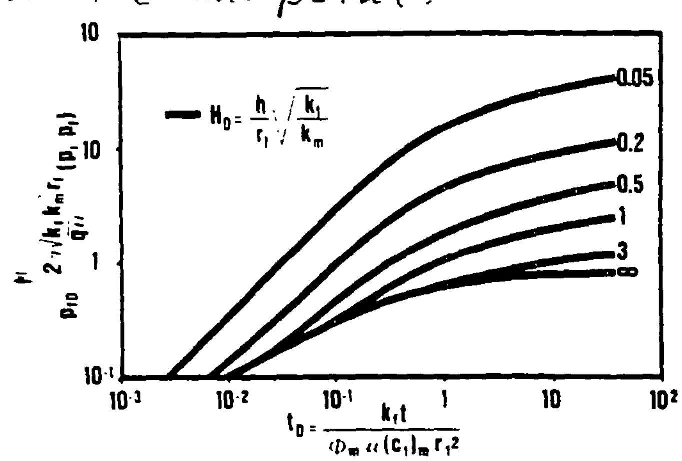

Figure Type curves for horizontal-fracture model with drawdowns measured at pumping well log-log method

Field data of log P_{fD} vs t_D is matched with type curve values for Δp, t, P_{fD}, t_D are obtained

k_f, k_m, and r_f can be calculated if storage $\phi_m C_m$ is known

$$P_{fD} = \frac{2\pi \sqrt{k_f k_m}\, r_f}{q\mu} \Delta P \quad (16)$$

$$t_D = \frac{k_f t}{\phi_m C_m \mu r_f^2} \quad (17)$$

$$h_D = \frac{h}{r_f} \sqrt{\frac{k_f}{k_m}} \quad (18)$$

h_D can be obtained from type curve

Beyond a critical radius for observation wells

$$r_c = r_f + 2h \sqrt{\frac{k_f}{k_m}} \quad (19)$$

a homogeneous isotropic solution (Theis) can be used.

Straight Line Methods: (semilog method)

when applicable a straight line method can be used for both of Gringarten's vertical and horizontal fracture methods using equations available in the papers.

Double Porosity Models

Warren and Root: (1965) Semilog method

Assumptions:

1. Orthogonal horizontal and vertical fractures with identical cubic blocks
2. Matrix blocks are homogeneous and isotropic
3. water flows from blocks into fractures and from fractures into the wellbore
4. High contrast between K_f and K_m
5. Pseudo-steady state flow

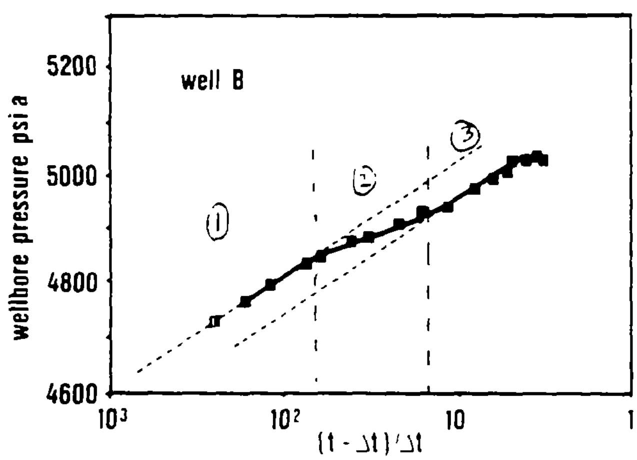

Figure Example of parallel semi-log straight lines (Warren and Root, 1965).

Curve can be divided into three sections.

① fracture flow only

③ fracture and matrix flow

② Transitional time period.

E_i = Exponential Integral Funct.

$E_i = \int \frac{e^{-u}}{u} du$

$$P_{fD} = \frac{1}{2}\left[0.80908 + \ln t_D + E_i\left(\frac{-\lambda t_D}{\omega(1-\omega)}\right) - E_i\left(\frac{-\lambda t_D}{1-\omega}\right)\right] \quad (20)$$

$$t_D = \frac{k_f\, t}{(\phi_m c_m + \phi_f c_f)\mu r^2} \qquad k_f = \sqrt{k_{fx}\, k_{fy}} \quad (21)$$

$$\lambda = \alpha \frac{k_m}{k_f} r_w^2 \quad (22)$$

$$\omega = \frac{\phi_f c_f}{\phi_m c_m + \phi_f c_f} \quad (23)$$

At early times - Flow is in fracture only

$$P_{fD} = -\frac{1}{2} E_i\left(-\frac{\phi_f c_f \mu r^2}{4 k_f t}\right) \quad (24)$$

At long times — Flow in fracture and matrix

$$P_{fD} = \frac{1}{2}\left[\ln \frac{k_f\, t}{(\phi_f c_f + \phi_m c_m)\,\mu\, r^2}\right] \qquad (25)$$

Reservoir acts equivalent homogeneous porous medium with permeability equal to fracture permeability.

At intermediate times - Transition from fracture flow to fracture-matrix flow during which the pressure remains constant (pseudo steady state).

$$P_{fD} = \frac{1}{2}\left(\ln \frac{1}{\omega}\right) \qquad (26)$$

or

$$P_{fD} = 1.15 \log_{10} \frac{1}{\omega}$$

$$\omega = e^{-2.3\left(\frac{\Delta P}{m}\right)} \qquad (27)$$

ΔP = vertical separation of the intersect of assymtote lines and the y-axis

m = slope of assymtote lines

$$P_{fD} = \frac{1}{2} \ln 1.26 \left(\frac{1-\omega}{\lambda}\right) \qquad (28)$$

Kazemi; (1969)

1. Finite circular reservoir with pumping well at the center.
2. Flow is from matrix to fractures and from fractures to the well bore
3. Both radial and vertical flow
4. Unsteady - State
5. Fractures are horizontal
6. Matrix and fractures are homogeneous and isotropic
7. when contrast between k_f and k_m is small transition period is may dissappear from plot.

$$P_{fD} = \frac{1}{2}\left[-E_i\left(-\frac{r_D^2}{4t_D}\right) + E_i\left(-\frac{\lambda t_D}{\omega(1-\omega)}\right) - E_i\left(-\frac{\lambda t_D}{1-\omega}\right)\right] \qquad (29)$$

At late time

$$P_{fD} = \frac{1}{2}\left(\ln \frac{2.246\ t_D}{r_D^2}\right) \qquad (30)$$

$$t_D = \frac{a' t}{r_w^2} \qquad (31)$$

$$K = \frac{115\ q\ \mu_o B_o}{2\pi\ h\ \circ\ m} \qquad a' = 0.445\ \frac{r^2}{t_0} \qquad (32) \text{ and } (33)$$

when $\Delta P = 0$; $t = t_0$

$$t = \frac{0.445\ (\phi_f C_f + \phi_m C_m)\ \mu\ r^2}{K} \qquad (34)$$

t is equal to the time at the deflection of straight line.

De Swann (1976)

① Radial Flow
② Flow from blocks to fractures is uniform at all surfaces
③ Response from blocks is slower than response from fractures

Early time is fracture flow only (radial flow)

Find k_f from

$$\Delta P_f = \frac{q\ \mu_o B_o}{4\pi h_f\ k_f} \cdot \ln\left(\frac{4\ \eta_f\ t}{\gamma\ r_w^2}\right) \qquad (35)$$

η_f = diffusivity of fracture
γ = 1.78 in cm-sec units.

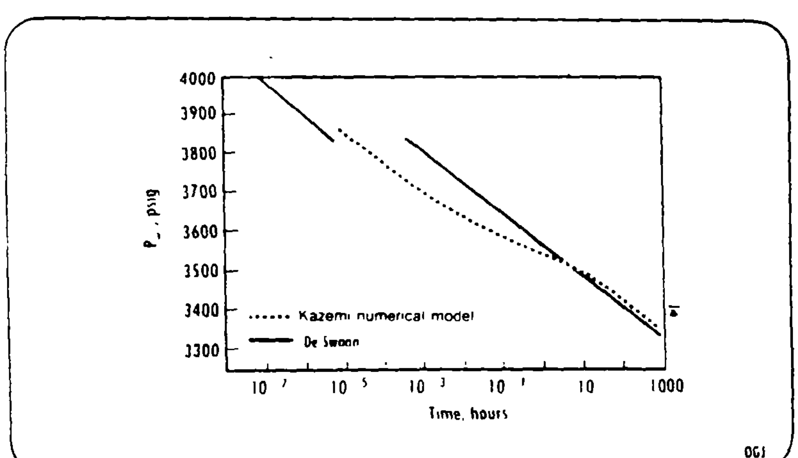

At late time

Flow is combination of fracture and matrix